

POLITECNICO DI TORINO

Master's Degrees in Civil Engineering



Master's Thesis

Comparison of Safety Formats for non-linear analyses of reinforced concrete columns

Supervisors

Dr. Eng. Paolo Castaldo

Dr. Eng. Diego Gino

Candidate

Giovanni Orazio Del Prete

April 2019

*A Mamma e Papà,
strepitosi artefici di vera ed eterna ricchezza.*

Abstract

The subject of the study is based on a comparison of the different Safety Formats for non-linear analyses of reinforced concrete columns with increasing slenderness values. The mentioned above Safety Formats allows to perform structural verification according to global approach, accounting for, separately, aleatory and epistemic uncertainties by means global safety factors.

The aim of the study is to analyze the results deriving from the different Safety Formats. To this purpose, the dependences from the column slenderness comparing the outcomes of the different safety formats is highlighted. The influence of the failure mode is also discussed, as affects significantly the ultimate design capacity.

Finally, as the Safety Formats are methodologies devoted to estimate the ultimate design capacity of RC structures by means of the implementation of probability theory with different degrees of simplification, the possible application of the Levels of Approximations approach proposed by fib Model Code 2010 is discussed and proposed.

Sommario

L'oggetto dello studio si basa su un confronto di differenti Safety Formats per l'analisi non lineare, applicati a colonne in cemento armato aventi valori di snellezza crescenti. Il Safety Format permette di identificare la resistenza strutturale in termini globali, tenendo conto di fattori di sicurezza indipendenti, associati ad incertezze aleatorie e di modello.

Lo scopo dello studio è quindi quello di analizzare e discutere i risultati relativi all'applicazione di differenti Safety Formats. A tal proposito, è stato interessante notare come i valori di resistenza globale ottenuti, evidenzino una dipendenza dalla snellezza, che ha condotto ad un'analisi relativa al tipo di collasso.

Infine, guardando al Safety Format come una metodologia di calcolo relativamente semplice, atta a identificare il carico di collasso allo stato limite ultimo, in ambito probabilistico e con l'accettazione di ipotesi più o meno semplificative, è stata discussa la possibile applicazione di un approccio riferito ai Livelli di Approssimazione, proposta nel *fib Model Code 2010*

Contents

1	INTRODUCTION TO STRUCTURAL RELIABILITY METHODS	- 1 -
1.1	LIMIT STATES.....	- 2 -
1.1.1	ULS – Ultimate Limit State	- 2 -
1.1.2	SLS – Serviceability Limit State	- 2 -
1.2	LIMIT STATE DESIGN AND RELIABILITY METHODS	- 3 -
1.2.1	Level III method.....	- 5 -
1.2.2	Level II methods	- 5 -
1.2.3	Level I method	- 6 -
1.2.4	Level 0 method.....	- 7 -
1.3	TARGET VALUES FOR RELIABILITY INDEX.....	- 8 -
2	SAFETY FORMATS FOR NON-LINEAR ANALYSIS	- 11 -
2.1	TYPE OF UNCERTAINTIES	- 12 -
2.1.1	Model Uncertainties	- 13 -
2.2	SAFETY FORMATS FOR NON-LINEAR ANALYSIS.....	- 14 -
2.2.1	Introduction of global safety factor γ_G	- 15 -
2.2.2	Probabilistic Method PM.....	- 16 -
2.3	GLOBAL RESISTANCE METHODS GRMs	- 18 -
2.3.1	Global Resistance Factor GRF	- 18 -
2.3.2	Estimation of Coefficient of Variation ECOV	- 19 -
2.3.3	Simplified Mean Value Method SMVM.....	- 20 -
2.3.4	Partial Factor Method PFM.....	- 21 -
2.3.5	Schlune method.....	- 22 -
2.3.6	Global Safety Format GSF.....	- 24 -
3	THEORY AND DESIGN FOR INSTABILITY	- 27 -
3.1	INTRODUCTION TO NON-LINEAR FIELD	- 27 -
3.2	BUCKLING HARDENING BRANCHING.....	- 30 -

3.3	<i>CRITICAL LOAD FOR AXIALLY LOADED COLUMNS</i>	- 32 -
3.3.1	<i>Instability of linear elastic columns</i>	- 33 -
3.3.2	<i>Instability of inelastic columns</i>	- 36 -
4	<i>EXPERIMENTAL DATABASE FOR RC COLUMNS</i>	- 39 -
4.1	<i>BIBLIOGRAPHY REFERENCES</i>	- 39 -
4.2	<i>EC2 COLUMNS REQUIREMENTS</i>	- 43 -
5	<i>STRUCTURAL MODEL FOR REINFORCED CONCRETE COLUMNS</i>	- 51 -
5.1	<i>MATERIAL BEHAVIOR</i>	- 51 -
5.1.1	<i>Compressive concrete behavior</i>	- 51 -
5.1.2	<i>Tensile concrete behavior</i>	- 54 -
5.1.3	<i>Reinforcement behavior</i>	- 56 -
5.2	<i>SOFTWARE</i>	- 56 -
5.2.1	<i>Models for non-linear simulations</i>	- 58 -
6	<i>RESULTS AND DISCUSSION</i>	- 61 -
6.1	<i>PROBABILISTIC METHOD RESULTS</i>	- 61 -
6.2	<i>SAFETY FORMATS RESULTS</i>	- 65 -
6.3	<i>COMPARATION OF SAFETY FORMATS</i>	- 66 -
6.3.1	<i>ECOV - Increasing overestimation</i>	- 67 -
6.3.2	<i>GRF – GSF - Independence from slenderness</i>	- 69 -
6.3.3	<i>PFM – SMVM - Growth and decline of Resistance values</i>	- 70 -
6.4	<i>COMPARISONS OF GLOBAL RESISTANCE FACTORS γ_R</i>	- 71 -
6.5	<i>CONCLUSIONS RELATED TO ACTUAL SLENDERNESS VALUES</i>	- 73 -
7	<i>FAILURE MODE-BASED SAFETY FACTOR</i>	- 79 -
7.1	<i>IDENTIFICATION OF THE FAILURE MODE</i>	- 79 -
7.1.1	<i>Global load-deflection diagrams</i>	- 80 -
7.1.2	<i>Local stress-strain diagram</i>	- 82 -
7.2	<i>FAILURE MODE</i>	- 85 -
7.3	<i>PROPOSAL OF FAILURE MODE-BASED SAFETY FORMAT FACTOR</i>	- 86 -

7.4	<i>FAILURE MODE SENSITIVITY</i>	- 87 -
8	<i>LEVELS OF APPROXIMATION</i>	- 89 -
9	<i>APPENDIX A – PROBABILITY DENSITY FUNCTIONS AND CUMULATIVE DENSITY FUNCTIONS OF COLUMNS GLOBAL RESISTANCE LOG-NORMAL DISTRIBUTIONS</i>	- 99 -
10	<i>APPENDIX B – GRAPHICS RELATED TO PRELIMINARY NON-LINEAR ANALYSES (NLA1 AND NLA2): GLOBAL AXIAL LOAD – DEFLECTION DIAGRAM AND LOCAL FIBER STRESS – STRAIN DIAGRAM</i>	- 105 -
11	<i>APPENDIX C – EXAMPLE OF OPENSEES C++ CODE</i>	- 119 -
12	<i>APPENDIX D – DIFFERENT INTERPOLATIONS OF GLOBAL RESISTANCE FACTOR γ_R RELATED TO SEVERAL SAFETY FORMATS</i>	- 129 -

1 Introduction to structural reliability methods

At the base of structural safety, or generally at the base of simple conception of safety, there is statistics and probability theory. Contrary to what ordinary people may think, total certainty of security against structural collapse can not exist, that is why it is impossible to think a structural engineer like a designer able to ensure full safety of structure. So, nature imposes man to deal with risk and it should be accepted in several fields of science. A particularly important topic in the civil area is risk of loss of human life, that represents one of important input data in phase of formulation of technical design codes. In order not to disturb the sensitivity of reader, it is right to underline the fact that the high or low risk of death is present in several and common situations of our life, like to take an airplane flight or to conduct a trip by car.

Structural reliability of a generic structure depends by several factors that can be considered data of probabilistic analysis. In this chapter, we will introduce structural reliability methods, starting to definition of limit state equation and concluding to explain various level methods. For a correct introduction to Safety Format field, it will be correct to introduce in this phase the reliability index and the reliability differentiation about structures with different importance, for which are accepted different failure probabilities.

1.1 Limit states

A limit state is a condition in which a structure, or a part of this, does no longer fulfil its performance requirements. Depending on these performance requirements, it is possible to define a specific limit state that can be more or less compromising and so it can be associated to high or low level of failure probability. We can distinguish ULS and SLS.

1.1.1 ULS – Ultimate Limit State

Ultimate Limit State is the most important because it is associated directly to safety of people contained in a structure. It refers obviously to structural collapses (also partial collapse) and it aims to define ultimate bearing capacity.

The following ULS can be considered:

- Loss of static equilibrium of the system or a part of it ;
- Fracture or great deformation in critical sections or particular connections;
- Fatigue and other phenomenon depending on time ;
- Collapse deriving from the formation of mechanism ;
- Instability phenomena or divergence of equilibrium of system (buckling, lateral buckling, aero-elastic instability) .

1.1.2 SLS – Serviceability Limit State

Serviceability Limit State refers to comfort of the users, visual aspects and generally to the performance of the structure during normal use. Its verification regards:

- Deformations that can compromise the functionality of the structure, penalizing visual aspect, comfort of users or various installations.
- Vibrations that clearly causes discomfort problems ;
- Damages such as cracks that have a negative effect on visual aspects but also on the durability of the structure.

Another differentiation can be made between irreversible SLS and reversible SLS. In case of reversible SLS the critical value is no longer crossed after removal of load. This differentiation permitted us to distinguish a permanent local damage such as a temporary deflection by a different problem of cracks in prestressed or simple reinforced concrete. In case of irreversible SLS, design criteria are similar to those for ULS. It can be quickly figured by the great sensitivity of prestressed concrete respect to the phenomenon of pitting, which makes the crack opening a structural damage. Alternative serviceability requirements can be expressed depending on the acceptability of crossing a limit value, their frequency and duration.

1.2 Limit state design and reliability methods

A generic limit state of a cross section or a particular construction element can be described by a limit state equation as:

$$g(X) = Z = 0$$

where X is a vector of n basic variables:

- Material properties
- Geometrical properties
- Actions and loads
- Model uncertainties.

For each basic variable it is possible to consider an appropriate probabilistic model to describe variable values and their changing. However, variables can be expressed with a deterministic approach in case of negligible variation in time or space.

Having defined the limit state function $g(X)$ like a function depending on probabilistic variables, it is possible to consider the function $g(X)$ like a random variable denoted Z . The function is defined so that $g(X) > 0$ corresponds to safe condition, and in reverse, $g(X) < 0$ to failure. Defining as $f_X(X)$ the n -dimensional probability density function relative to the n basic values, the failure probability P_f can be expressed as the integral of the pdf $f_X(X)$ calculated into the domain in

which the limit state function $g(X)$ is defined negative. It is good to note that explaining the integral domain in a certain way, this definition will allow to define the failure probability as a cumulative density function (see further). In analytical way, we can define P_f as:

$$P_f = \int_{g(X)<0} f_X(X) dX \quad (1.1)$$

The elaboration and the application of this definition may lead having different level of complexity and accuracy. It is easy to realize that, the main issue of the formula is given by the presence of more variables in the definition of the limit state function. That is why it is not sure to solve the aforementioned integral using analytical formulation or numerical integration. In order to explain better the concept of limit state function and the meaning of his integration, it is useful to note that if $n=2$, the result of failure probability integral is volume under the joint probability density function corresponding to the domain where $g(X) < 0$.

A simple example can be consider by midspan cross section of a simply supported isostatic beam, subject to distributed load. By a simple analysis, we can define a resisting bending moment M_R of the cross section and a bending moment M_E registered in midspan point, because of applied load. In this way the limit state function of the bending moment in midspan became:

$$g(X) = Z = M_R - M_E = 0$$

representing with R the resistance values and with E the load effects, the limit state equation becomes:

$$g(X) = Z = R - E = 0$$

It can be expressed in a (R,E) plain like a straight line that represent the boundary between survival domain $D_s(Z>0)$ and failure domain $D_f(Z<0)$.

So the failure probability integral of the 1.1, can be rewritten as:

$$P_f = \int_{D_f} f_{RE}(r, e) dr de = P [R - E < 0]$$

1.2.1 Level III method

The reliability method of III level corresponds to a simple and theoretical resolution of the integral (1.2), obtaining the failure probability P_f by analytical formulation, numerical integration or Monte Carlo simulations. As underlined before, the theoretical resolution can be countered by the number of basic variables, so by the complexity of the cases. In particular, we can relate to analytical formulation only when the case in question is simple. Most of the time, little complexities of the study require us to follow other resolution ways, for example numerical integration. Also in this case, it is right to remember that a numerical integration can be conducted only if there is a little number of basic variables. A most general resolution way is entrusted to Monte Carlo simulation, that remains a good accuracy method but has an high computational cost.

The clear aim of the analysis is to considered structure safe, calculating a failure probability P_f smaller than a predefined target value P_0 . The failure probability P_f and the reliability index β (see later) are conventional values that give a target of acceptable risk of the community, but if we want to be more precise, they do not correspond to a real failure frequencies because of some factors, like human errors that can sometimes be reason of collapse, are very difficult or impossible to take into account in a probabilistic analysis.

The values of P_f and β are however useful and valid, in order to calibrate partial factors for code and to compare several structural safety levels.

1.2.2 Level II methods

In case of level II method only the mean values of the basic variables and the moments of first and second order are used in most cases. The first simplification

is given by a linearization in the design point of the limit state function and an easier probability density function (*pdf*). As design point, it can be taken the point on $g(X) = 0$ with the highest probability density. It can be start to be clear the expression “first order approximation” for the limit state function and in particular the expression “FOSM = First Order Second Moment” which will be better investigated further.

As specified before, the reliability index β can be considered a measure of safety level of a structure: if we change its sign, it will correspond to the fractal of failure probability, respect to an appropriately standardized limit state function . So the reliability index β is directly related to failure probability thanks to the following relation, in which Φ represents the limit state function:

$$P_f = \Phi(-\beta)$$

The table 1.1 contains the numerical relation between β and P_f .

Table 1.1 - Relationship between P_f and β

P_f	10^{-1}	10^{-2}	10^{-3}	10^{-4}	10^{-5}	10^{-6}	10^{-7}
β	1,28	2,32	3,09	3,72	4,27	4,75	5,20

Explain P_s like the success probability, thanks to probability properties, it is possible to write:

$$\Phi(-\beta) = 1 - \Phi(\beta) \text{ and as a consequences: } P_s = \Phi(\beta).$$

1.2.3 Level I method

Going down with the levels, the aim, in order to solve the theoretical issue, becomes to simplify the calculation method; that is why we will introduce a level I that is a semi-probabilistic method. The variables taken into account with a probabilistic distribution, in this method, are represented by characteristic values calculated as a low percentile, in case of strength distributions, or a high percentile, in case of distribution related to actions.

It is important to underline that the partial factor using in this method is calculated with values that are based on above mentioned level II.

In EN 1990 we can find the basic verification format, that consists of to verify that the limit state is not exceeded when, in the limit state equation, all basic variables are replaced by so-called design values, designated by subscript “d”. In case of a simple limit state function (like mentioned before in the case of the bending moment in a simple supported beam), it is translated by an inequality in which the design Resistance R_d is at least equal to the design value of the load effect E_d . So :

$$E_d \leq R_d$$

where :

$$E_d = E(F_{d1}, F_{d2}, \dots, a_{d1}, a_{d2}, \dots, \theta_{d1}, \theta_{d2}, \dots) ;$$

$$R_d = E(X_{d1}, X_{d2}, \dots, a_{d1}, a_{d2}, \dots, \theta_{d1}, \theta_{d2}, \dots) ;$$

in which :

F is an action ;

X is a material property ;

a is a geometrical property ;

θ is a variable representing the model uncertainty .

1.2.4 Level 0 method

Increasing simplicity of treatment, we end up leaving the probabilistic approach and so we introduce the level 0, which is a deterministic method that use a nominal or deterministic value of the basic variables and just one empirical global safety factor that have to cover up all the uncertainties. Verification is performed according to an equation with the following format:

$$R_{nom} \geq \gamma \cdot E_{nom}$$

This is sufficient to understand that, a certain treatment is too easy to summarize such important subject as structural safety. So, the introduction of probability-based calculation methods was due to the observation that the deterministic

methods resulted in scattered safety levels and no coherent with the safety methodology that is available in case of new technology material.

1.3 Target values for reliability index

As explained before, reliability index and safety level are closely associated, that is why the choosing of a specific β value corresponds to choose the acceptable failure risk in the design phase. It is clear that, the bond to statistics leads to define a failure probability depending on time and, in particular, on the years of life of the structure that changes with its importance (i.e. 50 years for a structure such as our house, that we can considered standard construction, or 100 years for a more importance structure such as a bridge). The definition of structural importance is released by statistics and it takes to think to the structural failure consequences respect to the loss of human life but also respect to economic, social and environmental consequences. So the importance of the failure consequences allows to define a reliability differentiation related to Consequences Classes explained in table 2 (Annex B of EN 1990).

Table 1.2 - Definition of Consequences Classes

Consequence Classes	Description		Examples
	Consequences with respect to loss of human lives	Economic, social and environmental consequences	
CC3	High	Very Large	Tribunes, Public buildings with high consequences of failure (concert, hall,...)
CC2	Moderate	Considerable	Home and office buildings, public buildings with moderate consequences of failure (offices,...)

CC1	Low	Small or negligible	Agricultural building where people do not normally enter (depositories, greenhouses,...)
-----	-----	---------------------	--

The three consequences classes CC1, CC2 and CC3 are closely related to three reliability classes RC1, RC2 and RC3, respectively.

Annex C of EN 1990 indicates target values for β for reference period of 1 and 50 years, designed β_1 and β_2 respectively. In the following table, target value β for reliability class RC2 are indicated.

Table 1.3 - Target Value β for a Reliability Class RC2

Limit State	$t_{ref} = 1 \text{ year}$	$t_{ref} = 50 \text{ years}$
Ultimate Limit State	4,7	3,8
Serviciability Limit State	2,9	1,5

It is worthy to underline that in the framework of EN 1990 to EN 1999 the following assumption for the distribution type have been considered:

- Lognormal or Weibull distribution for material properties, strength and eventually model uncertainties ;
- Normal distribution for self-weight ;
- Extreme value distribution for variable actions (sometimes normal distribution like simplifications).

Moreover, when the uncertainty source are related to actions of which the yearly maxima are mutually independent, the following relationship can be used to convert β value in equivalent to different reference period:

$$\phi(\beta_n) = [\phi(\beta)]^n$$

With β_n the reliability index for $t_{ref} = n \text{ years}$ and β_1 the reliability index for $t_{ref} = 1 \text{ year}$.

Finally, minimum value β for ULS (Ultimate Limit State), recommended to EN 1990, are shown in the following table, divided for reliability class RC.

Table 1.4 - Recommended minimum values β (ULS)

Reliability Class	$t_{\text{ref}} = 1 \text{ year}$	$t_{\text{ref}} = 50 \text{ years}$
RC1	5,2	4,3
RC2	4,7	3,8
RC3	4,2	3,3

2 Safety Formats for non-linear analysis

Non-linear analysis can be seen as a powerful and precise calculation method to estimate load capacity of civil structure. It is clear that, according to *fib* Model Code 2010 approach, such analysis is related to high level of approximation, in which, with elevate computational cost, the aim is to find a more realistic collapse load, thanks to better model description of mechanical material properties. It is worthy to underline that, a new proposed approach of Levels of Approximation, can be related to accuracy, simplifications and computational cost, regarding to singular non-linear analysis. Non-linear analysis uses realistic constitutive law of materials and it is based on concepts of equilibrium and compatibility of deformations. A more detailed model so represented an appropriate material behavior, material geometry and other general structural parameters. In the classic design phase, several limits, like calculation time or the lack of structural resistance distribution, do not allow to evaluate analyses with an high level of approximation and usually designer engineer deals with mean values of material parameters. So, the aim of a Safety Format for non-linear analysis is to determinate actual structural behavior by means of a simple formula, able to find the most probable structural resistance, starting from mean values of parameters.

Starting by low level of approximation, verification of structures is considered as local because of it is conducted on section level. According to Eurocode [1] structure can be verified thanks to following inequality:

$$E_d \leq R_d \quad (2.1)$$

in which E_d is the design value of the effects of actions and R_d the corresponding resistance. According to EN 1992-1-1 [2] the design value E_d can be calculated by the designer engineer by means of :

- Linear elastic analysis ;
- Linear elastic analysis with limited redistribution ;

Performing non-linear analysis on generic concrete structure, in order to calculate design value of effects actions E_d , it has been verified that the use of a design value in the analysis, leads to an overestimation of the structure deformability and so an incorrect assessment of the load bearing capacity, e.g. an unrealistic redistribution of internal actions occurs in case of beams and slender columns. By comparison with experimental test, it is emerged that the actual structural resistance can be better evaluated with a non-linear analysis that uses mean values of material properties. In this way we are so arrived to a discrepancy related to Eq. (2.1), given by the fact that E_d is evaluated with mean values, in order to respect a better distribution of internal actions, while R_d is estimated with the design values, respecting semi-probabilistic approach. As previously mentioned, *SFs* have been proposed to solve this discrepancy with a methodology that calculates structural resistance with mean values of material resistances.

2.1 Type of uncertainties

The words “most probable resistance” start to give an idea of uncertainty related to structural constructions. Several simulations of a civil structure and its materials can not exist without uncertainties that, obviously, depend on the singular contexts and applications. Therefore, it is impossible to create a classification of uncertainty, with the aim to analyze them and so find an analytical solution able to give a value at the actual structural resistance. However, civil engineering recognizes two types of uncertainties: aleatory and epistemic.

Aleatory derives from latin “alea” that means the rolling of dice. It is clear that the word aims to consider all the randomness of a scientific phenomenon. In the structure field, it is possible to identify a great number of intrinsic randomness of variables related to structure, such as the measurement of a physical quantity (e.g. concrete strength measure).

The word epistemic derives from Greek “episteme” which means knowledge. Epistemic uncertainty points out the lack of knowledge in the definition of the structural model, that so becomes inexact or incomplete also because of it accepts simplifications. A practical instance of epistemic uncertainty can be given by the assumption of an hinge as connection model between two structural element: during the construction phase , it is not sure that the connection will work as a hinge; however this simplification is accepted in order to speed up the computation.

2.1.1 Model Uncertainties

In the previous chapter, the calculation model of SLU function has been presented depending on relevant variables X_i as follows:

$$R = f(X_1, X_2, X_3, \dots, X_n)$$

In case of X_i are supposed exact and the model $f(\dots)$ is complete and exact, the outcome R can be evaluated without any error or particular simplifications. But it has already been explained that, this is not an ordinary situation because of difficulties or impossibilities to define an accurate value to represent variables X_i . The previous exposition of different probabilistic levels methods, is finalized to arrive to a simple level method in which, lack of knowledge and model simplification are accepted. In a more accurate analysis, it becomes important to define model uncertainties and a methodology for their qualification and treatment in practical applications. The difference between model prediction and real outcome can be expressed as follows:

$$R = f'(X_1, X_2, X_3, \dots, X_n; \theta_1, \theta_2, \theta_3, \dots, \theta_n)$$

Where θ_i are variables which comprise model uncertainty and are treated as random variables. Their statistical properties can be evaluated from experiments and observations.

Generally, model uncertainty can be obtained by a simple comparison between model results and outcomes of a physical tests. Fig 2.1 shows a general concept for the assessment of model uncertainties. All parameters that affect tests, model

results and real structure behavior depend on both structural members and failure mode.

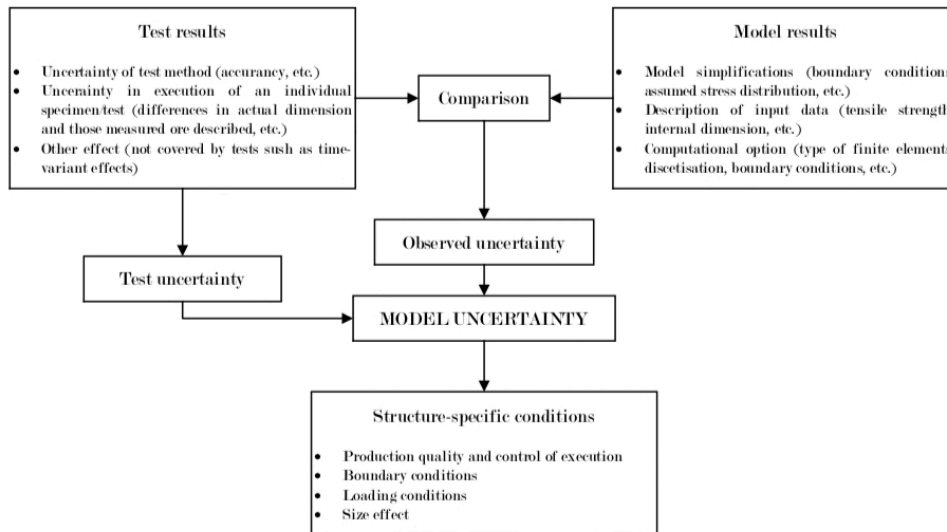


Figure 1 - General concept of the assessment of model uncertainties [Milan Holicky et al.]

- Test results: test methods based on general experience and calibration accuracy.
- Model results: the choose of a particular FEM model, all the uncertainties related to input data and all the possible simplifications.
- Structural conditions: it leads to investigate the differences between real structure and tests under ideal conditions.

In *SF* field, model uncertainties are generally summarized with γ_{Rd} . It is worthy to underline that the evaluation of γ_{Rd} is not topic of this thesis. Thanks to its independent from other uncertainty coefficient, from here on, γ_{Rd} is assumed equal to 1 in the all next calculation parts [see later].

2.2 Safety Formats for non-linear analysis

The *fib Model Code 2010* proposes a design condition associated to higher level of approximation, in which verification of structure does not considers resistance

at section level, as explained in Eq.(2.1) , but it aims to take into consideration global actual behavior of structure and progressive redistribution of internal forces of RC structures. (A more detailed exploitation about different fields of the Levels of Approximations is reported further).

Regarding Safety Format in *fib MC2010*, a new global inequality can be written in the domain of actions :

$$F_d \leq R_d \quad (2.2)$$

where F_d is the design value of actions and R_d is the design resistance, that can be estimated by means of two methods that start to differentiate the Safety Formats:

- PM. Probabilistic Method ;
- GRMs. Global Resistance Methods :
 - GRF Global Resistance Factor
 - ECOV Estimation of the Coefficient of Variation
 - SMVM Simplified Mean Value Method
 - PSF Partial Safety Factor
 - SHLUNE METHOD
 - GSF Global Safety Format

2.2.1 Introduction of global safety factor γ_G

The first generalized safety format for non-linear analysis was proposed in 1995 [8] and it is based on the idea that in a structures, only sensitivity of the overall structural behavior has to be investigated. It is also assumed that structural variable (e.g. material properties) are associated to aleatory distribution function (it will see that the log-normal distribution is considered as the better for material properties distribution function) .

The global safety factor γ_G was introduced like a coefficient related to the overall structural resistance, in order to cover uncertainties of material which mechanical property values are represented by means of statistics distribution function. By a first approach, γ_G is defined after the definition of distribution function of structural resistance, as the ratio between the mean value R_m and the design value R_d :

$$\gamma_G = \frac{R_m}{R_d} \approx \exp(\alpha_R \beta V_R) \quad (2.3)$$

where R_m is the mean resistance that corresponds to the outcome of NLFEA, performed with the mean values of the material properties, while R_d is the design value defined thanks to a probabilistic relationship of EuroCode [1] :

$$R_d = R_m \exp(-\alpha_R \beta V_R)$$

where :

- β is the reliability index ;
- α_R is the FORM (First Order Reliability Method) resistance sensitivity factor ;
- V_R is the coefficient of variation related to the resistance distribution .

The values $\beta = 3,8$ and $\alpha = 0,8$ are used for an expected structural life of fifty years. The coefficient of variation V_R can be obtained by Monte Carlo simulation .

The just described definition of global coefficient factor can be exploit thanks to previous definition of statistical distribution function of structural resistance, that in general is taken as log-normal thanks to a number of favorite study cases on material properties; but it is worthy to underline that the hypothesis of log-normal distribution may not be verified because of both log-normal distribution and global resistant factor depend on the analyzed structure and on the failure mode. It is so possible to underline that the global resistance factor may not be unique.

2.2.2 Probabilistic Method PM

The Probabilistic Method descends from calculation of several non-linear analysis with different parameters in order to create a distribution of structural resistance R that can be different from log-normal one. The number of NLFEAs to execute, require sampling techniques like Latin Hypercube, to optimize the input data, and Monte Carlo simulation. After obtaining R distribution, the design value R_d of global structural resistance is expressed in function of a specific reliability index with Eq. :

$$R_d = \frac{R^{-1}[\phi(-\alpha_R\beta)]}{\gamma_{Rd}}$$

where :

- R is the structural resistance predicted by NLFEA ,
- α_R is the resistance sensitivity factor ,
- β is the reliability index thanks to is possible to directly assess the design value of the global structural resistance ,
- γ_{Rd} is the model uncertainty factor

E.g. in the common case of ULS, with moderate consequences of failure and a reference period of 50 years, the aforementioned values can be considered [1]:

- $\gamma_{Rd} = 1,06$
- $\alpha_R = 0,8$
- $\beta = 3,8$

Admitting the two-parameters log-normal distribution as the better for concrete resistance, the previous eq. can be rewritten as:

$$R_d = \frac{\mu_R[\exp(\alpha_R\beta V_R)]}{\gamma_{Rd}} \quad (2.4)$$

Where μ_R and V_R are the mean value and the coefficient of variation of the distribution of global resistance described by the model. At this point, it is clear the need of Monte Carlo simulation in order to estimate the just mentioned distribution parameters. Therefore, PM requires two models; the first is a non-linear finite element model which represents the structure response; the second is a probabilistic model for the uncertainty of the model parameters as mechanical and geometrical material properties, boundary conditions or other effects. Finally, it is interesting to note that at numerator of Eq. (2.4) we can recognize the global safety factor γ_G described in (2.3). A new formal representation will be presented in the next paragraph, in order to introduce the other *SFs*.

2.3 Global Resistance Methods GRMs

The previous presentation of several SFs in *fib* Model Code 2010 puts *GRF*, *ECOV* and *PFM* under the voice *Global Resistance Methods*. The idea to define all *SFs* as global method, is justified by the theoretical formula (Eq. 2.5) that can summarize the calculation procedures, in which the design structural resistance is evaluated dividing the global resistance, obtained through NLFEA, by global safety factors γ_R and γ_{Rd} .

$$R_d = \frac{R(f_{rep})}{\gamma_R \gamma_{Rd}} \quad (2.5)$$

in which:

- R is the global resistance, result of non-linear analysis ;
- f_{rep} represents the generical material parameters that are input of the non-linear analysis ; their values depend on several Safety Formats and are different for each one ;
- γ_R is the uncertainty material coefficient, different for each SF.
- γ_{Rd} is the uncertainty model coefficient, different for each SF.

2.3.1 Global Resistance Factor GRF

The Global Resistance Factor uses the aforementioned global safety factor γ_G as unique uncertainty value which proposed value is $\gamma_G = 1,27$. It can be considered as a product of material properties uncertainties and model uncertainties :

$$\gamma_G = \gamma_R \cdot \gamma_{Rd}$$

According to [15] , for the uncertainty material factor γ_R is proposed a value of 1,20 ; like consequence, the estimation of uncertainty model coefficient γ_{Rd} has to take a value of 1,06 in order to obtain a global coefficient of 1,27 :

$$\gamma_G = \gamma_R \cdot \gamma_{Rd} = 1,20 \cdot 1,06 = 1,27 \quad (2.6)$$

As regarding global structural resistance obtained by means of NLFEA, the *GRF* requires as analysis inputs the following representative material parameters:

- f_{ym} for steel ;
- f_{cmd} for concrete ;

where f_{ym} is the mean yield stress, calculated in function of f_{yk} (characteristic yield stress) as:

$$f_{ym} = 1,1 f_{yk} \quad (2.7)$$

and f_{cmd} is a reduced resistance value for the compressive concrete strength, able to take into account the difference of material property uncertainties between concrete and steel. Remembering that, according to Euro Code, the partial safety coefficients related to concrete and steel are respectively $\gamma_c = 1,5$ and $\gamma_s = 1,15$, the f_{cmd} definition is similarly to (2.7) :

$$f_{cmd} = 1,1 f_{ck} \frac{\gamma_s}{\gamma_c} = 1,1 f_{ck} \frac{1,15}{1,5} = 0,85 f_{ck} \quad (2.8)$$

Finally the (2.5) can be rewritten for *GRF* as :

$$R_d = \frac{R(f_{cmd}, f_{ym})}{\gamma_R \gamma_{Rd}} \quad (2.9)$$

with:

- $\gamma_R = 1,20$
- $\gamma_{Rd} = 1,06$

2.3.2 Estimation of Coefficient of Variation *ECOV*

The global structural resistance R requires by *ECOV* is calculated with a NLFEA using the mean material parameters f_{cm}, f_{ym} both for concrete and steel. The particularity of this method is easy to understand thanks to its name. The global resistance factor γ_R is calculated in function of the coefficient of variation V_R of global structural resistance R distribution (Eq. 2.10). It is so important to underline

the necessity to define this distribution that, for hypothesis, can be taken as a two-parameters log-normal distribution. The hypothesis is justified by the good approximation that log-normal distribution has to describe the material properties as random variables. So, in linear analysis field, the two log-normal hypothesis related to the global resistance and the material property are redundant, but with non-linear analysis, the global structural distribution can obviously be different to material parameters distribution; this difference is as big as the analysis tending to non-linearity. That is why we can conclude that the *ECOV* approximation is closely related to the non-linearity magnitude of problem case. The aim of *ECOV* is represented by Eq. (2.10), valid in the hypothesis that the resistance follows a log-normal distribution :

$$V_R = \frac{1}{1,65} \ln \frac{R_m}{R_k} \quad (2.10)$$

in which R_m and R_k are the results of global resistance obtained with two NLFEMs using respectively mean values and characteristic values of material properties.

Thanks also to the aforementioned reliability index β and resistance sensitivity factor α_R , the global resistance factor γ_R can be calculated as:

$$\gamma_R = \exp(\alpha_R \beta V_R) \quad (2.11)$$

Finally the (2.5) can be rewritten for *ECOV* as :

$$R_d = \frac{R(f_{cm}, f_{ym})}{\gamma_R \gamma_{Rd}} \quad (2.12)$$

with:

γ_R expressed by (2.11) and $\gamma_{Rd} = 1,15$ [37].

2.3.3 Simplified Mean Value Method *SMVM*

The simplified mean value method *SMVM* takes by *ECOV* the same idea to estimation of coefficient of variation, but in a more simple way. As expressed in

Eq (2.13), the *SMVM* puts a coefficient of variation V_R equal to 1,15 , without to consider the distribution type of global resistance.

$$V_R = 0,15 \quad (2.13)$$

At this point the global resistance factor γ_R can be calculated by means of (2.11).

As regarding the value of global structural resistance R presented in (2.5), it has be calculated through NLFEA performing with the mean material parameters f_{cm}, f_{ym} both for concrete and still. It can be considered an other similarly with *ECOV* method.

Finally the (2.5) can be rewritten for *SMVM* as :

$$R_d = \frac{R(f_{cm}, f_{ym})}{\gamma_R \gamma_{Rd}} \quad (2.12)$$

with:

γ_R expressed by (2.11), using $V_R = 0,15$ (2.13) and $\gamma_{Rd} = 1,15$ [37].

2.3.4 Partial Factor Method *PFM*

Partial Factor Method is the most simple method in theoretical line. It advises just a single NLA with extremely low material parameters i.e. design parameters, without to take into account any type of distribution function regarding parameters or structural resistance.

It is clear that using low values of resistance material, the non-linear analysis will return an underestimation of global structural resistance R (related to PM global structural resistance which has been considered the most reliable value at the start of this study).

In addition to resistance underestimation, another deficit of *PFM* can be considered reliability of analysis results, performed with design values. As explained into introduction regarding Eq. (2.1), the use of design parameters generates an erroneous assessment of global resistance, also connecting to failure mode

problems. So in non-linear field, actual bearing capacity can be better calculated by means of means material parameters, that is why PFM is recommended only in case of absence of more refined solution.

In order to reconduct to the form of Eq.(2.5), the PFM can be summarized as:

$$R_d = \frac{R(f_{cd}, f_{yd})}{\gamma_R \gamma_{Rd}} \quad (2.13)$$

in which γ_R is considered as unit coefficient, and $\gamma_{Rd} = 1,15$ [37].

2.3.5 Schlune method

After the *fib* Model Code 2010, two new methodology were formulated. The first was proposed in 2011 by Schlune et al. [5]. The second was published in 2013 by Allaix et al. [11].

The great innovation brought by Schlune method in *fib* MC2010 is the possibility to estimate global structural reliability taking into account not only of bending moment and normal force, but also of issues related to shear failure. The formulation is a little different respect to the other *SFs*, but as any of them, Schlune method considers for the material resistance, the log-normal distribution function, that permits to uses similar equations of other *SFs*. The classical formal equation implies a NLFEA performed with mean value properties and can be rewritten as:

$$R_d = \frac{R(f_{cm, is}, f_{ym}, a_{nom})}{\gamma_R} \quad (2.14)$$

in which :

- $f_{cm, is}$ is the mean in situ concrete compressive strength ;
- f_{ym} is the mean yield strength of steel reinforcement ;
- a_{nom} is the nominal value of geometrical parameters ;
- γ_R is a single global safety coefficient, described below.

At this point, the aforementioned hypothesis of log-normal distribution for material resistance material permits to define γ_R as :

$$\gamma_R = \frac{\exp(\alpha_R \beta V_R)}{\vartheta_m} \quad (2.15)$$

The new factor ϑ_m takes into account the model uncertainties and it is defined as the mean ratio between the experimental and predicted resistances. His value can space between 0,7 and 1,2 and it depends on failure mode. While the coefficient of variation V_R takes into consideration uncertainties related to geometry, model and material. It is calculated as:

$$V_R = \sqrt{V_g^2 + V_m^2 + V_f^2} \quad (2.16)$$

where V_g , V_m and V_f are the coefficients of variation respectively of geometrical, model and material uncertainties. The material coefficient can be estimate as :

$$V_f \approx \frac{\sqrt{\left(\frac{R_m - R_{\Delta f_c}}{\Delta f_c}\right)^2 \sigma_{f_c}^2 + \left(\frac{R_m - R_{\Delta f_y}}{\Delta f_y}\right)^2 \sigma_{f_y}^2}}{R_m} \quad (2.17)$$

where :

- σ_{f_c} is the standard deviation of concrete compressive strength and σ_{f_y} is the standard deviation related on yield stress of the steel ;
- Δf_c , Δf_y are the finite variations of the material resistance ;
- $R_{\Delta f_c}$, $R_{\Delta f_y}$ are the resistance results of non-linear analysis performed with the values $(f_{cm} - \Delta f_c)$ for the concrete compressive strength and $(f_{ym} - \Delta f_y)$ for the yield stress.

It is so clear that this method needs the performance of three NLFAs: one using mean values of material properties, and the others using respectively $(f_{cm} - \Delta f_c)$ for concrete and $(f_{ym} - \Delta f_y)$ for still.

2.3.6 Global Safety Format *GSF*

The new Format introduced by Allaix et al. [11] , as Schlune method, takes into consideration nominal values of geometrical dimensions a_{nom} and considers log-normal distribution to describe material behavior. It is important to notice that the *GSF* requires the assumption of log-normal distribution only for material resistances; any distribution assumption is done for the global structural resistance R (see later).

The usual SF formulation can be rewritten as :

$$R_d = \frac{R(f_{cm}, f_{ym}, a_{nom})}{\gamma_R \gamma_{Rd}} \quad (2.18)$$

You immediately notice that the global structural resistance R , output of just one NLFEA, requires mean values of material properties both for concrete and for steel and the nominal values of geometrical dimensions a_{nom} .

The global resistance factor γ_R is derived by the same formulation introduced for *ECOV*, Eq.(2.11) :

$$\gamma_R = \exp(\alpha_R \beta V_R)$$

The difference is that *GSF* does not accept an estimation of the coefficient of variation V_R after assumed log-normal distribution also for global resistance R , but requires a more precise calculation of V_R using a probabilistic simulation by means of Monte Carlo simulation. Basically, a Monte Carlo simulation requires a high number of non-linear analysis performed with different random values of material resistances. The use of this simulation technique creates, of course, an high computational and temporary cost, but permits to obtain results closer to Probabilistic Method. Moreover, Monte Carlo performance returns an actually distribution of global structural resistance R , that no longer needs to be estimated as log-normal.

The model uncertainty factor γ_{Rd} wants to consider the difference between real and numerical model behavior of the structure. That is why, it is predominantly evaluated by means of a comparison between experimental tests and numerical

calculations, but also through probabilistic considerations. If the distribution of resistance model uncertainty ϑ_R is given, γ_{Rd} can be calculated as :

$$\gamma_{Rd} = \frac{1}{\exp(-\tilde{\alpha}_R \beta V_{\theta R})} = \exp(\tilde{\alpha}_R \beta V_{\theta R})$$

Where $\tilde{\alpha}_R = 0,4\alpha_R$ is the sensitivity factor for the resistance model uncertainty and $V_{\theta R}$ is the coefficient of variation of the resistance model uncertainty ϑ_R . However, by simplifying, γ_{Rd} can be taken equal to 1,15 as previous *SFs* [37].

3 Theory and design for instability

3.1 Introduction to non-linear field

Theory of elastic line defines the problem of elastic beam by means of static and kinematic equations, which are related in order to calculate internal actions and so stress field. In the practicality of design area, stress domain allows to designer engineer to establish the structural local resistance, without give particular importance to strain domain and so to global stress-strain behavior related to the structure. At the base of elastic theory, the static equations, which define equilibrium, are constructed after kinematic equations, in the undeformed configuration. Such formulation is possible thanks to the hypothesis of little displacement, characteristic of linear elastic field. In other words, in linear field, the elastic displacements are little enough to mistake undeformed and deformed configuration. However, this simplification can not be considered valid in particular cases in which, geometrical parameters play a particular role on global level and do not allow to obtain linearity of global stress-strain relationship (it can be noticed also in external load – displacement graphic). The non-linearity of this process, encourages to analyze static equilibrium starting from undeformed configuration: it will lead to the distinction of stable, unstable and indifferent equilibrium and it could have important consequences on the global structural resistance.

The entry in the non-linear field for the material properties, starts to counter hypothesis of little displacements and so it does not enable to neglected the undeformed configuration. Anyway, the writing of static equation that rules problem, could not be influenced by non-linearity of the geometric parameters. To this purpose,

figure 3.1 reports two different cases of load applied at the same column, with an elastic constrain at the base. In the first case, we have only the presence of a transversal concentrated load (P_t), which requires the columns works like a cantilever; in the second case we see also the presence of a second concentrated force (P), acting as a peak load.

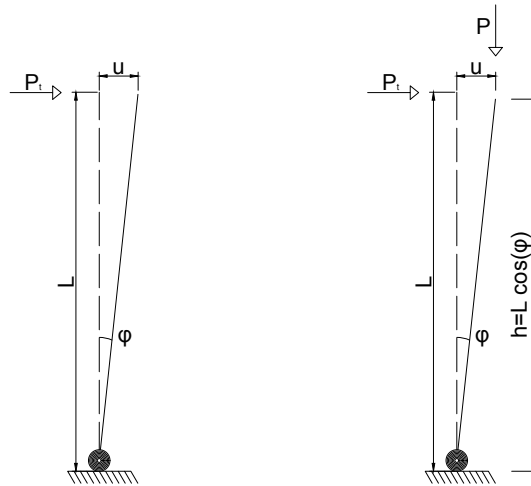


Figure 3.1 - Load cases with different nature

The static equations of the similar systems of the figure 3.1, are following :

$$P_t \cdot L \cdot \cos(\varphi) = W \cdot \varphi \quad (3.1)$$

$$P_t \cdot L \cdot \cos(\varphi) + P \cdot L \cdot \sin(\varphi) = W \cdot \varphi \quad (3.2)$$

Both equations obtained by equilibrium show a non-linear relationship, even though the supposition of a linear elastic behavior of the restraint. At this point, the hypothesis of low displacement values, allows to rewrite :

$$\cos(\varphi) \cong 1 \quad (3.3)$$

$$\sin(\varphi) \cong \varphi \quad (3.4)$$

And the Eq. (3.1) and (3.2) can be rewritten in linear form, related to undeformed situation :

$$P_t \cdot L = W \cdot \varphi \quad (3.5)$$

$$P_t \cdot L + P \cdot L \cdot \varphi = W \cdot \varphi \quad (3.6)$$

When the peak load P is present (2nd case) could not be legitimate to write static equilibrium in the undeformed configuration, even if the values of the displacements remain little. The hypothesis of negligible displacements is not only related to their entity but also to nature of the load condition. In these particular cases, the stability loss becomes an important element for the global resistance; in the cantilever case, it can be read as a rapid increase of displacement as result of a little growth of load value. The figure 3.2 shows the differences between the two load line of the two previous case. It presents the trend of the transversal concentrated load P_t in function of the rotation at the base φ . In the second case, the value of the peak load P is taken equal to P_t .

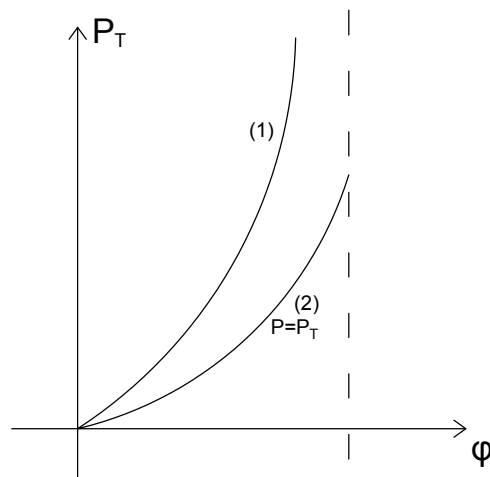


Figure 3.2 - Load lines

The dotted line is related to the case of presence of the peak load and it diverges from linear trend. His anomalous behavior represents the loss of equilibrium stability. So, the previous graphic shows two structural global behavior that can be considered representative of the plastic failure and the buckling failure of the columns cases under exam. The load line shape can give an idea about the global resistance and so about the failure mode which characterizes the single column case. More detailed graphics, products of failure mode analysis, are reported in Appendix B .

The differentiation between plastic collapse and buckling failure is closely related to mechanical and geometrical parameters. Structural failures caused by material failure is typical for shorten columns and is given by the achieving ultimate material resistance. Concrete crushing or steel yielding allows to the structure to benefit from all material resistance, independently by structural geometry and size. On the contrary, structural failure caused by buckling is typical for structures having high slenderness values. For slender structures, some loads, having particular entity or particular nature, force the structure to an instability domain in which material properties play an less important role, for the benefit of geometrical properties. In fact, when the failure instability occurs, the materials do not reach their strength limits.

3.2 Buckling hardening branching

This form of instability is typical of our column cases. It occurs in axially loaded elastic element such as column and it is characterized by a rapid change of configuration: the unbuckled and buckled states are very near, but buckling structural deformation is completely different by structural deformation in pre-buckling state. The figure 3.3 shows an hinge supported beam loaded with an axial force N . Its stability loss can be described by graphic which express the axial concentrated load N in function of deflection u (figure 3.4) .

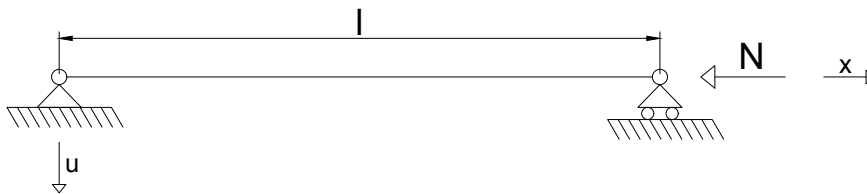


Figure 3.3 - Simply supported beam with axial load

It is clear that the deflection u is a dual deformation respect to second order bending. In the undeformed configuration, u will destined to remain equal to zero,

while analyzing the deformed shape, it enables to define different equilibrium states: stable, unstable and neutral.

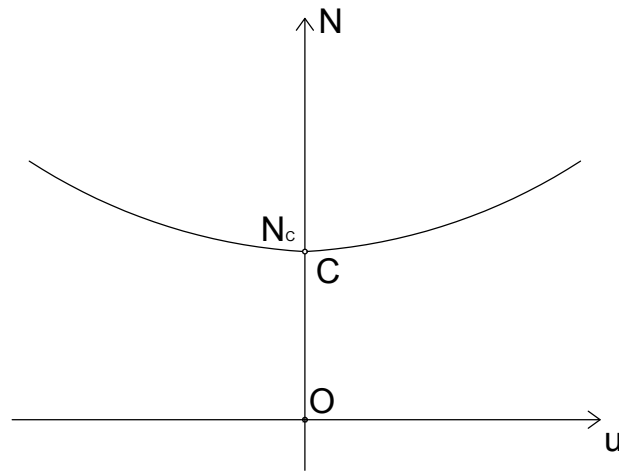


Figure 3.4 - Buckling hardening branching

Loading the beam with the increasing concentric force N , we do not have any deflection until achieving the critical load N_c . So the segment OC can represent stable equilibrium: in this phase the external load N takes on values that can be considered too low to compromise the equilibrium stability. In the point C , the axial load arrives to critical value N_c ($N=N_c$): from here, equilibrium stability is undermined. The system can be still considered in equilibrium, but this kind of equilibrium is unstable.

Theoretically, after the achievement of N_c ($N>N_c$), it is possible to continue along the N axis, without any deflection, until to arrive to maximum plastic value of axial load, given by the material strength and calculated on the cross section. In reality, the overcoming of critical value N_c and so the entry in the instability equilibrium state, makes equilibrium precarious; which means that a little equilibrium perturbation, such as an imposed deformation or a simple geometrical inaccuracy, is enough to diverge equilibrium and so to lead to collapse.

This particular phenomenon is analytically justified by existence of two stable and symmetric branches, starting to the point C , that give origin to a bifurcation of two symmetric ways in which equilibrium persists and lives in presence of deflection. The branches are obtained by resolution of a transcendent equilibrium equation

and they give a different equilibrium solution respect to the obvious configuration of pure compression in which $u=0$.

As explained before, the loss of equilibrium stability determines a fast increase of deformation in compliance with a little growth of axial load. It is clear that, the two buckling branches lead to a fast achievement of strain limit, that causes buckling failure, without going as far as exploiting the strength material limit.

With regard to buckling branches trend, it is interesting to underline that the present case of simply supported beam, leads to define a rigid-hardening buckling behavior, characterized by an associated growth of force and deformation that allows to define a stable behavior. Such behavior can be distinguished respect to other cases of rigid-softening buckling branch, in which, after the achievement of critic load, the displacements start to increase in compliance with a decrease of force value. Such rigid-softening behavior is defined unstable and it can be analyzed by potential stationarity study. For a better deepening about hardening and softening branches, please refer to [33] *Carpinteri A. -Scienza delle Costruzioni 2, Pitagora, Bologna, 1992.*

3.3 Critical load for axially loaded columns

In the previous paragraph, references was made about a critical load N_c that marks border line between stable and unstable equilibrium. It is well known that slender structures suffer from instability loss: for them critical load of course represents strength limit that, if exceeded, leads to failure.

The columns under exam in this study are only loaded with an axial force, rather than concentrated bending moment (there are only two case in which the axial force is constant and collapse takes place because of an increase transversal concentrated load). That is why, in first place, it was decided to report the theoretical example of simple supported beam loaded whit concentric load (static scheme was previously reported in *Fig.3.3*) which allows to define Euler's equation. It was also reported problem related to inelastic material behavior, which we consider characteristic of non-linear analysis and hence near to constitutive laws in exam.

3.3.1 Instability of linear elastic columns

The *Figure 3.3* shows a simply supported beam loaded with a concentrically axial force. It is inserted in a reference system, marked by x coordinate, with origin in hinge. If secondary order effects are taken into account, the axial force N causes a bending moments which can not be found until the deflections are determined. The column is therefore statically indeterminate, and it is necessary to solve the differential equation for the deflection curve of the column. The section rigidity EI is constant along the column. As the secondary effects are taken into account, the moment equilibrium gives as follow :

$$M - N \cdot u = 0 \quad (3.1)$$

where u is the displacement along the transversal direction of the column axis. The bending moment (M) is determined by the well-know formula:

$$M = -EI \frac{d^2u}{dx^2} \quad (3.2)$$

which inserted in the Eq. (3.1) gives the following differential equation:

$$EI \frac{d^2u}{dx^2} + N \cdot u = 0 \quad (3.3)$$

This is an ordinary homogeneous second order differential equation, which can be solved using the following boundary conditions:

$$u(x = 0) = 0 \quad u(x = l) = 0 \quad (3.4)$$

It can be introduced the factor α as follows:

$$\alpha^2 = \frac{N}{EI} \quad (3.5)$$

The *Eq.(3.3)* can be rewritten as:

$$\frac{d^2u}{dx^2} + \alpha^2 \cdot u = 0 \quad (3.6)$$

The complete solution of Eq. (3.6) is:

$$u = A\cos(\alpha x) + B\sin(\alpha x) \quad (3.7)$$

The two constants A and B are determinate from the boundary conditions (discarding the trivial solution A=B=0) and as a result, the solution of Eq. (3.7) is given by:

$$\sin(\alpha l) = 0 \rightarrow \alpha l = \pi + n\pi \quad (n = 0,1,2, \dots) \quad (3.8)$$

The axial loads N obtained through this solution are the eigenvalues and the corresponding solutions u(x) are eigenfunctions. The eigenfunctions give the information about the column deformed shape, but the deformed magnitude can not be determinate. When n = 0, $\alpha l = \pi$, which gives the first and lowest value of N, which corresponds to the Euler's equation:

$$N_{cr} = \frac{\pi^2 EI}{l^2} \quad (3.9)$$

The corresponding eigenfunction u(x) matches to curve with n=0 inflection point. It is shows in Fig. 3.5. It is clear that when n=0 we have just one concavity of the deflection curve.

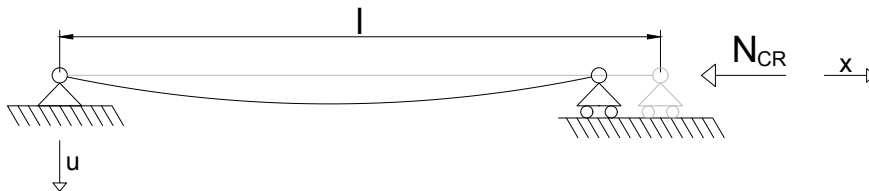


Figure 3.5 - Eigenfunction $u(x)$ with $n=0$

The Euler's equation (3.9) can be used to define the critical buckling stress:

$$\sigma_{cr} = \frac{N}{A} = \frac{\pi^2 EI}{A l^2} = \frac{\pi^2 E \rho^2}{l^2} \quad (3.10)$$

Introducing the slenderness factor λ , defined as the ratio of the length of the column over the radius of gyration of the transversal section, the Eq. (3.10) can be rewritten as:

$$\sigma_{cr} = \frac{\pi^2 E}{\lambda^2} \quad (3.11)$$

This equation means that when the material characteristics are fixed, the strength critical value (σ_c) depends only by λ . Moreover, it shows that the critical buckling stress (that can be seen as the load-carrying capacity) goes to infinity when $l \rightarrow 0$. By this equation, it is possible to define a theoretical failure condition, represented by Euler hyperbola. It is clear that this condition can not be physically possible and the materials have a well known limited strength, which Euler's equation must deal with. That is why the real failure condition can be represented by strength curve with a cut off at the corresponding material strength σ_p (see Fig. 3.6).

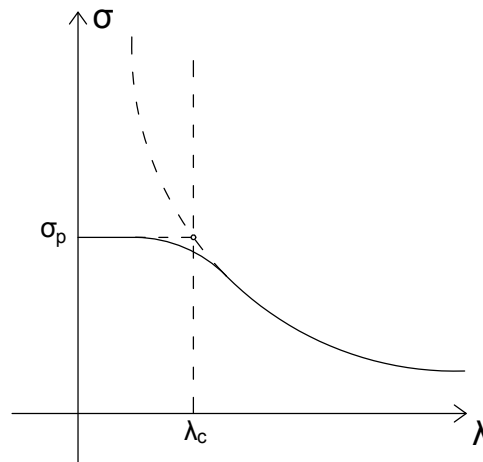


Figure 3.6 - Euler's hyperbola

Therefore, for slender columns, critical stress is usually lower than the compressive strength. As contrary, a stocky column has a critical buckling stress higher than the compressive strength, which means that the element reaches the material capacity. The blue curve in Fig. 3.6 identifies an interaction between the two types

of failures which have the aim to represent the actual strength behavior. If there was no interaction, a critic slenderness λ_c could be identified as:

$$\lambda_c = \pi \sqrt{\frac{E}{\sigma_p}} \quad (3.12)$$

The expression σ_p wants to identify strength limit which is related to plastic failure.

3.3.2 Instability of inelastic columns

Structural problems related to instability can occur when applied loads generate stress beyond the elastic limits. In this case, the structure behavior depends on two non-linearities: the rigidity decrease due to the compression force and the deformability increase of the material due to stress beyond the linear limits.

Engesser's method

Engesser's method is based on the Euler's equation, with a modification of the modulus of elasticity. He introduces the tangent modulus of the stress-strain relationship at the current stress level. Therefore, the corresponding inclination is used as elastic modulus (E_σ) of the material (see Fig. 3.7). Hence, the critical stress can be calculated as:

$$\sigma_{cr} = \frac{N_{cr}}{A_c} = \frac{\pi^2 E_\sigma}{\left(\frac{l}{i}\right)^2} \quad (3.13)$$

For a reinforced concrete column, it possible to consider a parabolic stress-strain behaviour of the concrete. The tangent modulus is determined as:

$$E_\sigma = E_0 \sqrt{1 - \frac{\sigma}{\sigma_p}} \quad (3.14)$$

where σ_p must be taken equal to f_c for concrete. Eq.(2.14) can be inserted into Eq. (2.13) to derive the critical stress (σ_{cr}).

As this column is reinforced, the influence of the steel can be taken into account as a contribution calculated on the basis of the critical stress assumed for the concrete.

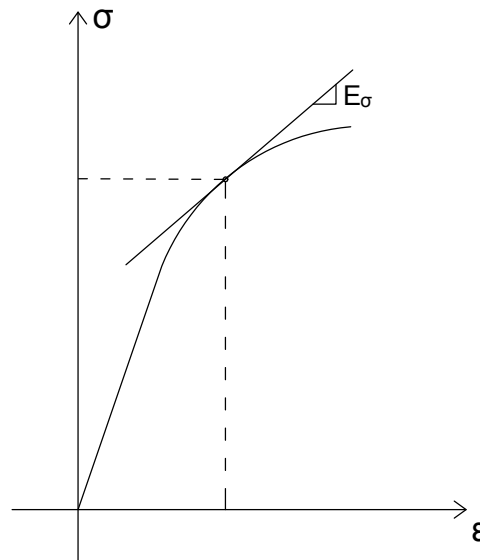


Figure 3.7 - Stress-strain curve typical for concrete

Thus, the critical load (N_{cr}) for the column can be calculated as:

$$N_{cr} = \sigma_{cr}bh + \sigma_s A_s \quad (3.15)$$

However, this simplification returns a σ_{cr} value that is underestimated since the stiffness of the reinforced column is higher than the stiffness of the unreinforced column.

Ritter's method

Ritter took the Engesser's method introducing a simplification. His theory determined the stiffness-stress relation of concrete as follows:

$$E_\sigma = E_0 \left(1 - \frac{\sigma}{\sigma_p} \right) \quad (3.16)$$

which leads a difference between the stiffness corresponding to a parabolic law (calculated with Engesser's method) and the Ritter stiffness (see Eq. (3.16)). Substituting the Eq. (2.16) into Eq. (2.13) leads to:

$$\sigma_{cr,Ritter} = \frac{\sigma_c}{1 + \frac{\sigma_c}{\pi^2 E_{c0}} \left(\frac{l}{i}\right)^2} \quad (3.17)$$

4 Experimental database for RC columns

4.1 Bibliography references

In this chapter are presented all informations regarding experimental tests performed on slender columns , which data have been taken from literature. The presentation is divided for bibliography references. The columns have different geometrical and mechanical properties; the only common factor is related to the shape of them section: They always have rectangular or square section.

1. Kim, J.K. and Yang, J. K. 1993 [16]

In this investigation, 30 tests on simply supported columns were reported. Two of the columns failed at the ends and are therefore disregarded from the list. The investigation contained three different levels of compressive strength (low, medium and high). For the purposes of the analysis, just 8 columns, with a low compressive strength, were considered. Furthermore, two different reinforced ratios were tested, 1.98% and 3.95%. Columns characterized by a reinforced ratio of 3.95% present reinforcement placed at the center of the cross-section. The data are reported in the appendix, section A.1.

2. Mehmel, A., Schwarz, H.,Kasperek, K. H. and Makovi, J. 1969 [17]

This investigation contained 16 tests. Fourteen of these present the same eccentricity in both ends and two have different eccentricities at the ends. For this

reason, those two columns, were disregarded. Three different types of reinforcement were used and the cross-section had three different sizes. The data are reported in the appendix, section A.2.

3. Drysdale, R. G. and Huggins, M. W. 1971 [18]

This investigation contained 58 tests, but just 4 columns were considered because those tests are characterized by short term loading to failure and eccentricity along principal axes of inertia. Those columns were characterized by a square cross-section and a reinforcement ratio of 3.14%. The data are reported in the appendix, section A.3.

4. Khalil, N., Cusens, A. R. and Parker M. D. 2001 [19]

In this investigation 20 columns were tests. Just 11 columns are considered because they are characterized by a short-term load. The considered columns have a constant width of 152mm. The slenderness and the reinforcement ratio were varied. The data are reported in the appendix, section A.4.

5. Saenz, L. P. and Martin, I. 1963 [20]

This test campaign were performed at the University of Havana with 52 rectangular section concrete columns. Reinforcement ratio and slenderness were varied. Columns were restrained at the ends, but the authors declared that there were no certainty that absolute fixedness was developed. The data are reported in the appendix, section A.5.

6. Foster, S. J. and Attard, M. M. 1997 [21]

In this investigation, the data related to 68 eccentrically loaded conventional and high-strength concrete columns were reported. Just 26 conventional concrete

columns were considered. The columns were 150 x 150 mm at the mid-section and two different percentage of steel reinforcement ratio were used. The data are reported in the appendix, section A.6.

7. Pancholi, V. R. 1977 [22]

The tests were performed on 38 columns and those included creep investigations. Hence, just 29 columns were considered. Those elements were characterized by a high slenderness ratio, two different dimensions of square cross-section and two different reinforcement ratios. The load were applied at the centre of gravity of the section, then no eccentricity were considered. The data are reported in the appendix, section A.7.

8. Dracos, A. 1982 [23]

This paper included short and long term studies, hence, just 36 columns were considered. Slenderness, cross-section, reinforcement ratio and eccentricity were varied. All columns were simply supported. The data are presented in the appendix, section A.8.

9. Iwai, S., Minami, K. and Wakabayashi, M. 1986 [24]

A total of 396 column with rectangular cross sections, including square sections, were testes. The ratio of column length to minimum depth ranged from 6 to 26. Loads were applied monotonically at each column end with equal eccentricities at various angles from an axis of symmetry. For this reason just 11 columns were considered. The data are reported in the appendix, section A.9.

10. Chuang, P. H. and Kong, F. K. 1997 [25]

In this investigation, 26 eccentrically loaded simply supported columns were tested. Normal strength concrete as well as high strength concrete was used, then, just 20 columns were considered. The concrete cross-section had two different sizes and three types of reinforcement and reinforcement ratio were used. The data are reported in the appendix, section A.10.

11. Barrera, A. C., Bonet, J. L., Romero, M. L. and Miguel, P. F. 2011 [26]

In this experimental program, 44 rectangular columns with different sections were executed. The length of the columns are 3 m for all the specimens and these were subjected first to a constant axial load and later to a monotonic lateral force up to failure. These specimens symbolize two semi-columns connected by a central element, which represents the stiffener effect of an intermediate floor or the connection between a column and the foundation, represented by a stub element. Normal strength concrete as well as high strength concrete was used, then, just 23 columns were considered. The data are reported in the appendix, section A.11.

12. Baumann, O. 1935 [27]

The experimental investigation made by Baumann was subdivided into two sections, a pilot series and a main series. Both series consider both axially and eccentrically loaded columns. The pilot series consists of 12 tests and the main series of 31 tests. The columns in the pilot series and in the first 15 tests of the main series were simply supported. In the remaining data of the main series, the end conditions were changed, and, consequently all these columns were disregarded. The cross-section was varied in many of the tests . The data are presented in the appendix, section A.12.

Fig. 4.1 shows column types, with end supports and applied loads. It is important to underline that also A, B and C column types are taken in consideration in the

non-linear model calculation. Type A columns have theoretical null eccentricity, that in the model has been taken equal to 0,5mm , in order to represent a little value of geometrical eccentricity and also to give a direction input to columns deflections. Type B columns have a first order eccentricity e_1 , that was also considered in the model; while, for type C columns anyone eccentricity value was considered in the model because of its different load models (see chapter 5).

All columns were verified for Euro Code requirements which ensure safety, serviceability and durability. They are explained in the following paragraph.

In Tab. 4.1 the number and the type of tests made by each investigator is presented.

4.2 EC2 Columns requirements

The following requirements are taken by [2]. This requirements deal with columns for which the larger dimension b is not greater than 4 times the smaller dimension h .

Longitudinal reinforcement

- Longitudinal bars shall have a diameter of not less than φ_{\min} . The recommended value is 8 mm.
- The total amount of longitudinal reinforcement shall not be less than $A_{s,\min}$. The recommended value is $0.002A_c$.
- The area of longitudinal reinforcement shall not exceed $A_{s, \max}$. The recommended value is $0.04A_c$.

A minimum areas of reinforcement are given in order to prevent a brittle failure, wide cracks and also to resist forces arising from restrained actions.

Transverse reinforcement

- The transverse reinforcement shall be anchored adequately.
- The diameter of the transverse reinforcement shall not be less than 6 mm or one quarter of the maximum diameter of the longitudinal bars, whichever is the greater.
- The spacing of the transverse reinforcement along the column shall at maximum of $s_{cl,tmax}$. The recommended value is the least of the following three distances:
 - 20 times the minimum diameter of the longitudinal bars;
 - the lesser dimension of the column;
 - 400 mm.
- Every longitudinal bar placed in a corner shall be held by transverse reinforcement. No bar within a compression zone shall be greater than 150 mm from a restrained bar.

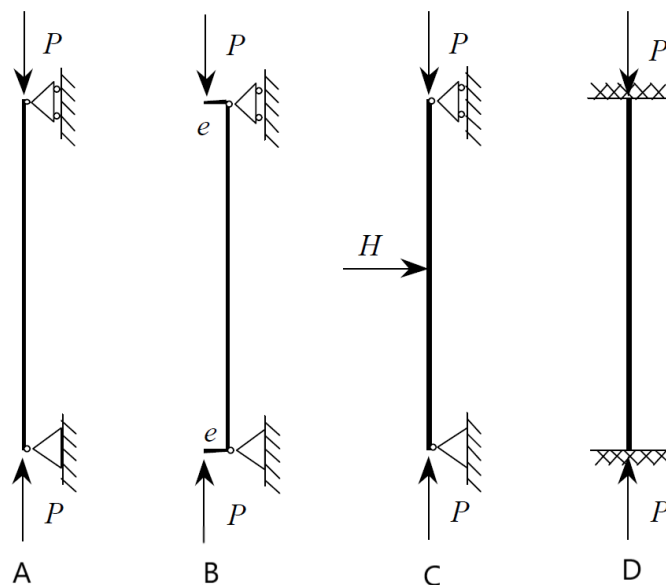


Figure 4.1 - Column types

Table 4.1 – Complete database of columns

Referen ces	Investigators	Year	Number of tests	Type of tests
[16]	Kim, J.K. and Yang, J. K.	1993	8	B
[17]	Mehmel, A., Schwarz, H.,Kasperek, K. H. and Makovi, J.	1969	14	B
[18]	Drysdale, R. G. and Huggins, M. W.	1971	4	B
[19]	Khalil, N., Cusens, A. R. and Parker M.D.	2001	11	B
[20]	Saenz, L. P. and Martin, I.	1963	52	D
[21]	Foster, S. J. and Attard, M. M.	1997	23	B
[22]	Pancholi, V. R.	1977	29	A
[23]	Dracos, A.	1982	36	A
[24]	Iwai, S., Minami, K. and Wakabayashi, M.	1986	11	4 A and 7B
[25]	Chuang, P. H. and Kong, F. K.	1997	20	B
[26]	Barrera, A. C., Bonet, J. L., Romero, M. L. and Miguel, P. F.	2011	23	C
[27]	Baumann, O.	1935	27	14 A and 13 B

The geometrical properties of the 40 investigated columns are explained in following tables (*Tab. 4.2 - 4.3 - 4.4 - 4.5*). The informations are also given for material mechanical properties and about literature bearing collapse, which represents the actual collapse load obtained by experimental tests.

Table 4.2 - Geometrical properties of investigated columns - pt.1

n°	Reference	Test n°	l_{tot} [mm]	L [mm]	l/h [-]	λ [-]
1	[21]	2L20-30	1450	650	10	33
2	[21]	2L20-60	1450	650	10	33
3	[24]	C000	680	600	6	20
4	[21]	2L8-120R	1450	650	10	33
5	[24]	C020	680	600	6	20
6	[21]	4L8-30	1450	650	10	33
7	[21]	4L20-120	1450	650	10	33
8	[21]	4L8-120R	1450	650	10	33
9	[27]	III	3210	3000	23	79
10	[24]	B020	1880	1800	16	54
11	[26]	N30-10.5-C0-3-30	3300	2940	24	82
12	[27]	3.3	3400	2700	21	74
13	[25]	A-17-0.25	3400	2800	17	59
14	[17]	5.1	3400	2700	22	75
15	[26]	H60-10.5-C0-1-30	3300	2940	24	82
16	[27]	Va	3240	3000	23	80
17	[27]	I	3210	3000	32	111
18	[20]	24D-2	2697	2697	30	104
19	[25]	C-31.7-0.25	3800	3260	32	110
20	[24]	RL300	3000	2920	25	87
21	[27]	2	3230	3010	26	90
22	[17]	4.1	4500	3800	30	104
23	[27]	8	3230	3010	26	89
24	[27]	VI	3000	3000	33	113
25	[20]	15E -2	3597	3597	40	139
26	[23]	S28	5000	5000	48	167
27	[27]	9	6510	6310	40	139
28	[23]	S30	5000	5000	48	167
29	[27]	12	6510	6310	40	139
30	[27]	6	6510	6310	41	141
31	[27]	15	6510	6310	40	140
32	[27]	3	6510	6310	41	141
33	[23]	S25	6000	6000	58	200
34	[22]	17A	4940	4940	65	225
35	[22]	5	6004	6004	60	208
36	[22]	6	6004	6004	60	208
37	[22]	8	6004	6004	79	274
38	[22]	20	5327	5327	70	243
39	[22]	18	5327	5327	70	243
40	[22]	7	6004	6004	79	274

Table 4.3 - Geometrical properties of investigated columns - pt.2

n°	Reference	Test n°	b [mm]	h [mm]	d _b [mm]	d' _b [mm]	d _h [mm]	d' _h [mm]
1	[21]	2L20-30	150	150	127,7	22,4	127,7	22,4
2	[21]	2L20-60	150	150	125,7	24,4	125,7	24,4
3	[24]	C000	120	120	100,0	20,0	100,0	20,0
4	[21]	2L8-120R	150	150	122,7	27,4	122,7	27,4
5	[24]	C020	120	120	100,0	20,0	100,0	20,0
6	[21]	4L8-30	150	150	122,7	27,4	122,7	27,4
7	[21]	4L20-120	150	150	124,7	25,4	124,7	25,4
8	[21]	4L8-120R	150	150	127,7	22,4	127,7	22,4
9	[27]	III	140	140	126,0	14,0	126,0	14,0
10	[24]	B020	120	120	100,0	20,0	100,0	20,0
11	[26]	N30-10.5-C0- 3-30	140	150	120,0	20,0	130,0	20,0
12	[27]	3.3	254	159	134,0	25,0	134,0	25,0
13	[25]	A-17-0.25	300	200	280,0	20,0	180,0	20,0
14	[17]	5.1	253	158	128,0	30,0	128,0	30,0
15	[26]	H60-10.5-C0- 1-30	140	150	120,0	20,0	130,0	20,0
16	[27]	Va	178	140	164,0	14,0	126,0	14,0
17	[27]	I	200	100	190,0	10,0	90,0	10,0
18	[20]	24D-2	127	90	74,0	15,9	74,0	15,9
19	[25]	C-31.7-0.25	200	120	180,0	20,0	100,0	20,0
20	[24]	RL300	120	180	100,0	20,0	160,0	20,0
21	[27]	2	250	125	237,5	12,5	112,5	12,5
22	[17]	4.1	253	150	125,0	25,0	125,0	25,0
23	[27]	8	250	126	237,4	12,6	113,4	12,6
24	[27]	VI	198	98	188,2	9,8	88,2	9,8
25	[20]	15E -2	127	90	74,0	15,9	74,0	15,9
26	[23]	S28	104	104	76,0	28,0	82,0	22,0
27	[27]	9	250	162	233,8	16,2	145,8	16,2
28	[23]	S30	104	104	76,0	28,0	82,0	22,0
29	[27]	12	250	162	233,8	16,2	145,8	16,2
30	[27]	6	250	160	234,0	16,0	144,0	16,0
31	[27]	15	247	161	230,9	16,1	144,9	16,1
32	[27]	3	250	160	234,0	16,0	144,0	16,0
33	[23]	S25	104	104	76,0	28,0	82,0	22,0
34	[22]	17A	76	76	58,5	17,5	58,5	17,5
35	[22]	5	100	100	74,0	26,0	74,0	26,0
36	[22]	6	100	100	74,0	26,0	74,0	26,0
37	[22]	8	76	76	58,5	17,5	58,5	17,5
38	[22]	20	76	76	58,5	17,5	58,5	17,5
39	[22]	18	76	76	58,5	17,5	58,5	17,5
40	[22]	7	76	76	58,5	17,5	58,5	17,5

Table 4.4 - Mechanical properties of investigated columns – longitudinal reinforce

n°	Reference	Test n°	100p [-]	A _s [mm ²]	φ _s [mm]	n° _{tot} [-]	n° _b [-]	n° _h [-]
1	[21]	2L20-30	2,044	459,96	12,10	4	2	2
2	[21]	2L20-60	2,044	459,96	12,10	4	2	2
3	[24]	C000	3,963	570,645	9,53	8	3	3
4	[21]	2L8-120R	2,044	459,96	12,10	4	2	2
5	[24]	C020	3,963	570,64	9,53	8	3	3
6	[21]	4L8-30	4,089	919,92	12,10	8	3	3
7	[21]	4L20-120	4,09	919,92	12,10	8	3	3
8	[21]	4L8-120R	4,089	919,92	12,10	8	3	3
9	[27]	III	1,600	314,00	10,00	4	2	2
10	[24]	B020	3,963	570,64	9,53	8	3	3
11	[26]	N30-10.5-C0- 3-30	3,231	678,58	12,00	6	2	3
12	[27]	3.3	1,100	452,39	12,00	4	2	2
13	[25]	A-17-0.25	3,270	1962,00	24,99	4	2	2
14	[17]	5.1	3,100	1256,64	20,00	4	2	2
15	[26]	H60-10.5-C0- 1-30	1,436	301,59	8,00	6	2	3
16	[27]	Va	2,500	615,00	14,00	4	2	2
17	[27]	I	1,600	314,00	10,00	4	2	2
18	[20]	24D-2	2,500	285,48	9,53	4	2	2
19	[25]	C-31.7-0.25	3,350	804,00	16,00	4	2	2
20	[24]	RL300	2,642	570,64	9,53	8	3	3
21	[27]	2	0,600	201,00	8,00	4	2	2
22	[17]	4.1	1,200	452,39	12,00	4	2	2
23	[27]	8	0,600	201,00	8,00	4	2	2
24	[27]	VI	1,600	314,00	10,00	4	2	2
25	[20]	15E -2	2,500	285,48	9,53	4	2	2
26	[23]	S28	4,183	452,39	12,00	4	2	2
27	[27]	9	0,800	314,00	10,00	4	2	2
28	[23]	S30	4,183	452,39	12,00	4	2	2
29	[27]	12	0,800	314,00	10,00	4	2	2
30	[27]	6	0,800	314,00	10,00	4	2	2
31	[27]	15	0,800	314,00	10,00	4	2	2
32	[27]	3	0,800	314,00	10,00	4	2	2
33	[23]	S25	4,183	452,39	12,00	4	2	2
34	[22]	17A	5,439	314,16	10,00	4	2	2
35	[22]	5	4,524	452,39	12,00	4	2	2
36	[22]	6	4,524	452,39	12,00	4	2	2
37	[22]	8	5,439	314,16	10,00	4	2	2
38	[22]	20	5,439	314,16	10,00	4	2	2
39	[22]	18	5,439	314,16	10,00	4	2	2
40	[22]	7	5,439	314,16	10,00	4	2	2

Table 4.5 - Mechanical properties of investigated columns – transversal reinforce

n°	Reference	Test n°	A _{sw} [mm ²]	Φ _{st} [mm]	n° _{staffe/m} [1/mm]	S [mm]
1	[21]	2L20-30	31,20	6,30	33,33	30,0
2	[21]	2L20-60	31,20	6,30	16,67	60,0
3	[24]	C000	15,90	4,50	16,67	60,00
4	[21]	2L8-120R	31,20	6,30	8,33	120,0
5	[24]	C020	15,90	4,50	16,67	60,0
6	[21]	4L8-30	31,20	6,30	33,33	30,0
7	[21]	4L20-120	31,20	6,30	8,33	120
8	[21]	4L8-120R	31,20	6,30	8,33	120,0
9	[27]	III	*	*	*	*
10	[24]	B020	15,90	4,50	16,67	60,0
11	[26]	N30-10.5-C0-3-30	28,27	6,00	10,00	100,0
12	[27]	3.3	28,27	6,00	8,33	120,0
13	[25]	A-17-0.25	78,54	10,00	6,67	150,0
14	[17]	5.1	28,27	6,00	6,25	160,0
15	[26]	H60-10.5-C0-1-30	28,27	6,00	10,00	100,0
16	[27]	Va	*	*	*	*
17	[27]	I	*	*	*	*
18	[20]	24D-2	7,31	3,05	10,99	91,0
19	[25]	C-31.7-0.25	28,27	6,00	6,67	150,0
20	[24]	RL300	15,90	4,50	16,67	60,0
21	[27]	2	*	*	*	*
22	[17]	4.1	28,27	6,00	7,14	140,0
23	[27]	8	*	*	*	*
24	[27]	VI	*	*	*	*
25	[20]	15E -2	7,31	3,05	10,99	91,0
26	[23]	S28	8,30	3,25	10,00	100,0
27	[27]	9	*	*	*	*
28	[23]	S30	8,30	3,25	10,00	100,0
29	[27]	12	*	*	*	*
30	[27]	6	*	*	*	*
31	[27]	15	*	*	*	*
32	[27]	3	*	*	*	*
33	[23]	S25	8,30	3,25	10,00	100,0
34	[22]	17A	8,30	3,25	13,16	76,0
35	[22]	5	8,30	3,25	10,00	100,0
36	[22]	6	8,30	3,25	10,00	100,0
37	[22]	8	8,30	3,25	13,16	76,0
38	[22]	20	8,30	3,25	13,16	76,0
39	[22]	18	8,30	3,25	13,16	76,0
40	[22]	7	8,30	3,25	13,16	76,0

Table 4.6 - Mechanical properties of investigated columns – Starting eccentricity – Bearing capacity

n°	Reference	Test n°	f_c [MPa]	f_y [MPa]	f_u [MPa]	e_0/h [-]	Type	N_{exp} [KN]
1	[21]	2L20-30	40,00	480,00	-	0,133	B	750,00
2	[21]	2L20-60	43,00	480,00	-	0,133	B	700,00
3	[24]	C000	27,0	347,16	516,81	-	A	559,58
4	[21]	2L8-120R	56,00	480,00	-	0,053	B	1092,00
5	[24]	C020	26,97	347,16	516,81	0,200	B	327,32
6	[21]	4L8-30	43,00	480,00	-	0,053	B	1100,00
7	[21]	4L20-120	40,00	480,00	-	0,133	B	900,00
8	[21]	4L8-120R	56,00	480,00	-	0,053	B	1247,00
9	[27]	III	16,08	294,20	-	-	A	343,23
10	[24]	B020	27,56	355,00	507,00	0,200	B	271,46
11	[26]	N30-10.5-C0- 3-30	29,50	538,00	645,00	-	C	280,00
12	[27]	3.3	35,30	509,90	-	0,082	B	782,57
13	[25]	A-17-0.25	38,20	493,00	-	0,250	B	1181,44
14	[17]	5.1	40,60	426,80	-	0,165	B	735,50
15	[26]	H60-10.5-C0-1-30	58,50	531,00	668,00	-	C	412,00
16	[27]	Va	26,38	281,84	-	-	A	684,50
17	[27]	I	15,20	294,20	-	-	A	264,78
18	[20]	24D-2	20,82	247,52	-	-	A	198,39
19	[25]	C-31.7-0.25	44,40	520,00	-	0,250	B	333,38
20	[24]	RL300	30,99	360,88	507,98	0,167	B	474,32
21	[27]	2	33,54	304,01	-	-	A	696,27
22	[17]	4.1	40,50	509,90	-	0,163	B	367,75
23	[27]	8	20,40	304,01	-	0,200	B	235,36
24	[27]	VI	24,91	294,20	-	-	A	392,27
25	[20]	15E -2	20,06	247,52	-	-	A	161,03
26	[23]	S28	24,43	304,00	-	0,144	B	44,00
27	[27]	9	24,52	294,20	-	0,200	B	205,94
28	[23]	S30	25,66	300,00	-	0,144	B	48,00
29	[27]	12	29,71	294,20	-	0,300	B	112,78
30	[27]	6	32,17	294,20	-	0,200	B	225,55
31	[27]	15	33,05	294,20	-	-	A	549,17
32	[27]	3	33,54	294,20	-	-	A	666,85
33	[23]	S25	24,72	282,00	-	0,144	B	36,00
34	[22]	17A	25,75	300,42	-	-	A	31,88
35	[22]	5	33,05	278,45	-	-	A	72,74
36	[22]	6	35,61	278,45	-	-	A	72,24
37	[22]	8	36,49	300,42	-	-	A	31,88
38	[22]	20	38,07	300,42	-	-	A	37,86
39	[22]	18	38,20	300,42	-	-	A	33,88
40	[22]	7	39,29	300,42	-	-	A	29,89

5 Structural model for reinforced concrete columns

The analysis conducted on several structures provides the creation of a structural model which can be explained describing how software works, structural restrains, external forces and started eccentricity. Moreover, it is important to focus on material mechanical behavior that gives an easy opportunity to underline non-linear factors and how they affect concretely the study.

In the classical linear SLU approach, anyone concrete tension resistance is taken into consideration and concrete compression behavior is simplified by classic Sargin parabola, followed by plastic plateau. Differently from classical linear SLU approach, in these study cases, a little bi-linear contribution of concrete in tension and a more important contribution of the concrete compression strength given by transversal bars contribution were considered. It will arrive to describe a material constitutive law totally different to classical parabola-rectangular; this takes origin by Ravzi-Saatcioglu model.

5.1 Material behavior

5.1.1 Compressive concrete behavior

The Ravzi-Saatcioglu model is assumed for stress-strain relationship of concrete in compression and is featured by different behavior between unconfined and confined concrete. The unconfined concrete strength just takes into account the

standard cylinder test result f_{cm} . The peculiarity of the model is represented by the confined concrete strength, called f_{ccm} , which takes into account triaxial state of stress generated by reaction of transversal reinforcement. It is possible to note that a longitudinal compression applied on a concrete cube generates not only a longitudinal compression strain but also a transversal tension strain depending on Poisson's coefficient that describes the relation between two axial strains for different materials. In the actual case of reinforced concrete columns, the transversal tension strains are prevented by transversal bars. This mechanism does not allow to concrete to expand in lateral direction and also causes a lateral pressure in the concrete which increases its strength according to:

$$f_{t2} = f_{u2} + k'_1 \cdot f_{t1} \quad (5.1)$$

where k'_1 is a function of the Poisson's coefficient (ν) and f_{t1} , f_{t2} and f_{u2} are stresses under triaxial and uniaxial stress conditions, acting in direction 1 (transversal) and 2 (longitudinal).

With best approximation, it is possible to define k'_1 as:

$$k'_1 = \frac{1 - \nu}{\nu} \quad (5.2)$$

The previous equations (5.1) and (5.2) are valid with linear elastic and isotropic material. In non-linear material case, Poisson's ratio varies with load and moreover the stress strain characteristics and Poisson's ratio can change in all three orthogonal directions.

However, in the case of non-linear elastic concrete, the previous Eq.(5.1) can be rewritten in terms of uniaxial strength and lateral confinement pressure:

$$f'_{cc} = f'_c + k_1 \cdot f_1 \quad (5.3)$$

where f'_{cc} and f'_c are respectively the confined and unconfined concrete strength and f_1 corresponds to the lateral confinement pressure, that depends on the diameter of the stirrups and their spacing. While the k_1 factor is not the same as k'_1 but it continues to preserve an indirect dependence on Poisson's ratio. Thanks to experimental data, it can be directly correlated to the lateral confinement pressure f_1 , which entity depends on Poisson's coefficient. To this purpose,

experimental tests permit to define a decreasing addition of k_1 respect to f_1 , according to:

$$k_1 \cong 6,7 \cdot (f_1)^{-0,17} \quad (5.4)$$

The fig.(5.1) is very important to capture the non-neglectable difference between compressive strength of confined concrete and unconfined concrete. It is reported to generic data and it has not the role to underline entity of strength increase buy only change of the shape in the constitutive law.

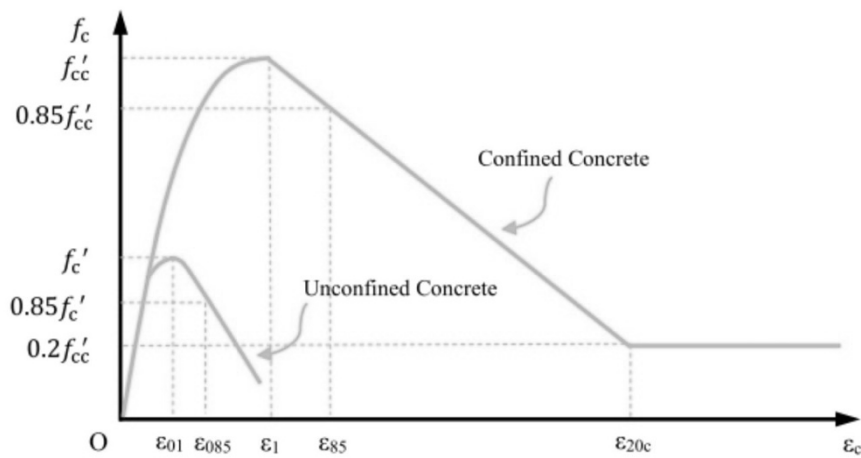


Figure 5.1 - Confined and unconfined compressive constitutive law

The Eq.(5.3) explains the relation between unconfined and confined concrete strength, while strain value in correspondence of strength peak of confined concrete ε_{c1} is given by :

$$\varepsilon_{c1} = \varepsilon_{c01} \cdot (1 + 5k) \quad (5.5)$$

where ε_{c01} is the strain corresponding to peak stress of unconfined concrete; it depends on f'_c as reported in Euro Code (see later). The k coefficient takes its value by the scale value of k_1 :

$$k = \frac{f_1}{f'_c} \cdot k_1 \quad (5.6)$$

The parameters related to unconfined concrete are the classical concrete parameters known from EC2. They are reported below with the same nomenclature used in Euro Code, which identifies concrete strength with its mean value f_{cm} ; in the previous graphic f_{cm} must be considered the value of the peak concrete stress.

Table 5.1 - Unconfined concrete parameters

Young's Modulus	$E_{cm} = 22 \left[\frac{f_{cm}}{10} \right]^{0,3}$
Compressive strain at the peak stress	$\varepsilon_{c01}(\text{‰}) = 0,7(f_{cm})^{0,31} < 2,8$
Compressive strain at 0,85 % of f_{cm}	$\begin{cases} \varepsilon_{c0.85} = 3,5 & f_{cm} \leq 58 \text{ MPa} \\ \varepsilon_{c0.85} = 2,8 + 27 \left[\frac{98 - f_{cm}}{100} \right]^4 & f_{cm} > 58 \text{ MPa} \end{cases}$

The concrete constitutive laws can finally be described as :

$$\sigma_c = \begin{cases} f'_c \cdot \left[2 \frac{\varepsilon}{\varepsilon_{c01}} - \left(\frac{\varepsilon}{\varepsilon_{c01}} \right)^2 \right] & \leq 0,2 \cdot f_c & \text{per } \varepsilon < \varepsilon_{c01} \\ f'_c \cdot \left[1 - 0,15 \cdot \left(\frac{\varepsilon - \varepsilon_{c01}}{\varepsilon_{c0.85} - \varepsilon_{c01}} \right) \right] & \leq 0,2 \cdot f_c & \text{per } \varepsilon > \varepsilon_{c01} \end{cases} \quad (5.7)$$

$$\sigma_{cc} = \begin{cases} f'_{cc} \cdot \left[2 \frac{\varepsilon}{\varepsilon_{c1}} - \left(\frac{\varepsilon}{\varepsilon_{c1}} \right)^2 \right]^{\frac{1}{1+2k}} & \leq 0,2 \cdot f_c & \text{per } \varepsilon < \varepsilon_{c1} \\ f'_{cc} \cdot \left[1 - 0,15 \cdot \left(\frac{\varepsilon - \varepsilon_{c1}}{\varepsilon_{c85} - \varepsilon_{c1}} \right) \right] & \leq 0,2 \cdot f_c & \text{per } \varepsilon > \varepsilon_{c1} \end{cases} \quad (5.8)$$

5.1.2 Tensile concrete behavior

Resistance model of concrete takes into account the tension strength contribution in order to achieve a more accurate results. Stress-strain tension curve is

considered with a bilinear law (fig.5.2). The two laws are divided by stress peak f_{ctm} .

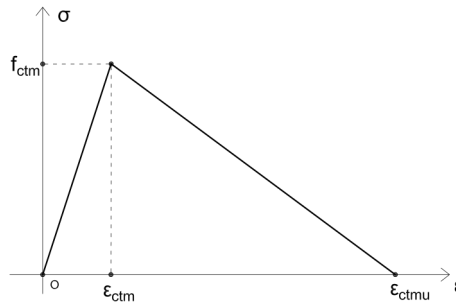


Figure 5.2 - Concrete tensile behavior

The value of concrete tensile strength suggested by EC2 [2] is :

$$f_{ctm} = \begin{cases} 0,30 \cdot (f_{cm} - 8[MPa])^{2/3} & f_{cm} \leq 58 MPa \\ 2,12 \cdot \ln\left(1 + \left(\frac{f_{cm}}{10}\right)\right) & f_{cm} > 58 MPa \end{cases} \quad (5.9)$$

While after the peak value, softening branch is linear and can be graphically described by its negative slope :

$$SLOPE = \frac{f_{ctm}}{\epsilon_{ctmu} - \epsilon_{ctm}} = \frac{f_{ctm}}{\epsilon_{ctm} \left(\frac{\epsilon_{ctmu}}{\epsilon_{ctm}} - 1\right)} \quad (5.10)$$

The ratio $\frac{\epsilon_{ctmu}}{\epsilon_{ctm}}$ depends on concrete compressive strength f_{cm} . It can be described by following graphic. However, concrete tensile behavior has been calibrated in each software, starting from first attempt, with the aim to best fit experimental results.

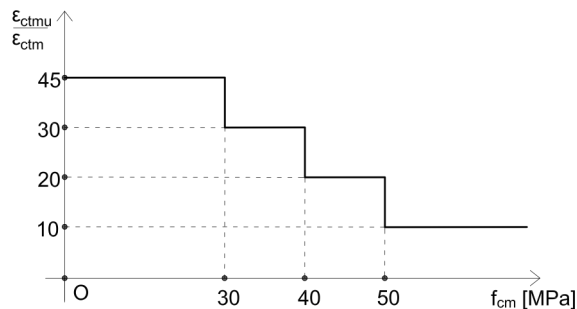


Figure 5.3 – Tensile softening slope

5.1.3 Reinforcement behavior

Also a simple model approach provides the same behavior for steel reinforcement in both compressive and tensile case; it can be graphically observed with a symmetry respect to origin in Fig.(5.4). The behavior is a simple bi-linear which wants to distinguish the first elastic field, characterized by a slope described by Young's Modulus E_s , taken always equal to 210.000 MPa, and a second plastic field that wants to simplified hardening behavior with a little leaning linear line. The two fields are divided by yield parameters of stress and strain. The value of f_{ym} is taken by the database, while when the ultimate tension still strength f_u is not declared by the authors, it is supposed as :

$$f_u = 1,03 \cdot f_{ym} \quad (5.11)$$

The value of f_u is supposed to correspond at a strain value of 70%.

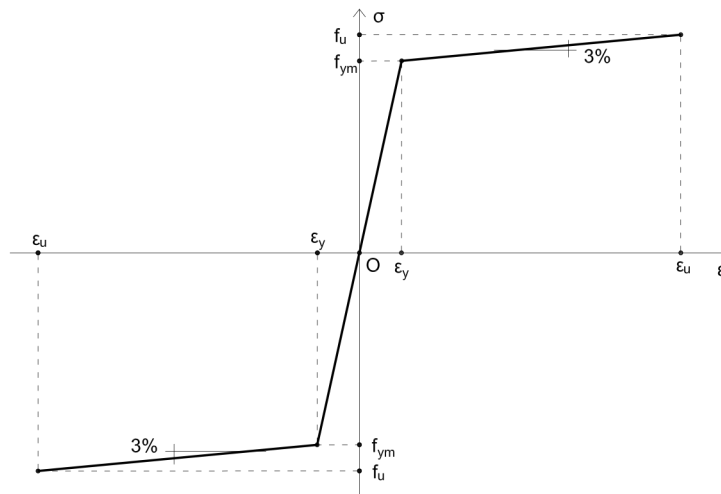


Figure 5.4 - Steel reinforcement stress-strain law

5.2 Software

Open System for Earthquake Engineering Simulation (OpenSees) is an object-oriented, software framework created at the Pacific Earthquake Engineering

Center. This software is used for the development of applications to simulate the performance of structural systems. The element used in the analysis for the modelling of the columns were fiber beam elements, which takes into account of a distributed plasticity (a simple distinction between concentrated and distributed plasticity is given in Fig. 5.5). Moreover, the force-based approach has been used, which means:

- Equilibrium between element and section forces is exact;
- Section forces are determined from the basis forces by interpolation within the basic system. Interpolation comes from static equilibrium and provides constant axial force and linear distribution of bending moment, in the absence of distributed element loads;
- A low number of nodes can be used.

Force based approach can be distinguished by displacement-based approach, which uses standard FEM procedure, with an interpolation of section displacement starting from approximate displacement field. Moreover, in order to approximate non linear element response, constant axial deformation and linear curvature distribution are imposed along element length; that is why mesh with a low number of nodes can not be able to represent high order distribution of deformations.

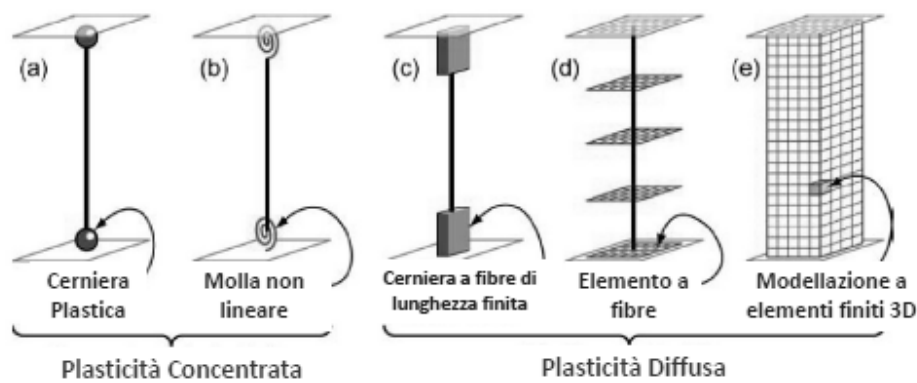


Figure 5.5 - Differences between concentrated and distributed plasticity

Finally, Fig 5.6 shows as every beam section can be considered as divided in different fiber areas with a specified material constitutive law.

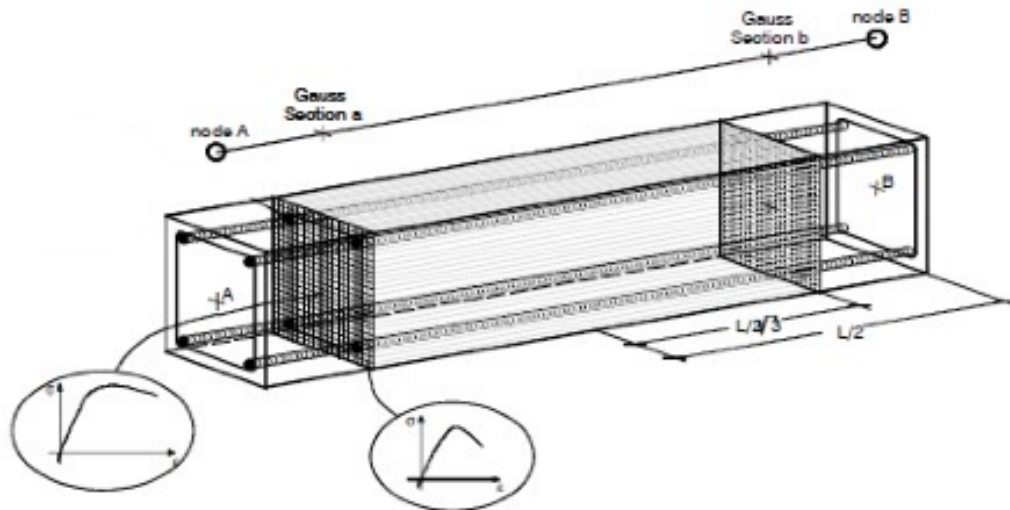


Figure 5.6 - Fiber beam elements

5.2.1 Models for non-linear simulations

As mentioned in chapter 4, the investigated columns have a static scheme of simple supported beam; anyway a distinction in three columns type can be done referring to starting eccentricity, singular local behavior of material and load models:

- Type A. It is referred to columns with none started eccentricity. Anyway, for the purpose to reproduce geometrical eccentricity and to give a direction input to column deflection, a little started value of eccentricity $e_0=0,5mm$ was considered in the model. Columns which presents massive elements at both ends, in these points are modelled with a linear material constitutive law, with the purpose to reflect a more rigid behavior in those parts of structure. Finally, the axial load is applied up to failure and a load path with displacement control were considered ;
- Type B. Differing to previous type, for type B columns have a physical started eccentricity which is obviously reported in the model as a first order eccentricity e_1 . Linear material constitutive law and load model are the same of type A ;

- Type C. This kind of scheme concerns only two columns of the domain. Its main feature is the presence of an increase transversal concentrated load applied on the middle span until up failure occurs, while the axial load remains constant. Anyone started eccentricity was considered and a more rigid behavior (obtained assigning a linear material constitutive law) was obtained not only at the ends of columns, but also in the middle span.

6 Results and discussion

The analysis conducted is aimed at comparison between various Safety Formats for non-linear analysis of RC columns with increasing slenderness values. We started from a rich database of columns, containing a complete description of the structures. The attention can be soon focused on mechanical and geometrical properties, which we can consider in this context like mean values: these allow to realize a computational model, able to identify a first bearing capacity to compare to the actual collapse load, that is nothing more than the experimental load value taken by literature. Abusing language, we can call “Mean Resistance” the resistance outcome of the analysis performed with mean material properties values. Up to this point, there was a high number of references to comparison, that is why it will be legitimate for the reader to think about a first real comparison between the just introduced resistance values. It is worthy to underline that, while literature reported results are given by reality, mean resistance is son of a calculation model which is influenced not only by material randomness, but also by model aleatory. Since this thesis does not aim to release model uncertainties, such comparison is considered meaningless for this study. In other words, we can conclude banishing every comparison between non-linear analysis outcome and bearing capacity coming from literature.

6.1 Probabilistic Method Results

For the purpose to fill the meaning of the previous comparison, we can take into consideration a structural resistance equal affected by model uncertainties, that can be justly compared with “Mean Resistance”. So, a first analysis is proposed to

identify N collapse loads of structures, using what could be defined as the most reliable of the Safety Formats, as well as the most expensive on a computational level: the Probabilistic Method. Reliability and computational cost just described, derive from the fact that at the base of the PM there is the well known Monte Carlo simulation technique. Assuming a lognormal distribution for resistance parameters of the materials (f_c, f_y) , the theoretical procedure provides that on each column, an high number of tests are carried out, having as input different resistance values of materials, randomly identified according to lognormal distribution.

Since civil engineering must deal with extremely low probability of structural failure, a good outcome of Monte Carlo simulation would require a number of tests with at least three orders of magnitude. The choice to perform a sampling selection of the input data through Latin Hypercube Sampling, is so compulsory, in order to perform a much lower number of tests. This probabilistic model was assumed in agreement with the Probabilistic Model Code and allowed to reduce probabilistic analysis to a domain of 40 columns, each of them having 30 cases of mechanical material characteristics [35] .

At the end of non-linear tests performed with the software “OpenSees”, the thirty load cases allow to identify for each column: the average μ_R of the collapse load, calculated on 30 results, and the coefficient of variation V_R of the distribution of the 30 collapse loads, obtained as outcomes. As described in the previous chapters, these data are useful to assess the global resistance factor γ_R , which can be evaluated as:

$$\gamma_R = esp(\alpha_R \cdot \beta \cdot V_R)$$

where $\alpha_R = 0,8$ is the FORM sensitivity factor, considered in the hypothesis of dominant resistance variable, and $\beta = 3,8$ is the reliability index for an ordinary structure corresponding to Reliability Classes *RC2*, with a lifetime of *50 years* [1]. In this way is possible to define the bearing capacity of Probabilistic Method as:

$$R_d = \frac{\mu_R}{\gamma_R \cdot \gamma_{Rd}}$$

where μ_R and γ_R are the aforementioned parameters defined in Monte Carlo simulation, while γ_{Rd} is the global safety factor for the model uncertainties, which

assessment is not subject of this thesis ; it can be taken equal to 1 . This simplification is implemented thanks to independence between the two global safety factor γ_R and γ_{Rd} ; which means that the choice of a specific value of γ_{Rd} does not influence the calculation of γ_R .

Considering the high computational cost, and also a base of reliable probability model, in this context, Probabilistic Method can be considered the principal Safety Format in terms of computational answers comparable to actual structure bearing capacity. That is why, a first congruent comparison can be express by the ratio between the bearing capacity of the previous called “Mean Resistance”, and that one of the Probabilistic Method (*Fig.6.1*). It is clear that the “Mean Resistance” has nothing to do with anyone safety coefficient and it does not take into consideration anyone probabilistic model of uncertainty; that is why, a great overestimation of the bearing capacity is expected. By *Fig.6.1* it is possible to note that all ratios bypass the unit value and it is also possible to see a dependence of ratios on slenderness that can anticipate several matters of this study. As regards slenderness dependence, it is useful to know that a previous study [35] on the assessment of the global safety factor for the model uncertainties γ_{Rd} , permits to exclude any dependence of γ_{Rd} on geometrical and mechanical properties, or other variables of the analysis. This represents a great hypothesis in order to apply the unit value for γ_{Rd} and so to consider the independence of model uncertainties in this study.

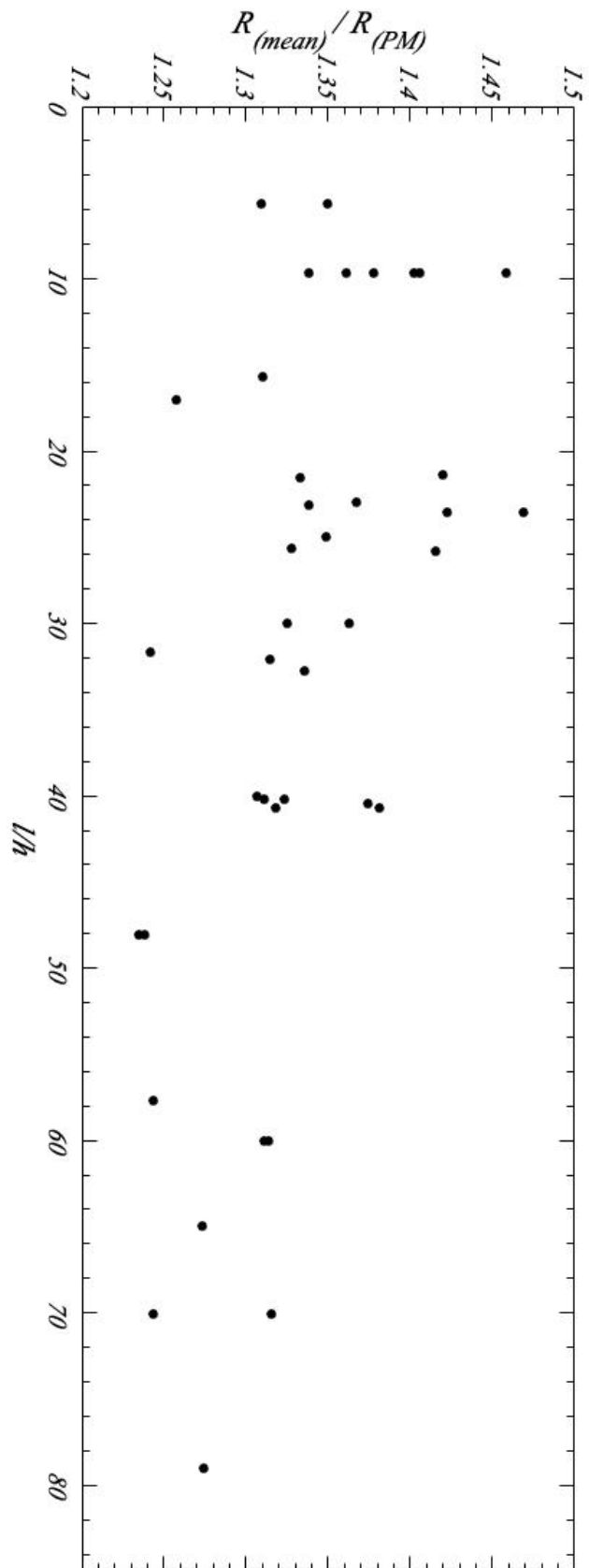


Figure 5.1 - Ratio between bearing capacities obtained by non-linear analyses performed with mean material properties values and Probabilistic Method

6.2 Safety Formats results

After Probabilistic Method, other five Safety Formats have been applied in order to compare different results of collapse loads. For this purpose, for each column are performed 4 non-linear analyses with following material properties:

- Mean properties f_{cm} , f_{ym} . ;
- Design properties f_{cd} , f_{yd} .
- Characteristic properties f_{ck} , f_{yk} .
- Representative properties f_{cmd} , f_{ym} .

Where $f_{cmd}=0,85 f_{cm}$ is considered a representative value.

The most conservative results are obtained by the design values of the Partial Safety Factor and the representative values of the Global Resistant Factor. Design values are calculated according to EC2 respectively for concrete and steel as:

$$f_{cd} = \frac{\alpha_{cc} \cdot f_{ck}}{\gamma_c}$$

$$f_{yd} = \frac{f_{yk}}{\gamma_s}$$

where $\alpha_{cc}=1$ is the reduction coefficient for long-lasting resistors (in Italy $\alpha_{cc}=0,85$);

$\gamma_c = 1,5$ the partial safety coefficient related to concrete ;

$\gamma_s = 1,15$ the partial safety coefficient related to steel.

A simplified summary of the theoretical basis of SFs is given in the following table (6.1):

Table 6.1 - Safety Format Formula

Safety Format	Formula	Global Resistance Factor
PM	$R_d = \frac{\mu_R}{\gamma_R \cdot \gamma_{Rd}}$	$\gamma_R = esp(\alpha_R \cdot \beta \cdot V_R)$ $V_R = \frac{\sigma_R}{\mu_R} \quad \text{Monte Carlo}$
PSF	$R_d = \frac{R(f_{cd}, f_{yd})}{\gamma_R \cdot \gamma_{Rd}}$	$\gamma_R = 1$
GRF	$R_d = \frac{R_{rep}(f_{cmd}, f_{ym})}{\gamma_R \cdot \gamma_{Rd}}$	$\gamma_R = 1,27^*$
SMVM	$R_d = \frac{R_m(f_{cm}, f_{ym})}{\gamma_R \cdot \gamma_{Rd}}$	$\gamma_R = esp(\alpha_R \cdot \beta \cdot V_R)$ $V_R = 0,15$
ECOV	$R_d = \frac{R_m(f_{cm}, f_{ym})}{\gamma_R \cdot \gamma_{Rd}}$	$\gamma_R = esp(\alpha_R \cdot \beta \cdot V_R)$ $V_R = \frac{1}{1,65} \ln \frac{R_m(f_{cm}, f_{ym})}{R_k(f_{ck}, f_{yk})}$
GSF	$R_d = \frac{R_m(f_{cm}, f_{ym})}{\gamma_R \cdot \gamma_{Rd}}$	$\gamma_R = esp(\alpha_R \cdot \beta \cdot V_R)$ $V_R = \frac{\sigma_R}{\mu_R} \quad \text{Monte Carlo}$

* γ_R is take equal to 1,27 in this context in which $\gamma_{Rd} = 1,00$

6.3 Comparison of Safety Formats

The overall comparison between all Safety Formats is provided by a summary on graphic in Fig.6.2 that shows the ratio R_i/R_{PM} , where R_i is the collapse load obtained with following SFs: PSF, GRF, ECOV, SMVM, GSF, while R_{PM} is the bearing capacity of Probabilistic Method, which represents for us the most reliable value of collapse

load. The NLA results are so plotted in function of the ratio l/h which, in our case of rectangular sections, can play the role of the column slenderness value.

The position order of Safety Formats in the graphic legend is not casual. It respects a theoretical hierarchy of the Levels of Approximation, born taking into account an increasing computational cost of the different methodologies.

Considering the Probabilistic Method results as the nearest to the actual bearing capacities, we are tempted to expect a consequent results hierarchy, able to create a standard trend for each column. This expected trend is disputed by the color trend observed in the previous graphic; this allows to focus on the changing of Safety Format results hierarchy, related to the Levels of Approximation (subject treated in further chapter).

The graphic highlights important dependencies by slenderness. For a more exhaustive explanation of study outcomes, they are made clear in the next different paragraphs.

Finally, at the end of this paragraph two explanatory tables (*Tab. 6.3 – 6.4*) are reported. They show all columns bearing capacities reads as NLAs outcomes and so as Safety Formats results (together with relative global resistance factor γ_R). For the purpose to contextualize and assess Safety Formats in probabilistic field, by log-normal distribution of each column global resistance, calculated Monte Carlo simulation effected by [35], SF result probabilities and its cumulative values have been identified for each columns. Appendix A shows a set of Probability Density Functions and Cumulative Density Functions, related to log-normal global resistance distribution, in which SF results appear with them relative fractal values.

6.3.1 ECOV - Increasing overestimation

The most remarkable result is of course the linear increasing trend of *ECOV*. By *Fig.6.2* it is possible to see a clearly growth of the yellow points that, starting to the ratio $h/l=60$, exceed the unit value: this result can be assessed like an overestimation respect the PM collapse value, which we consider exact in this context of analysis simulation independent by the model uncertainties. It is worthy to note that this exceeding respect to unit value and so this important overestimation of the collapse load, arises only with *ECOV* and in case of very slender columns. However this phenomenon represents a solid element to raise

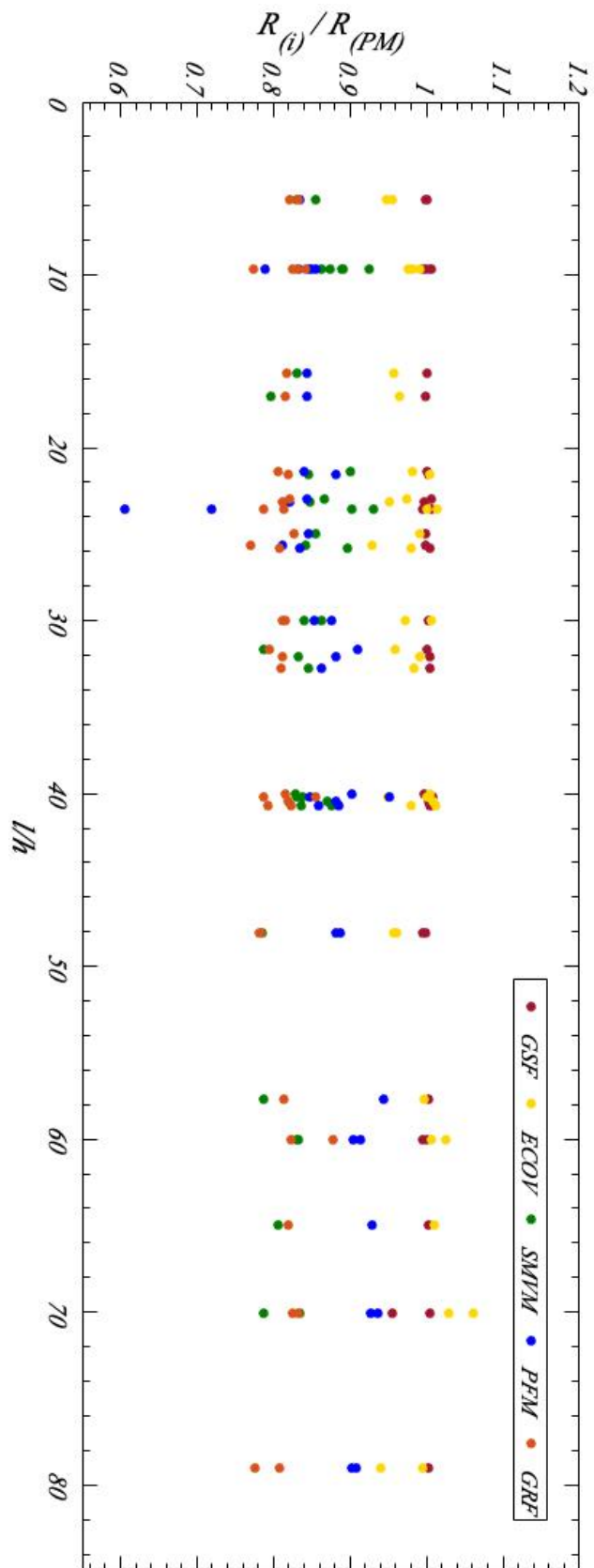


Figure 6.2 - Ratio R_i/R_{PM}

an issue of overestimation, which is fair to relate to a Eulerian failure mode because of high slenderness. The juxtaposition between the collapse value overestimation and an unexpected failure mode is matter introduced by Castaldo et al. , which will be discuss further, in order to identify a solution against overestimation.

Returning to the linear increasing trend, it should be pointed out that it arises not only with the Estimation of Coefficient of Variation, but also in others Safety Formats. The increasing trend dependent on lambda, is related to the evolution of the global resistance factor γ_R which also assumes a decrease fit in function of slenderness. The decrease trend of the global resistance factor γ_R has already been highlighted and justified in previous studies, but it regarded a computation related to the Probabilistic Method. The analytical differences between different Safety Formats outcomes are given by a different decreasing trend that the global resistance factor γ_R assumes in function of the Safety Format applied (See later).

6.3.2 GRF – GSF - Independence from slenderness

Nothing particular interest can be escape by these outcomes which do not show any dependence with slenderness values. Anyway it is worthy to underline that, while the Global Safety Format uses different values of the global resistance factor γ_R for each column, the Global Resistance Factor always uses the same value ($\gamma_R = 1,20$). Moreover, in the *GSF*, the global resistance factor γ_R is estimate for each column taking advantage from Monte Carlo Simulation. This computational effort, from one the one hand, permits to cover the differences between *GSF* and *PM* outcomes in every column case, but on the other side, it prohibits to consider *GSF* as more convenient than Probabilistic Method.

The Global Resistance Factor method performs the analysis with a representative value of material properties, obtained by means of the multiplication factor $0,85$, and then divides the analysis result by a fixed value of the global resistance factor γ_R . A similar process is proposed by the Partial Factor Method (which results are commented in the next paragraph) that in the previous presentation has been presented like a global resistance method with a unit value of γ_R . It uses the mean

material value for non-linear analysis and also provides for the division by a fixed value of the global resistance factor γ_R . The underlined similar procedure does not take directly into consideration the material properties uncertainties by means of a resistance coefficient of variation, that is why, it leads to think an incapacity of the methods with a constant value of the global resistance factor γ_R , to give a dependence of tests by from slenderness. This thesis can so justified the constant trend of *GRF* outcomes; moreover it is useful to note that *GRF* uses an high value of the global resistance factor ($\gamma_R = 1,20$) respect to *PFM*.

The exceptional case of slenderness independence with the variation of the global resistance factor γ_R for each column, is given by *GSF*, and its independency was justified by its analogy with Probabilistic Method, that leads very similar results.

6.3.3 *PFM – SMVM - Growth and decline of Resistance values*

In this paragraph we face to comment a slenderness dependence of global resistance, which arises with both Safety Formats that use a constant value of the global resistance factor γ_R : the Partial Factor Method and the Simplified Mean Value Method. In the previous paragraph, an allegation was made against the Safety Formats which use a fixed value of γ_R , because they can not take directly into consideration material properties uncertainties by means of a resistance coefficient of variation and so they permits to expected independence outcomes respect to slenderness. Regarding this idea, now we are called upon to justified results that show an increase (*PFM*) and a decrease (*SMVM*) trend in function of slenderness.

The Partial Safety Factor is the unique method to exploit a non-linear analysis performed whit the design values of the material parameters. These are derived by common formulae of Eurocode, that break down material resistance values. It is clear that a less value of material resistance leads to a little value of global resistance, but as mentioned before, in case of high slenderness values, the material properties and their related uncertainties play a less important role, to the benefit of geometrical issue associated to Eulero buckling. Therefore, the reduction of

material properties values is able to return little values of global resistance only in case of small slenderness, i.e. in the case in which the mechanical properties of the materials can better influence non-linear analysis performance. On the contrary, on high slenderness, a great reduction of material properties values does not allow to ensure an high safety level that the design values are common to give in a standard structure calculation.

A parallel matter can be related to the only decrease trend, given by Simplified Mean Value Method. After performing the analysis with the mean value of material properties, it uses a constant value of the global resistance factor $\gamma_R=1,58$, derived by a concrete coefficient of variation equal to 0,15. This hypothesis of uncertainty estimate is of course in favor of security (the global resistance obtained with *SMVM* is always lower than *PM*), but such estimate appears too precautionary for high slenderness; that is why the global resistance factor $\gamma_R = 1,58$ gives an excessive underestimation of global resistance.

6.4 Comparisons of Global Resistance Factors γ_R

After a full analysis of global resistance in terms of bearing capacity, it is remarkable underline and compare the associated trend of γ_R in the several methodologies of Safety Formats. *Fig. 6.3* contains different trend of γ_R in function of slenderness, marked by colors associated to Safety Formats. The trend were obtained by linear interpolation for all Safety Formats, except for *ECOV* which global resistance factor registers a more strong dependences on slenderness, that is why in that case second order polynomial interpolation was used. The particular graphic interpolations are reported in the Appendix D, together with a graphic contained the linear interpolation of ratio $\gamma_{R,ECOV}/\gamma_{R,PM}$ which have the goal to underline a more strong dependence on slenderness of *ECOV* respect to Probabilistic Method.

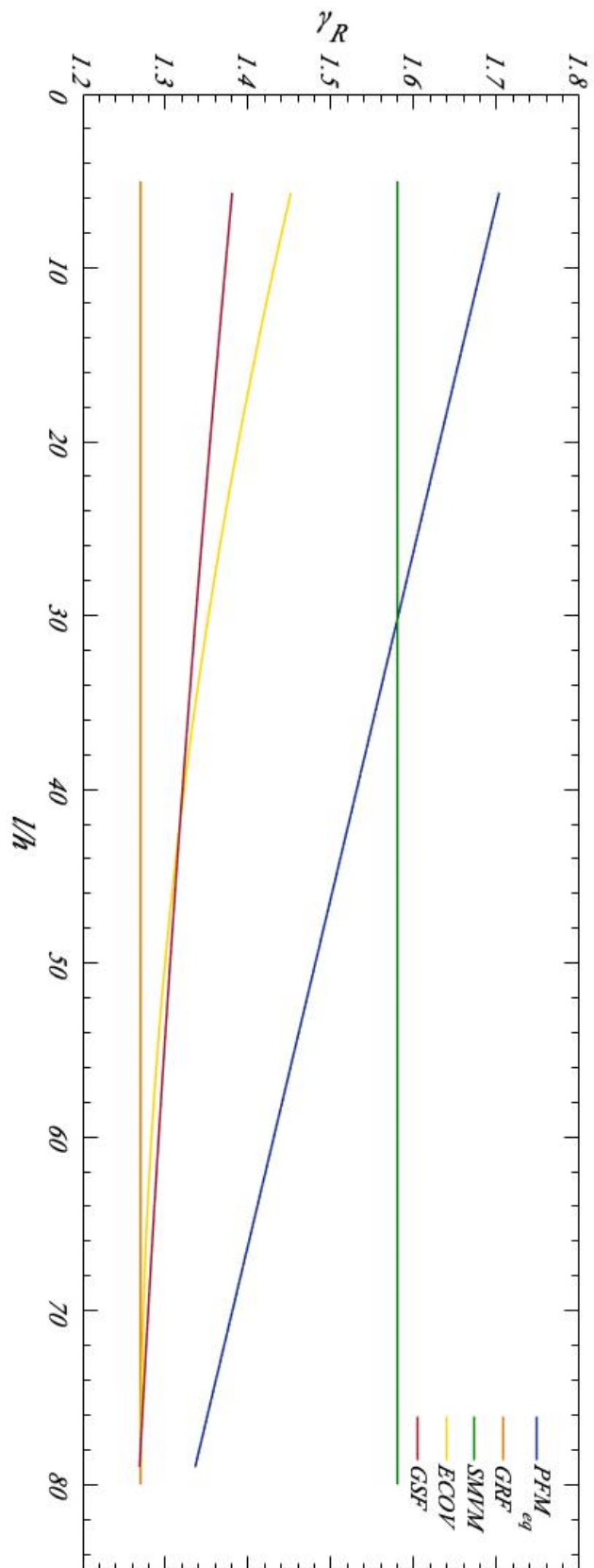


Figure 6.3 - Comparison of Global Resistance Factor γ_R

The peculiarity of Fig. 6.3 is the inclusion to comparison of a dummy global resistance factor related to PFM. It can be defined as “equivalent global coefficient” and it is calculated as ratio between global resistance obtained by analysis performed with mean mechanical properties values and global resistance obtained by analysis performed with design mechanical properties :

$$\gamma_{R,ECOV,eq} = \frac{R(f_{cm})}{R(f_{cd})}$$

Finally table 6.2 summarizes values taken by global resistance factor for each SF.

Table 6.2 - Values of global resistance factor γ_R

Safety Format	Range of variation	Mean Global Resistance Factor γ_R
PM - GSF	1,27 - 1,40	1,33
ECOV	1,27 - 1,45	1,35
PFM_{eq}	1,33 - 1,70	1,55
SMVM	constant	1,58
GSF	constant	1,27

6.5 Conclusions related to actual slenderness values

At the end of analysis, same considerations are given in order to define calculation validity about several Safety Formats. In previous paragraphs, dependences on slenderness was underlined for different Safety Formats and in just one case (ECOV), this dependence has led to a global resistance overestimation. For the purpose to formulate a final conclusion, it is worthy to underline that our column domain ranges on slenderness between $l/h=5$ and $l/h=80$. For conversion of the ratio l/h in the standard slenderness value λ , for rectangular cross section

columns, it will multiply for a value of $\sqrt{12}$. To this purpose, slenderness definition is reported:

$$\lambda = \frac{l}{\rho}$$

where ρ is the radius of gyration of cross section, that, related to rectangular section, can be write as :

$$\lambda = \frac{l}{\rho} = l \cdot \sqrt{\frac{A}{I}} = l \cdot \sqrt{b \cdot h \cdot \frac{12}{b \cdot h^3}} = \frac{l}{h} \cdot \sqrt{12}$$

Explaining the real slenderness value λ , the obtained values achieve very high levels that can not be considered in the structural standards (e.g. bridge piers can arrive to have slenderness equal to $\lambda = 90$). That is why, analyzing a restrained domain, given by common slenderness value, it is possible to conclude that:

- Slenderness continues to influence global resistant, but for relative low values, its influence is not so power to disturb the Safety Format hierarchy; which means that the results are comply with expectations related to levels of approximations. In other words, all stranger set of results occurs in very slender columns, and the domain restriction of columns is able to keep out outcome weirdness ;
- ECOV is confirmed very reliable Safety Format for a restrained columns domain with $\lambda_{max} = 170$. The global resistance overestimation respect to Probabilistic Method occurs only in cases with $170 < \lambda < 225$; such slenderness values are not typical of structural elements, that is why the assessment of ECOV performances can be considered positive.

In the *Fig. 6.4* is reported a different view about overall results, expressed in function on real slenderness λ . As underlined before, the graphic is important to the purpose to underline the global underestimation of all Safety Formats and also results accuracy respect to Probabilistic Method.

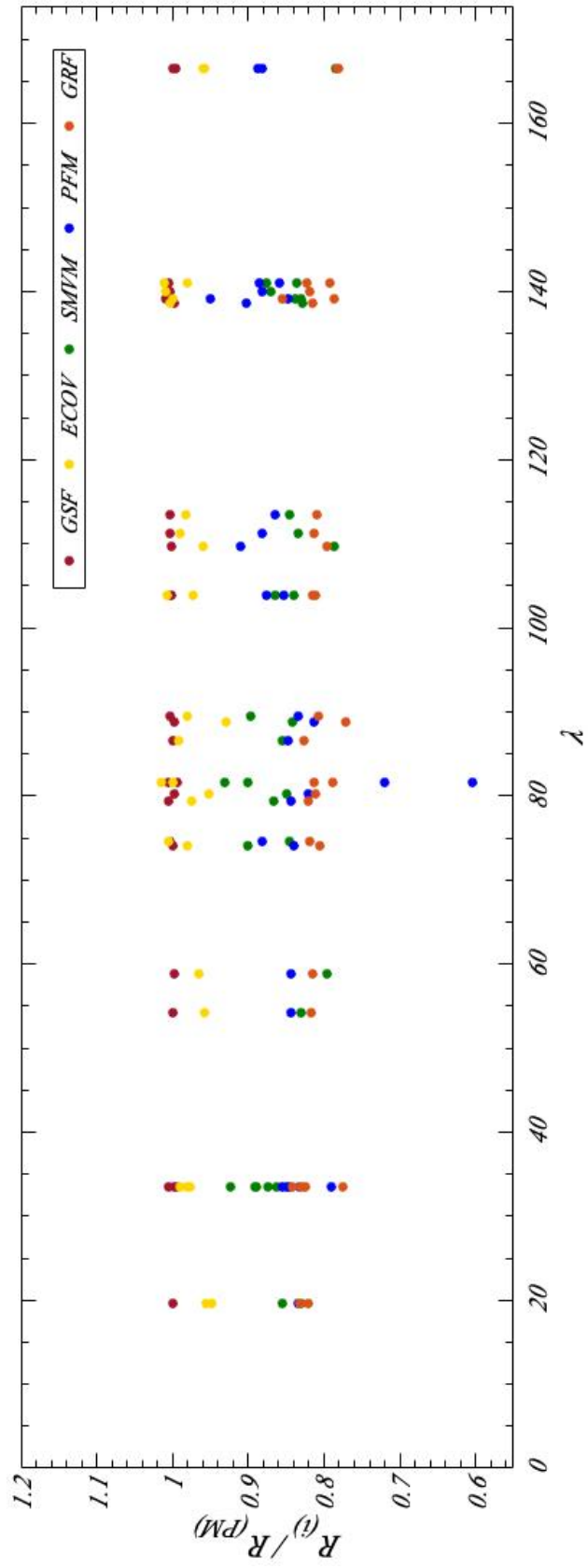


Figure 6.4 - $R^{(i)} / R^{(PM)}$ for common structural slenderness values

Table 6.3 - OpenSees analysis results

Test n°	l/h	Literature	OpenSees			
		N _{exp}	Mean Resistance	N (f _{cd} , f _{yd})	N (f _{ck} , f _{yk})	N (f _{cmd} , f _{ym})
2L20-30	9,7	750,0	694,0	389,9	527,6	485,7
2L20-60	9,7	700,0	739,0	438,1	609,1	552,9
C000	5,7	559,6	560,0	346,3	464,6	438,2
2L8-120R	9,7	1092,0	1152,0	657,2	928,5	826,8
C020	5,7	327,3	328,5	209,5	275,9	261,6
4L8-30	9,7	1100,0	1032,0	647,9	869,0	811,1
4L20-120	9,7	900,0	830,0	527,3	699,7	654,2
4L8-120R	9,7	1247,0	1319,0	809,6	1097,7	1009,0
III	22,9	343,0	347,0	214,0	289,0	264,6
B020	15,7	271,5	262,0	168,8	221,2	207,4
N30-10.5-C0-3-30	23,6	8,3	8,1	4,0	6,6	5,7
3,3	21,4	782,0	866,0	512,1	709,0	623,8
A-17-0.25	17,0	1181,0	1369,0	917,8	1186,7	1126,7
5,1	21,5	735,0	843,0	557,9	723,2	658,2
H60-10.5-C0-1-30	23,6	8,6	8,9	3,8	7,7	6,3
Va	23,1	684,0	680,4	417,7	565,8	523,6
I	32,1	265,0	258,0	172,9	221,3	202,5
24D-2	30,0	198,0	193,0	124,2	163,2	150,2
C-31.7-0.25	31,7	333,0	280,0	205,2	243,5	227,7
RL300	25,0	474,0	414,0	259,8	350,5	322,5
2	25,8	696,3	762,0	449,3	624,5	551,9
4,1	30,0	367,0	448,1	288,1	380,3	340,7
8	25,6	235,0	244,1	149,4	201,2	179,9
VI	32,8	392,3	363,2	234,9	307,7	279,5
15E - 2	40,0	161,0	129,0	89,1	111,9	102,3
S28	48,1	44,0	64,7	46,3	56,4	52,0
9	40,2	206,0	209,0	134,0	174,8	157,9
S30	48,1	48,0	66,3	47,4	57,8	53,2
12	40,2	113,0	172,6	125,2	157,2	143,0
6	40,7	225,0	240,0	156,3	204,5	183,2
15	40,4	549,0	558,0	358,0	471,9	422,8
3	40,7	667,0	563,0	361,0	475,5	425,5
S25	57,7	36,0	42,3	32,1	37,6	35,1
17A	65,0	31,9	37,1	27,1	32,8	30,3
5	60,0	72,7	78,0	54,2	68,2	62,1
6	60,0	72,2	82,0	56,6	71,1	69,7
8	79,0	31,9	31,0	22,1	27,1	24,9
20	70,1	39,8	37,9	28,2	34,8	31,9
18	70,1	33,9	39,8	28,3	34,8	32,0
7	79,0	29,9	32,3	22,9	27,4	25,0

Table 6.4- Safety Formats Results

Test n°	l/h	PFM	GFR	SMVM	ECOV		GSF		PM
		N _d [KN]	N _d [KN]	N _d [KN]	N _d [KN]	γ ^R ECOV	N _d [KN]	γ ^R MonteCarlo	N _d [KN]
2L20-30	9,7	389,9	382,4	439,9	418,2	1,66	495,7	1,40	493,6
2L20-60	9,7	438,1	435,3	468,4	517,1	1,43	524,1	1,41	527,2
C000	5,7	346,3	345,0	354,9	396,5	1,41	414,8	1,35	414,9
2L8-120R	9,7	657,2	651,0	730,2	773,3	1,49	794,5	1,45	790,0
C020	5,7	209,5	206,0	208,2	238,0	1,38	250,8	1,31	250,9
4L8-30	9,7	647,9	638,6	654,1	751,1	1,37	753,3	1,37	758,4
4L20-120	9,7	527,3	515,1	526,1	605,4	1,37	619,4	1,34	620,4
4L8-120R	9,7	809,6	794,5	836,0	939,3	1,40	962,8	1,37	957,4
III	22,9	214,0	208,4	219,9	247,5	1,40	255,1	1,36	253,8
B020	15,7	168,8	163,3	166,1	191,6	1,37	200,0	1,31	200,0
N30-10.5- CO-3-30	23,6	4,0	4,5	5,1	5,6	1,45	5,5	1,46	5,5
3,3	21,4	512,1	491,2	548,9	598,4	1,45	609,9	1,42	609,8
A-17-0.25	17,0	917,8	887,2	867,7	1051,3	1,30	1086,5	1,26	1088,7
5,1	21,5	557,9	518,3	534,3	635,1	1,33	633,8	1,33	632,3
H60-10.5- CO-1-30	23,6	3,8	4,9	5,6	6,8	1,31	6,2	1,43	6,3
Va	23,1	417,7	412,3	431,2	483,9	1,41	506,9	1,34	508,3
I	32,1	172,9	159,4	163,5	194,3	1,33	196,9	1,31	196,2
24D-2	30,0	124,2	118,3	122,3	141,6	1,36	146,2	1,32	145,7
C-31.7-0.25	31,7	205,2	179,3	177,5	216,4	1,29	225,8	1,24	225,5
RL300	25,0	259,8	254,0	262,4	304,4	1,36	306,7	1,35	306,9
2	25,8	449,3	434,6	483,0	527,6	1,44	540,4	1,41	538,4
4,1	30,0	288,1	268,3	284,0	331,0	1,35	329,5	1,36	328,8
8	25,6	149,4	141,7	154,7	170,7	1,43	183,5	1,33	183,8
VI	32,8	234,9	220,1	230,2	267,4	1,36	273,1	1,33	272,0
15E - 2	40,0	89,1	80,5	81,8	99,1	1,30	98,5	1,31	98,7
S28	48,1	46,3	40,9	41,0	50,2	1,29	52,2	1,24	52,2
9	40,2	134,0	124,3	132,5	150,2	1,39	158,3	1,32	158,0
S30	48,1	47,4	41,9	42,0	51,4	1,29	53,5	1,24	53,7
12	40,2	125,2	112,6	109,4	145,3	1,19	132,8	1,30	131,6
6	40,7	156,3	144,3	152,1	178,5	1,34	183,2	1,31	182,1
15	40,4	358,0	332,9	353,7	409,5	1,36	407,3	1,37	406,1
3	40,7	361,0	335,1	356,8	412,0	1,37	409,5	1,37	407,5
S25	57,7	32,1	27,7	26,8	34,0	1,25	34,1	1,24	34,0
17A	65,0	27,1	23,9	23,5	29,5	1,26	29,2	1,27	29,1
5	60,0	54,2	48,9	49,4	60,9	1,28	59,1	1,32	59,4
6	60,0	56,6	54,9	52,0	63,0	1,30	62,6	1,31	62,6
8	79,0	22,1	19,6	19,6	24,2	1,28	24,4	1,27	24,3
20	70,1	28,2	25,1	24,0	32,3	1,17	29,2	1,30	30,5
18	70,1	28,3	25,2	25,2	31,1	1,28	30,4	1,31	30,3
7	79,0	22,9	19,7	20,5	23,8	1,36	25,4	1,27	25,3

7 Failure Mode-based Safety Factor

Up to here it have not been given particular importance to failure mode of slender columns. It is well-known that possible collapse of a peak loaded column, can be obtained by insufficient material resistance, associated to a plastic collapse, or by a more complex problem of Eulerian instability in which structure can not exploit all its material resistance and finds the failure with smaller load values. Previously, a first distinction between two just explained collapses was done indirectly, thanks to the several dependences related to column slenderness. In fact, in the phase of trend evaluation of global resistance factor γ_R , it has been noticed interesting influences of slenderness λ , which can be considered indirectly proportional to γ_R in both cases of *ECOV* and *PM*. The decrease trend allows to associate smaller values of γ_R for columns with higher values of λ , which means that, in case of high slenderness, the aleatory uncertainty of the material properties has a little influences on the final resistance. The justification to this phenomenon was given by an automatic association between high slenderness and Eulerian instability collapse: when the failure is generated by instability issue, structure can not enjoy all material resistance, that is why material properties and so its randomness, play a less important role in the failure analysis.

7.1 Identification of the failure mode

After a first step of automatic and lawful association between high slenderness and Eulerian collapse, in this context, it can be interesting to evaluate data, in order to identify a more accurate collapse distinction. In this paragraph, the presentation of two kind of graphics is reported:

- Global load-deflection diagram ;

- Local stress-strain diagram related to most critical fiber of the cross-section.
- The assessment of both graphics will lead to define failure mode.

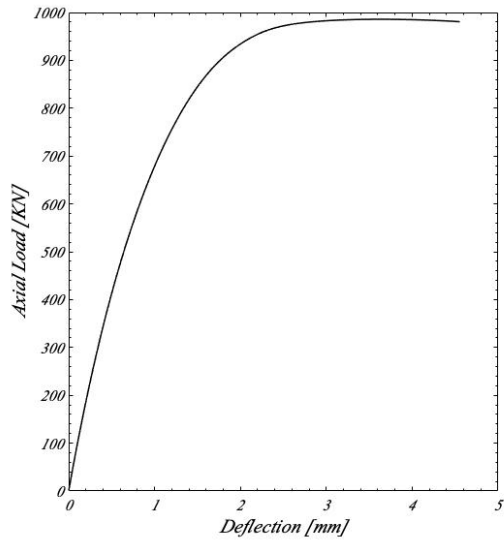
7.1.1 Global load-deflection diagrams

After explained theoretical concepts on the global displacement related to second order effects, in this practical phase, it was useful to represent the load line of same columns, expressed in function of global horizontal displacement, obviously associated to deflection, with a view to buckling evaluation.

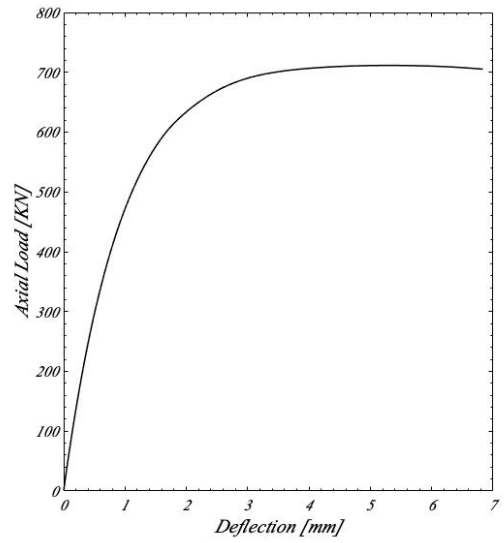
Of course, as underlined in Fig.(3.2), Eulerian collapse can be identified in cases in which load line records a fast increase of global deflection values u in compliance with a little growth of axial force N . This phenomenon leads to create a non-linear trend between N and u , that turns up with equilibrium instability. On the other side, the collapse can be considered plastic, so with a total strength material exploitation, in cases in which non-linearity related to second order effects does not appear.

To this purpose, it is worthy to underline that taking into account non-linear constitutive material laws, all load lines will be influenced by this other kind of non-linearity, related to material properties. In conclusion, the failure assessment deals to evaluation of two non-linearity kind: the first is related to material constitutive law and there is always; the second is related to second order effect and it is able to give a good idea about when buckling failure occurs.

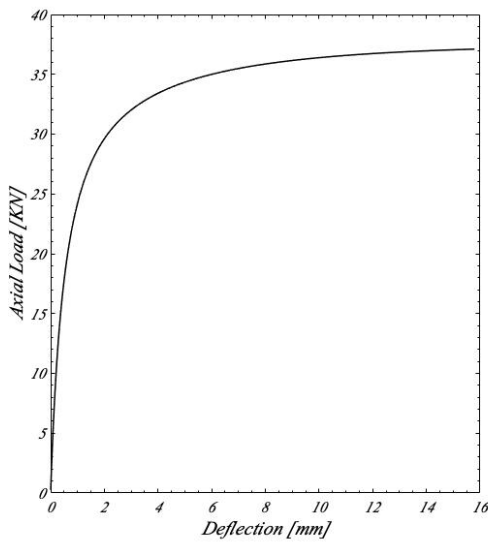
The following figures (*Fig.7.1 - 7.2 - 7.3 - 7.4*) show the applied axial load in function of the global deflection related to two test (4L8-30 and 17-A) performed with two different parameter set (see later NLA1 and NLA2) which uses mean value for concrete strength and design value for steel strength, for first case, and vice versa for the second.



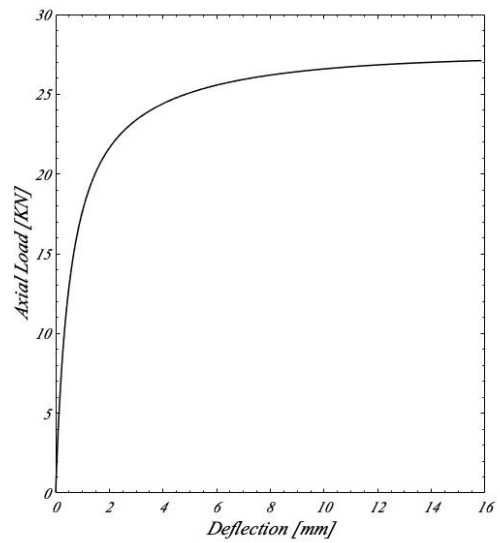
4L8-30 - NLA 1 - Global load-deflection diagram
 $\lambda = 33,60$
 Figure 7.1



4L8-30 - NLA 2 - Global load-deflection diagram
 $\lambda = 33,60$
 Figure 7.2



17-A - NLA 1 - Global load-deflection diagram
 $\lambda = 225$
 Figure 7.3



17-A - NLA 2 - Global load-deflection diagram
 $\lambda = 225$
 Figure 7.4

As expected, by figures, it is clear the non-linearity influence related to material properties. It can be noticed in all four diagrams. However, it is possible to focus on the different trend which axial load take in case of low slenderness (test 4L8-30) and high slenderness (test 17-A). Non-linearity related to second order effects can be noticed in *Fig 7.3 – 7.4* and it is characterized by a rapid deviation of the curve by the starting linear trend. On the contrary, *Fig 7.1 – 7.2* show a slow loss of non-linearity which can be so correlated to material constitutive law. At the end, it is possible to note the differences related to the entity of axial force values, that draws attention to strength material exploitation.

7.1.2 Local stress-strain diagram

On local level, it can be interesting to evaluate stress-strain trends related to particular fiber of the midspan cross-sections. In particular, every stress-strain diagram is created in the same time for :

- External concrete fiber of core section ;
- External concrete fiber of cover section ;
- Steel fiber in traction .

Analyzing the graphics, the main goal is to identify in which of three fibers failure occurs. To this purpose, on the horizontal axis the stress limits are reported whit a vertical red line that reports the strain value ε_{c0} corresponding peak stress point. The *Fig. (7.5 – 7.6 – 7.7)* shows the stress-strain diagrams related to the test 4L8-30 . It is referred to column whit a little slenderness value ($\lambda = 33,60$) for a preliminary non-linear analysis (see later NLA 1) performed with material properties using mean value for concrete and design value for steel.

By following set of three graphics (*Fig.7.5 – 7.6 – 7.7*), it is possible to finalize that failure occurs in the extreme fiber of the unconfined concrete. In particular, the *Fig.7.6* underlines a complete path of concrete constitutive law, with an exploitation of the softening branch that clearly leads to failure for strength limit.

On the other side, a typical case of buckling failure is reported in the next set of three graphics (*Fig.7.8 – 7.9 – 7.10*). It shows fiber outcomes related to test S28 ($\lambda = 166,62$). It is clearly visible that materials do not achieve ε_{c0} : failure occurs in elastic field with low stress values respect to limit strength.

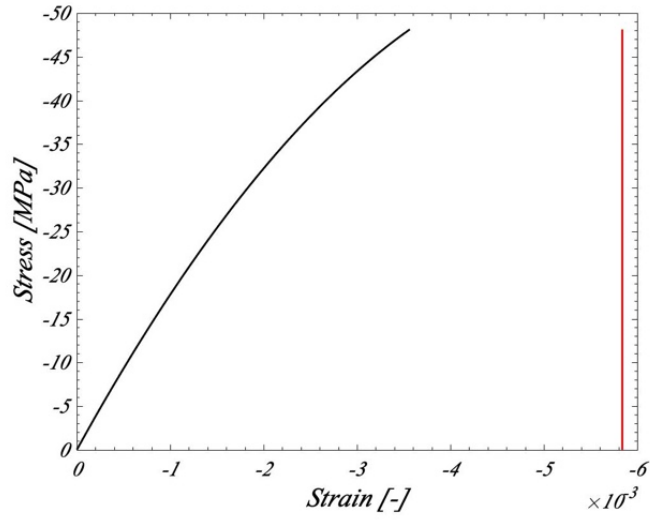


Figure 7.5 - **4L8-30** - NLA 1 - Confined concrete behavior

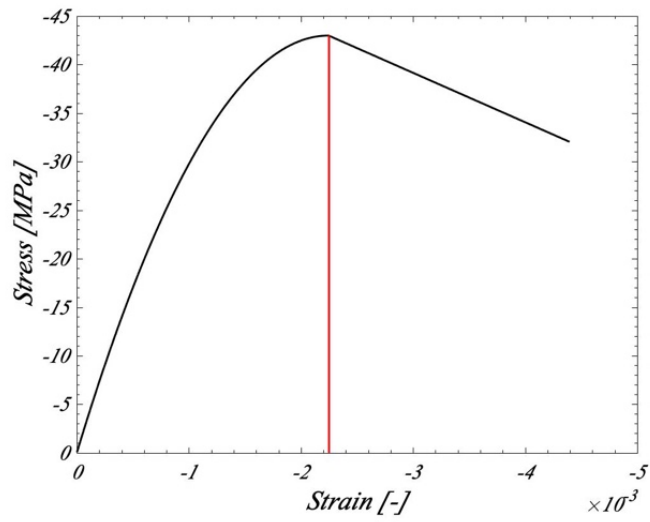


Figure 7.6 - **4L8-30** - NLA 1 - Unconfined concrete behavior

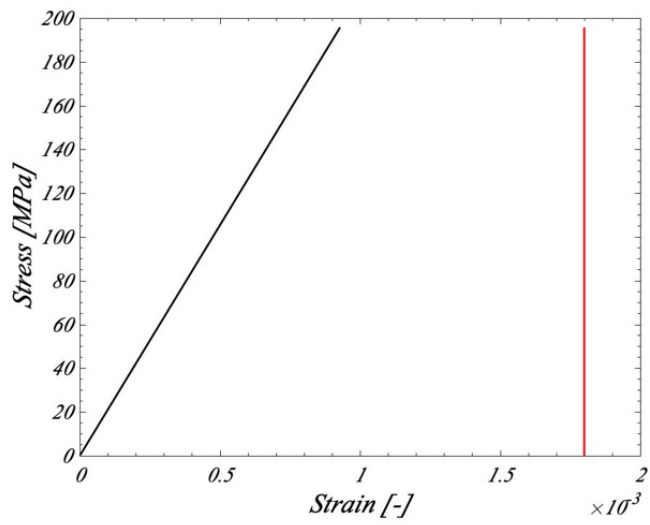


Figure 7.7 - **4L8-30** - NLA 1 - Steel behavior

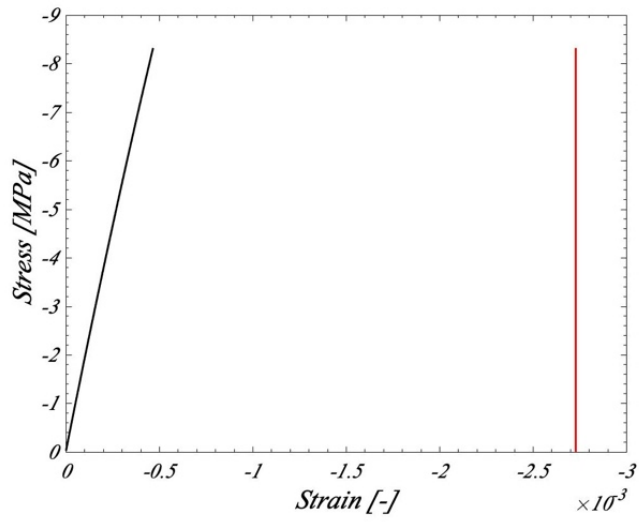


Figure 7.8 - S28 - NLA 1 - Confined concrete behavior

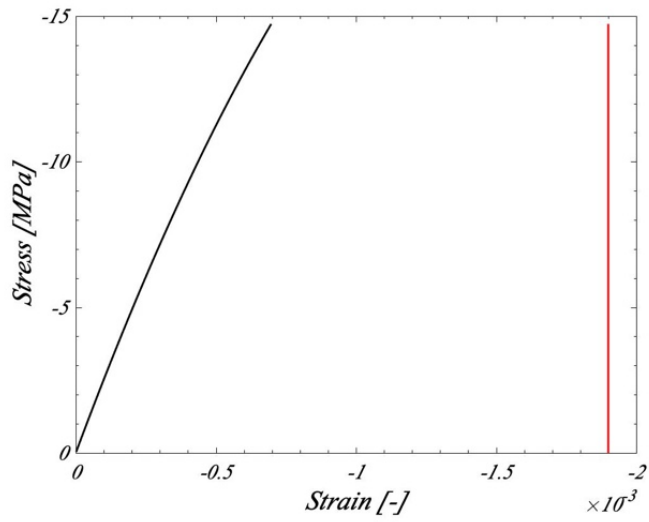


Figure 7.9 - S28 - NLA 1 - Unconfined concrete behavior

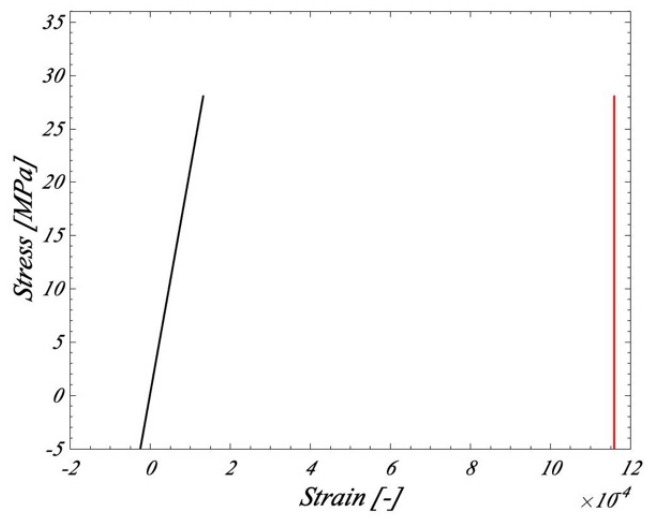


Figure 7.10 - S28 - NLA 1 - Steel behavior

7.2 Failure Mode

Generally, in a Safety Format discussion, it can be very interesting to focus on failure mode of structures. It is worthy to underline, in first place, that the *GRMs* have to be able to estimate the effective collapse load, by means of a global structural analysis and with a relatively low computational effort, and in second place, that the Probabilistic Method is obviously assumed as the reference safety format as explained above. Clearly, in order to ensure safety, *GRMs* have to identify global resistance values smaller than PM. In particular, the mean trend hierarchy of this study is composed as following: *GRF* – *PFM* – *SMVM* – *ECOV* – *GSF* . A specific chapter related to this matter is further reported; it is based on the Levels of Approximation for non-linear analysis in probabilistic fields and ends up creating a LoA hierarchy.

Studies conducted on flexural behavior of RC beams with regular square of circular web openings [14] allowed to show that some of these beams do not follow the conventional aforementioned hierarchy of SF results and the same beams are interested by different failure mode, depending on applied Safety Format. It is clear that hierarchy absence and different failure mode for different Safety Formats, are closely connected phenomena; that is why failure respecting of expected hierarchy, can be considered as an alarming element for purpose to identify a case in which, the Safety Format falls in mistake respect to failure mode evaluation, not respecting the security rules. An example of different failure mode can be given by the fact that, the failure mode affects both material and region: so in a simply supported beam, the bending mechanism involves both materials (concrete and steel) in the midspan, while shear mechanism involves only concrete near restraints.

According to Castaldo et al. , some structure cases allow to escape some imperfections of Safety Formats, given by incapacity to take into account the actual distribution of the structural resistance as a function of the possible failure mode. In other words, the *GRMs* sometimes can not be able to estimate effective failure mode, generating in this way a safety level not adequately guaranteed. A simple expectation can be done by the coefficient of variation in the *ECOV*, that is evaluated with a simplified approach which, obviously, does not consider any modification in the failure mode. Moreover, as explained before, the *GSF* assumes

the mean value of distribution of the global structural resistance equal to the value achieved from NLA, by employing the mean values of the material properties.

7.3 Proposal of failure mode-based safety format factor

The innovative proposal of a new coefficient γ_{FM} called failure mode-based safety factor has the aim to reduce the global resistance values obtained by *GRMs* in order to get resistance values nearest to reality. That is why γ_{FM} has been calibrated in order to obtain results, in terms of design global resistance R_d evaluated with the *GRMs*, in compliance with the resistance R_d estimated with the probabilistic method PM. The previously analytical definition of global resistance R_d can be modified as:

$$R_d = \frac{R_{rep}}{\gamma_R \cdot \gamma_{Rd} \cdot \gamma_{FM}} \quad (7.1)$$

It is important to underline that the proposal to use a new safety factor associated to failure mode, waives a prior analysis which evaluates the failure mode sensitivity of the particular structural case. A simple methodology for this purpose, is to conduct two NLAs:

- One NLA simulation using the mean values for the concrete properties and the design values for the reinforcement properties;
- One NLA simulation using the design values for the concrete properties and the mean values for the reinforcement properties.

If failure modes of these two analyses are the same, it is possible to evaluate structural case as independent to failure mode and so all the *GRMs* can be adopted to estimate design ultimate load as well as PM. In other way, it is possible to accept formula above admitting $\gamma_{FM}=1,00$. Whereas, if failure modes of two analyses are different, γ_{FM} coefficient becomes crucial in order to balance failure mode sensitivity of the particular case. Obviously in these cases, γ_{FM} can not be equal to one (recommended value according Castaldo et al. $\gamma_{FM}=1,15$).

7.4 Failure mode sensitivity

In order to check effectiveness of the previous methodology, a limited number of columns of database have been subjected to previous two preliminary NLAs with mean and design material properties for concrete and steel, as explained above. As concluded in paragraph (6.5) , the missing of hierarchy between several Safety Format results can be noticed for high slenderness values that can not be considered typical of structural problems. So it is reasonable to expect that the methodology of two NLAs will return equal failure modes. The appendix B reports previous described graphics related to preliminary analyses: it is clearly that global axial force-deflection diagrams and local stress-strain diagrams do not show any strong difference between NLA 1 and NLA 2.

It is possible to say that there is no worthy interaction between geometrical and material properties. In fact, failure mode remains the same also in case of change of material properties. This result, in first place, gratifies performance of non-linear preliminary analyses and so confirm γ_{FM} independence on slenderness values. For a theoretical respect of Eq. (7.1) in this study about slender columns, it is possible to assign $\gamma_{FM} = 1$.

8 *Levels of Approximation*

At the end of the analysis, a satisfying evaluation of Safety Formats leads to underline not only accuracy of results but also computational cost. As explained before, Probabilistic Method is undoubtedly the most expensive but return a great reliability of results. It is, therefore, legitimate to relate an high computational cost with a more accurate outcome. To this purpose, in this chapter, a little benefit-cost analysis is reported introducing concept of Levels of Approximation.

Before to explain how LoAs can adapt to non-linear analysis, it is worthy to call back some general concepts on structural analysis. This thesis started with a little description about non-linear analysis, related its to high level of approximation respect to linear analysis which deals with more simply material constitutive law. Moreover, the introduction in a structural analysis finalizing to assess global structural resistance, rather than local failure related to internal action of the critical cross section, leads to categorize this kind of analysis on accuracy levels requiring challenging efforts.

In view of new *fib* Model Code 2020, an easy classification about levels of approximation related to Safety Format for non-linear analysis is reported :

- *LoA I*, requires limited number of non-linear analysis with hypothesis related to the coefficient of variation of global structural response;
- *LoA II*, requires limited number of non-linear analysis with a simplified method for the estimation of the coefficient of variation of global structural response;
- *LoA III*, requires the definition of probabilistic models in order to perform the reliability analysis.

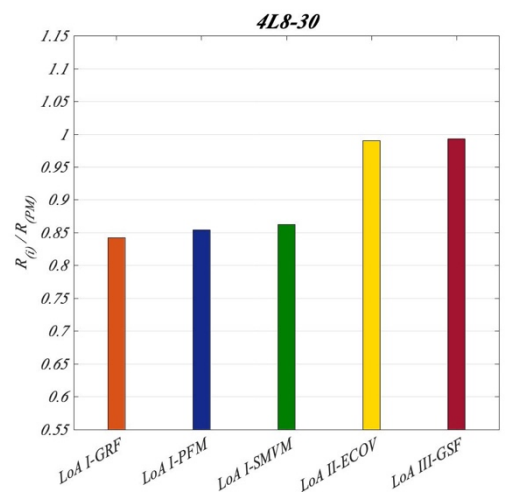
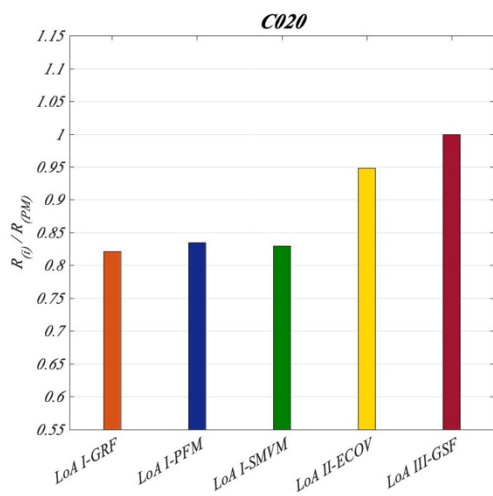
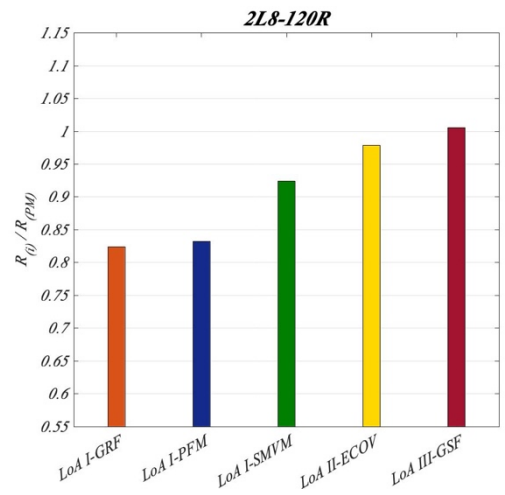
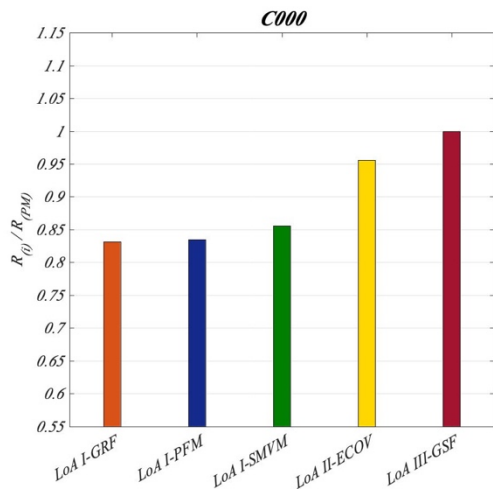
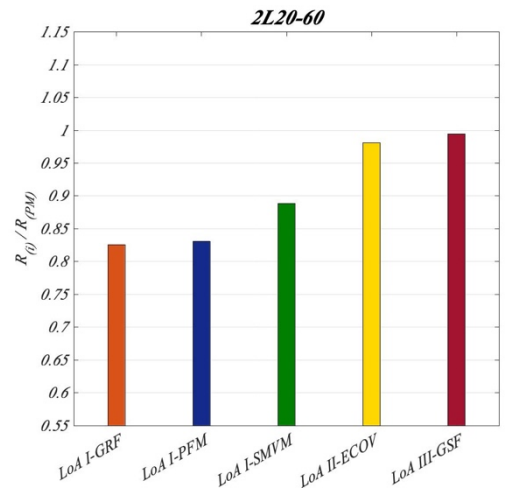
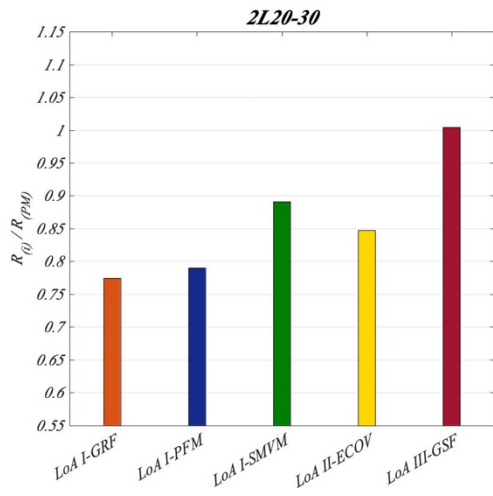
The relative response on the global resistance side, can be also related to LoAs thanks to specific level of reliability identified by the target reliability index β .

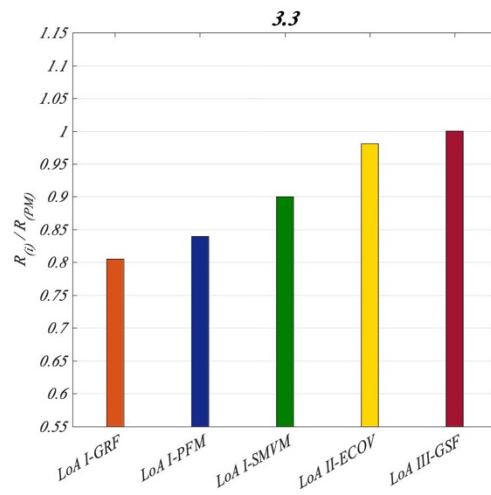
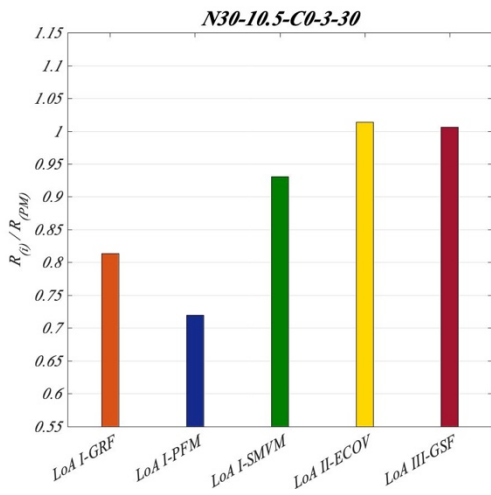
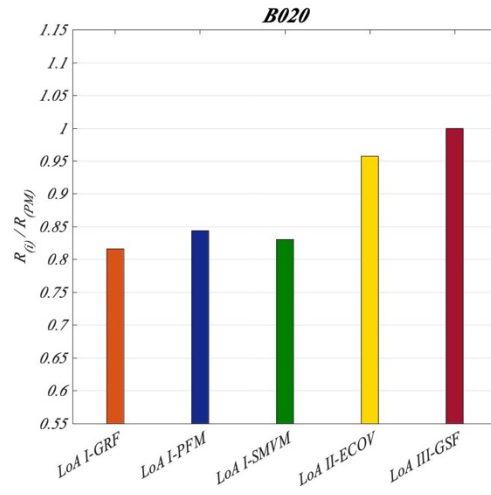
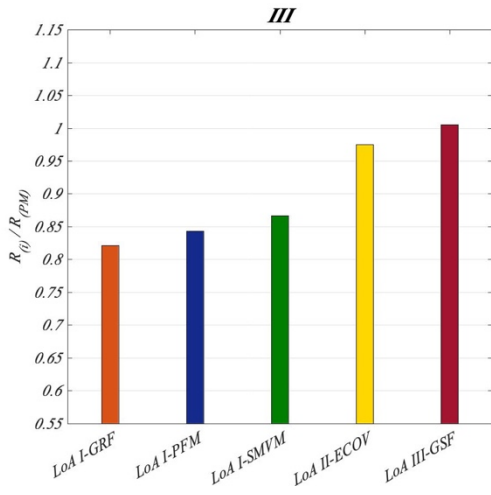
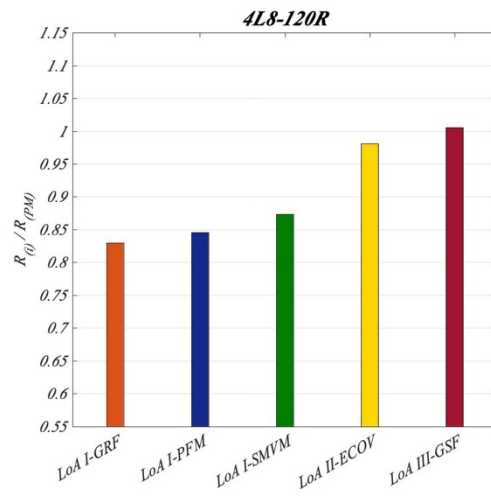
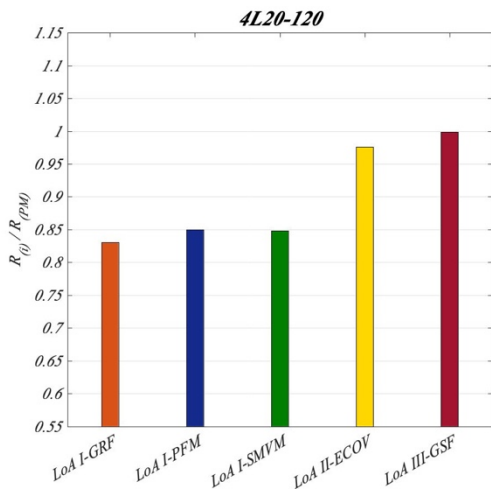
The further graphics show different representation of Safety Format results. For each column, a bar graphic underline the different ratios between R_i/R_{PM} . The exceeding of unit limit underline the already mentioned ECOV overestimation for very high slenderness values. However, in this phase, the aim is to discuss the changing of order in terms of resistance results. Like done for the graphic legend in Fig.6.2 , the horizontal axes of the bar charts are always consisting of the same order which is related to different Levels of Approximation:

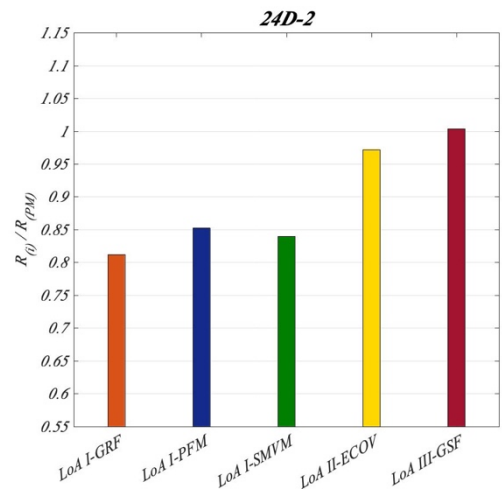
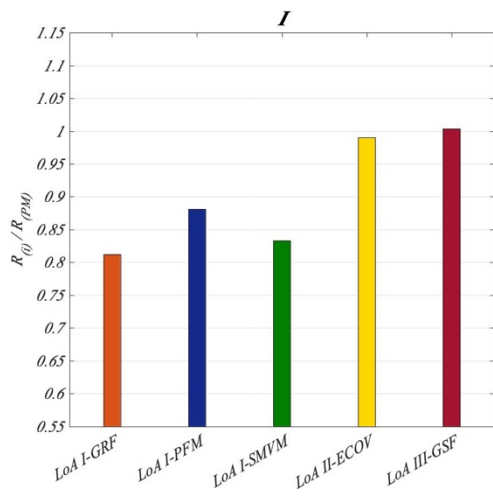
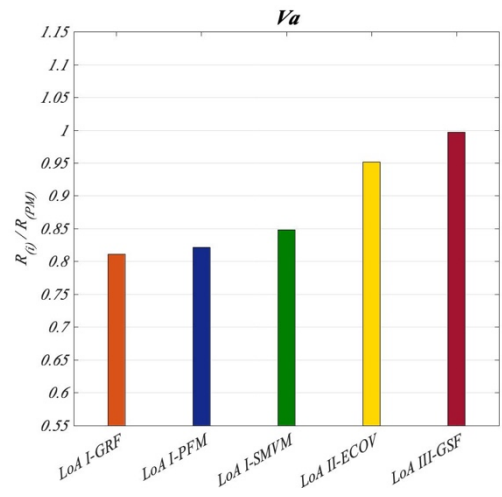
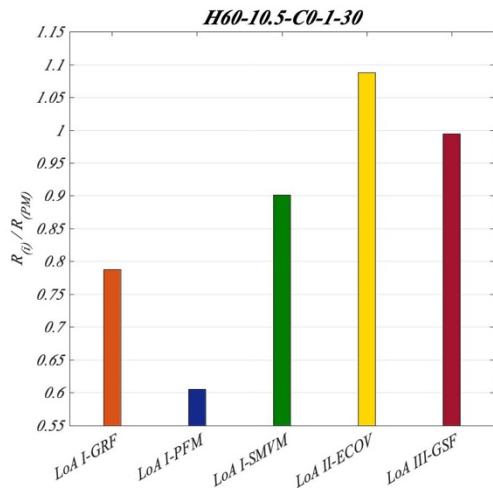
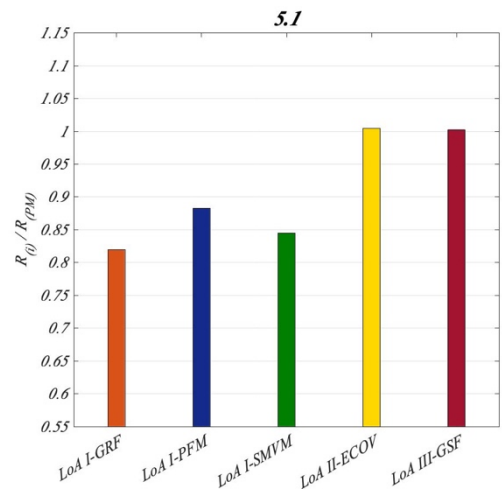
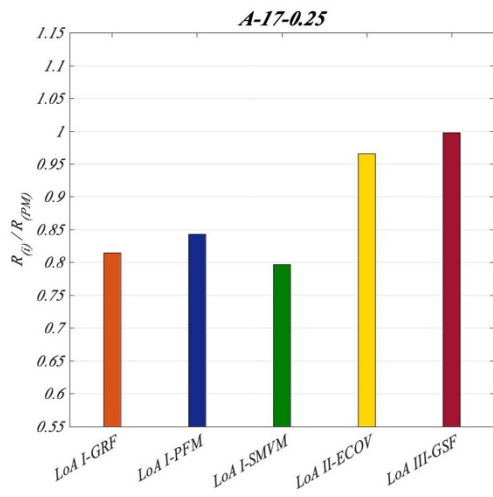
1. *LoA I – GRF*
2. *LoA I – PFM*
3. *LoA I – SMVM*
4. *LoA II – ECOV*
5. *LoA III – GSF*
6. *LoA III – PM*

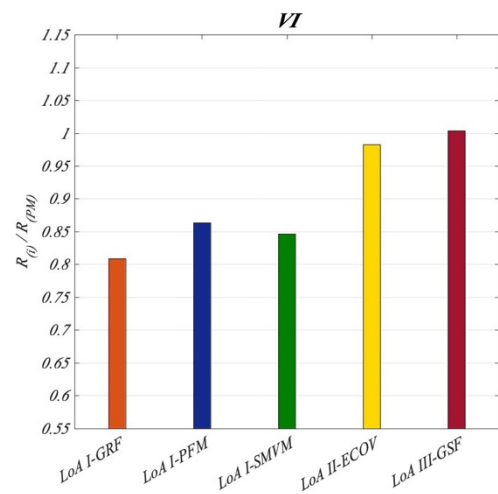
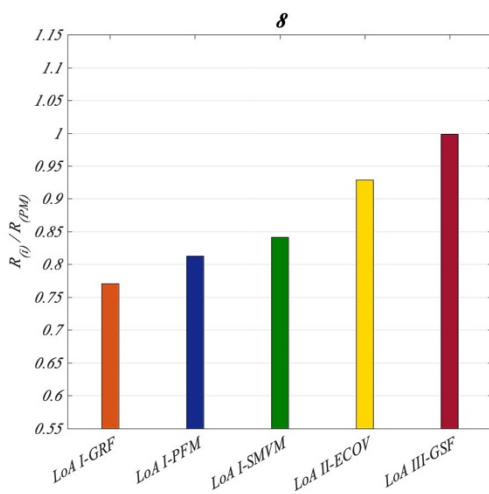
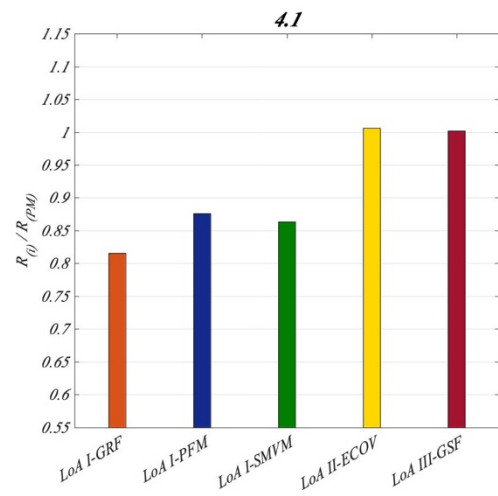
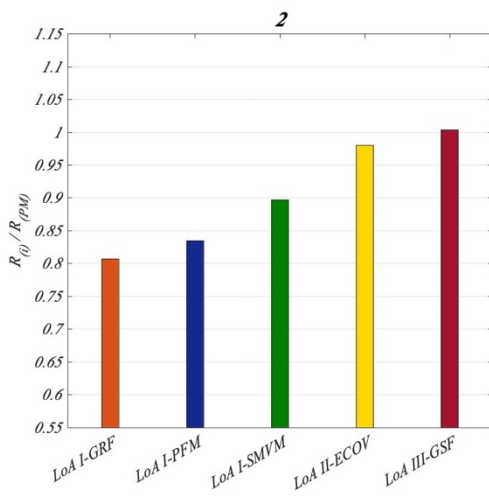
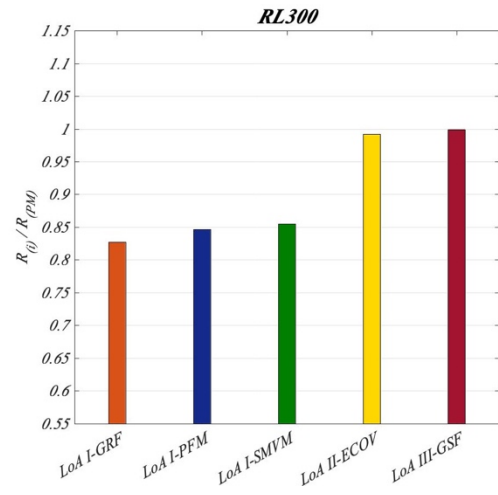
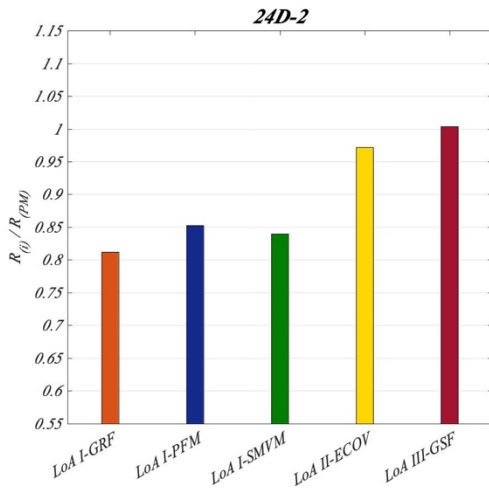
By this different representation, it is visible the Safety Format hierarchy in terms of results and accuracy respect to Probabilistic Method. Bar charts are reported by low to high slenderness; so the alteration of underestimation between *GRF*, *PFM*, *SMVM* occurs with good frequency but it does not represent an ambiguity because of they belong to same first levels of approximation. Particular attention can be focused on *ECOV* and its overestimation for very high slenderness values; anyway this equivocation , related to uncommon slenderness values in structural field, has already been addressed in paragraph 6.5.

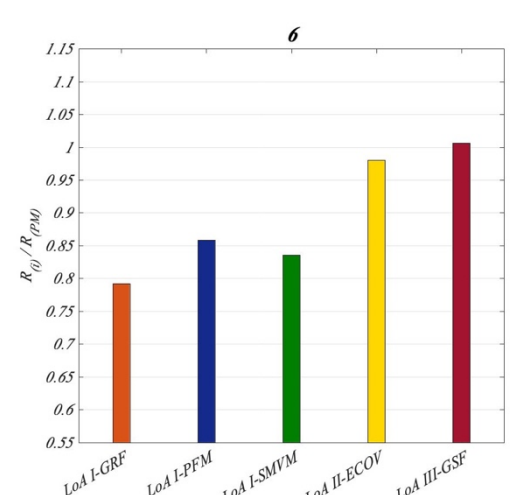
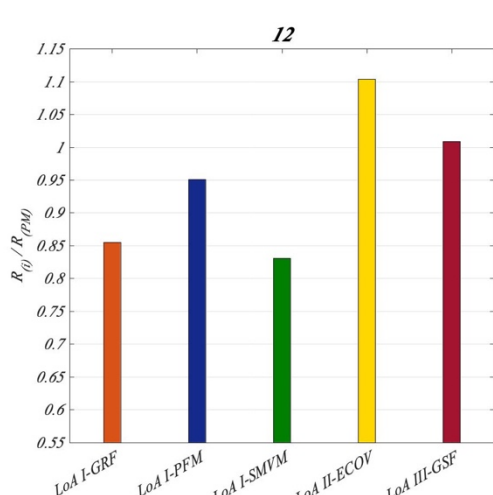
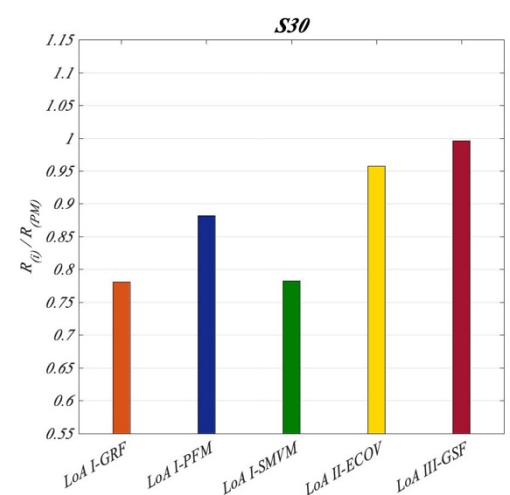
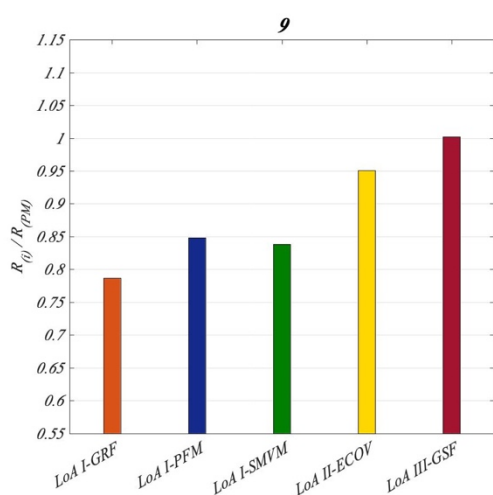
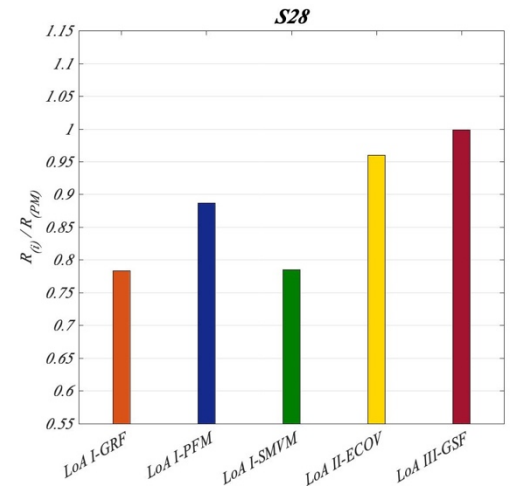
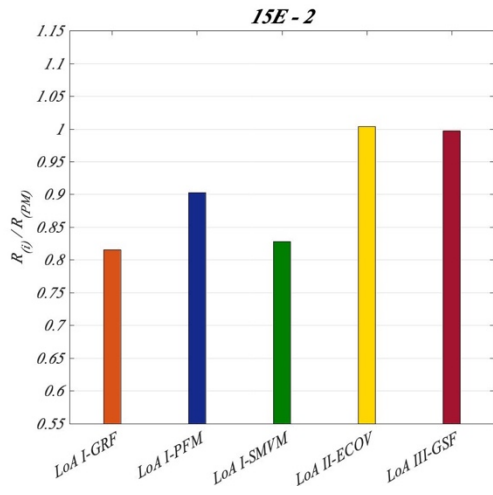
So for a restrained domain, it is possible to conclude that Safety Format hierarchy presents the expected results discuss in Chapter 7, with a little and legitimate overestimation respect to Probabilistic Method.

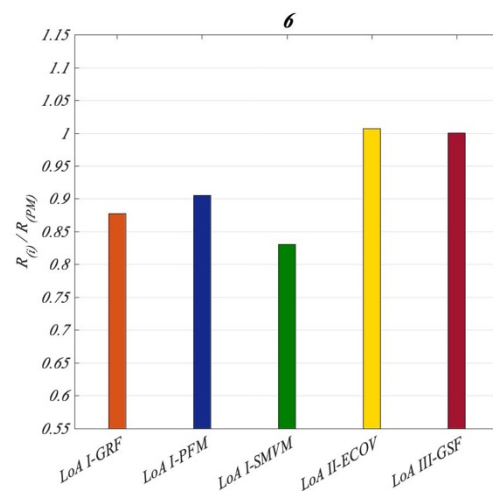
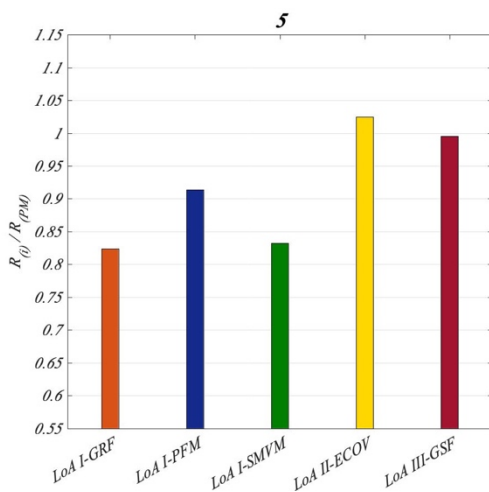
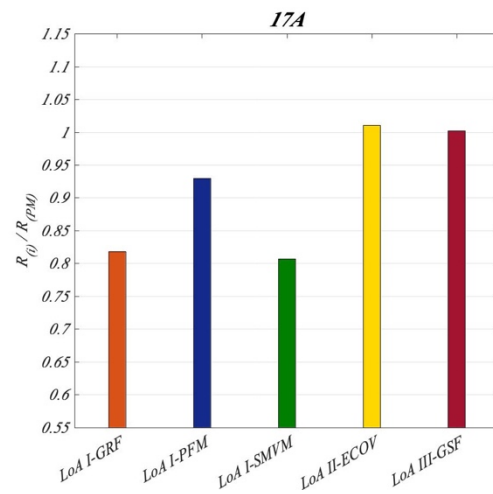
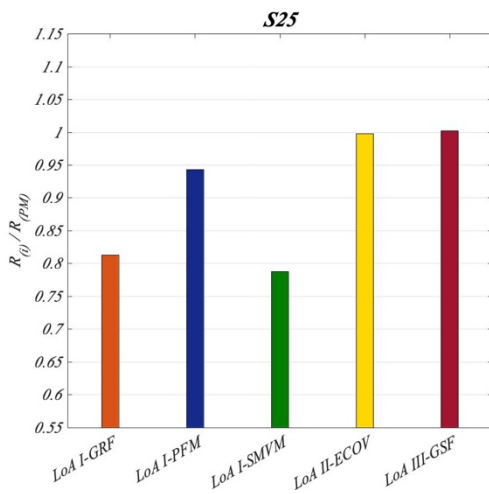
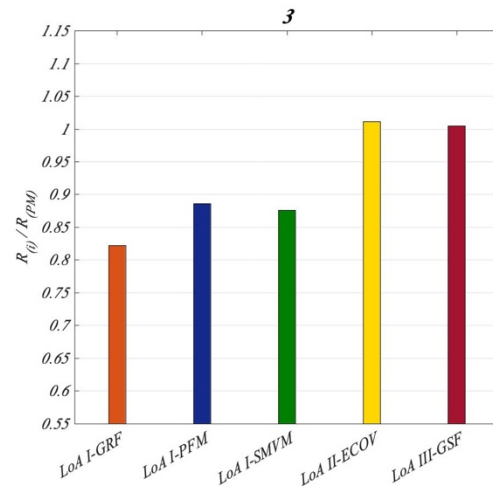
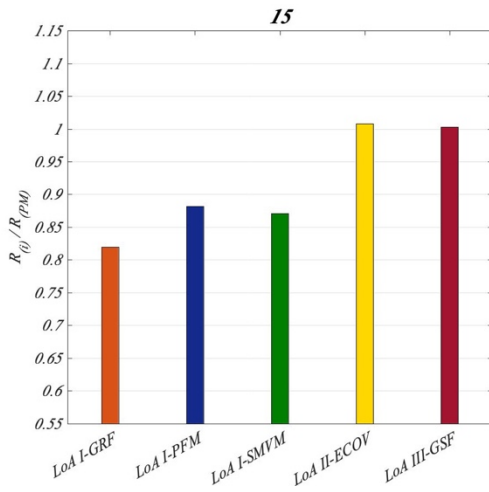


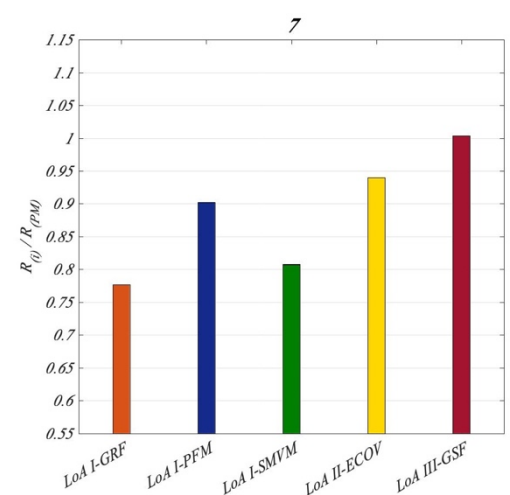
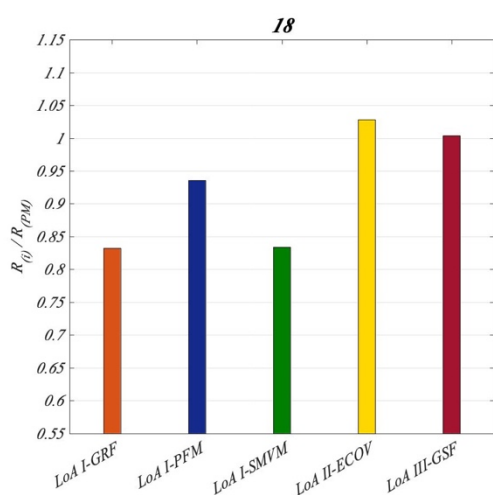
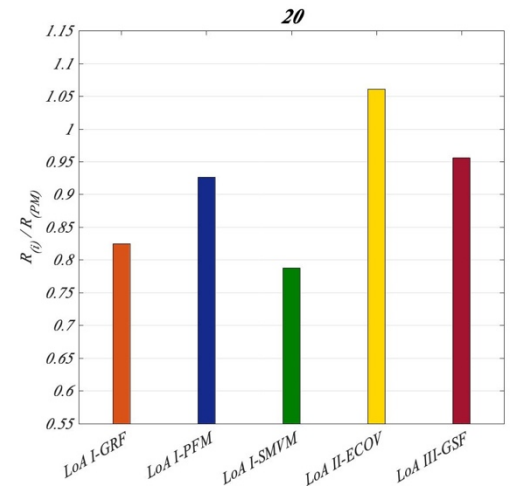
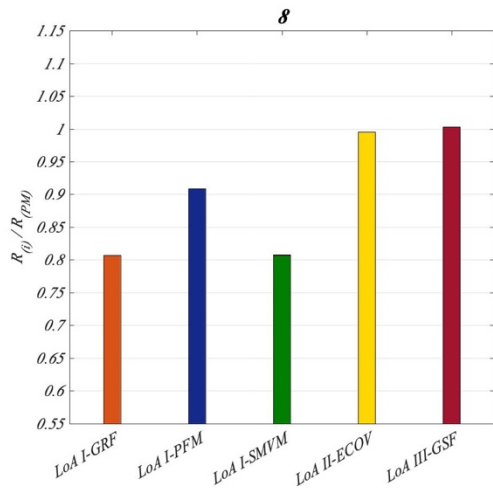




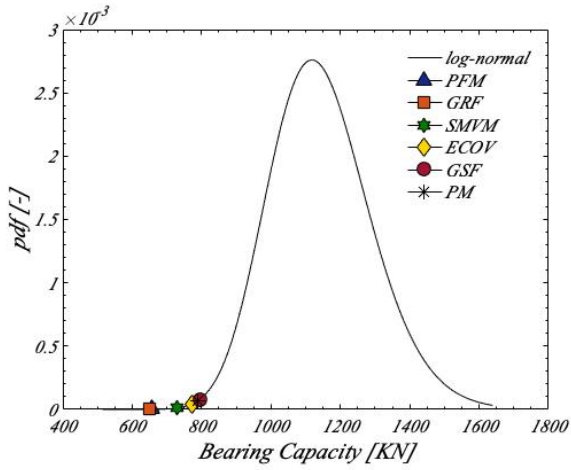






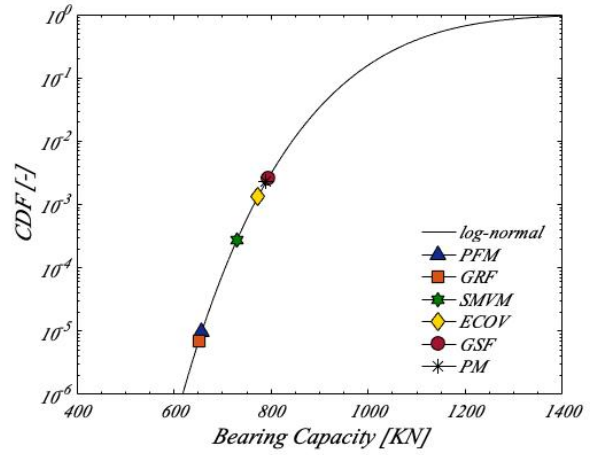


*9 Appendix A – Probability Density Functions and
Cumulative Density Functions of columns global resistance
log-normal distributions*



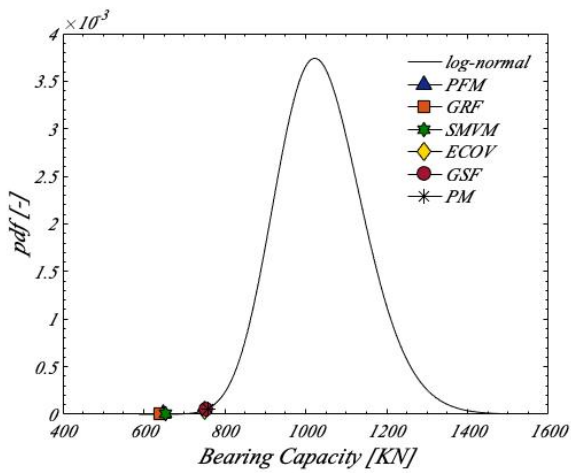
2L8-120R

log-normal - $\mu_N = 1146 \text{ KN}$ - $V_N = 0,1368$
 p-value=0,71



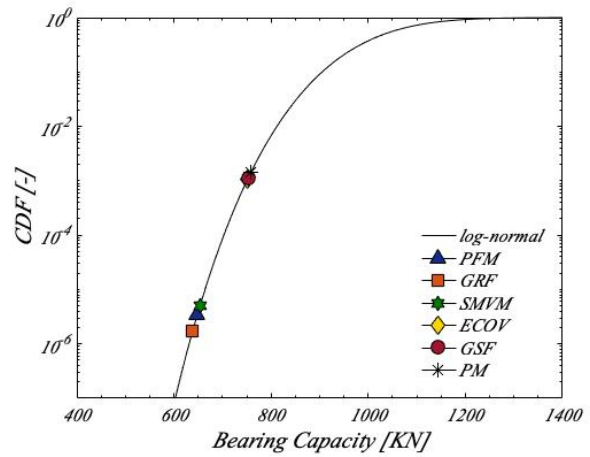
2L8-120R

log-normal - $\mu_N = 1146 \text{ KN}$ - $V_N = 0,1368$
 p-value=0,71



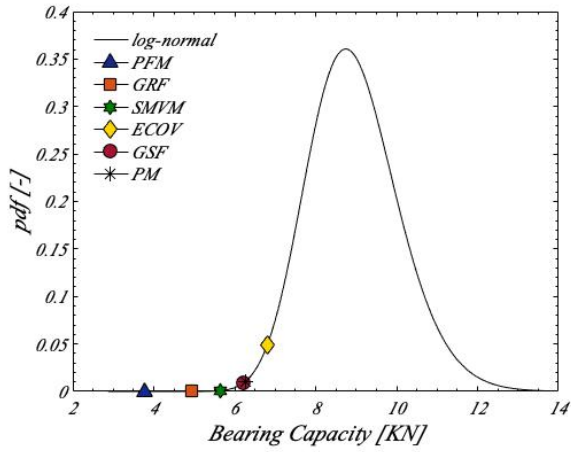
4L8-30

log-normal - $\mu_N = 1039,2 \text{ KN}$ - $V_N = 0,1093$
 p-value=0,81



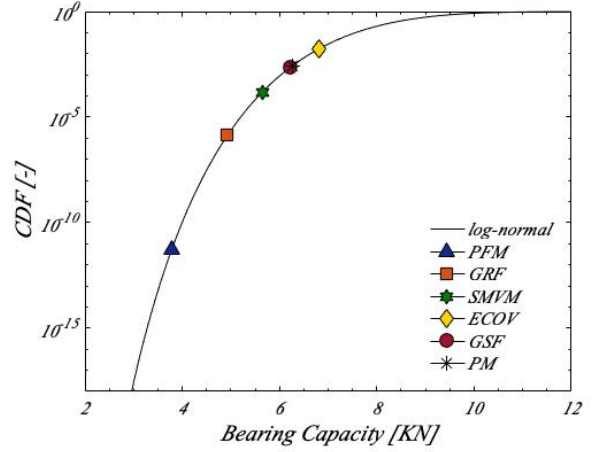
4L8-30

log-normal - $\mu_N = 1039,2 \text{ KN}$ - $V_N = 0,1093$
 p-value=0,81



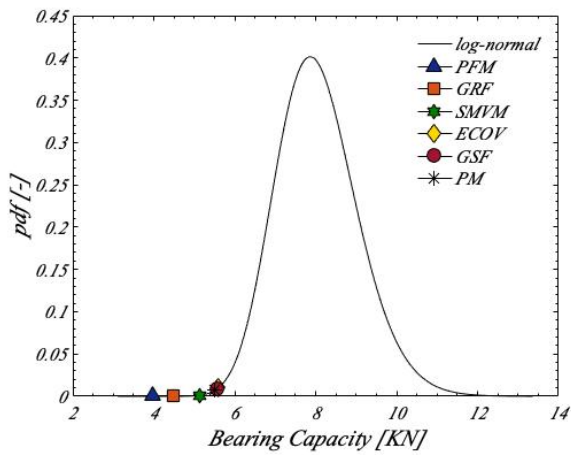
H60-10.5-C0-1-30

log-normal - $\mu_N = 8,95$ KN - $V_N = 0,1337$
 p-value=0,68



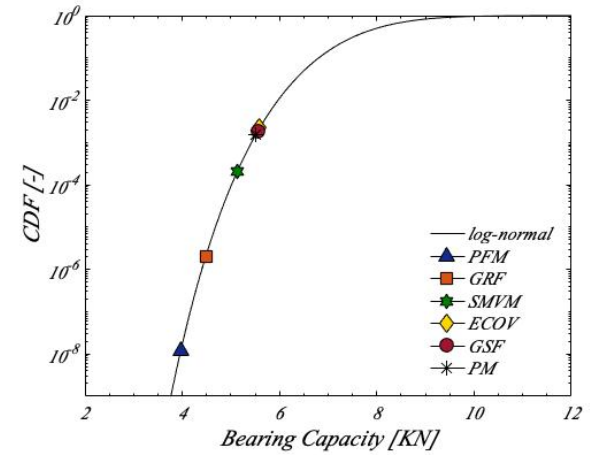
H60-10.5-C0-1-30

log-normal - $\mu_N = 8,95$ KN - $V_N = 0,1337$
 p-value=0,68



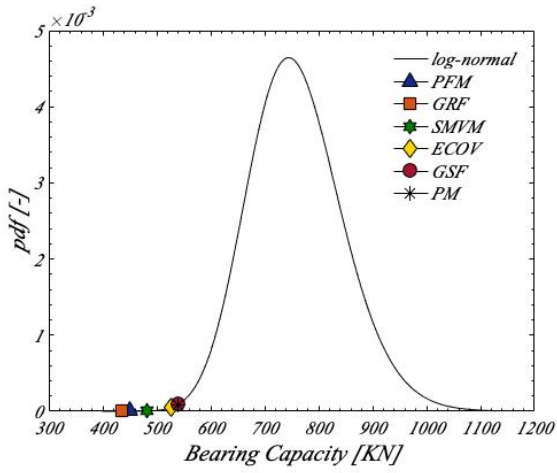
N30-10.5-C0-3.30

log-normal - $\mu_N = 8,05$ KN - $V_N = 0,1335$
 p-value=0,80



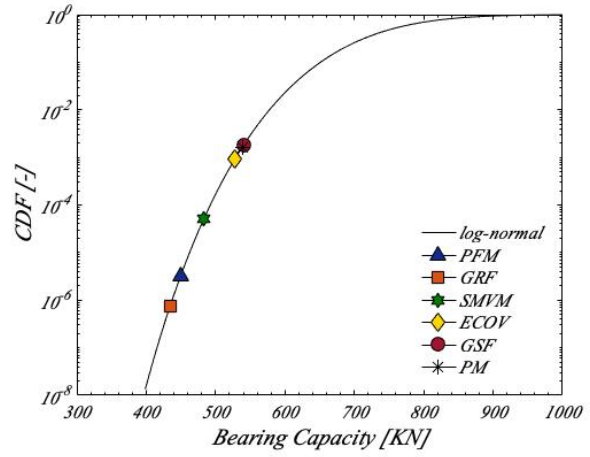
N30-10.5-C0-3.30

log-normal - $\mu_N = 8,05$ KN - $V_N = 0,1335$
 p-value=0,80



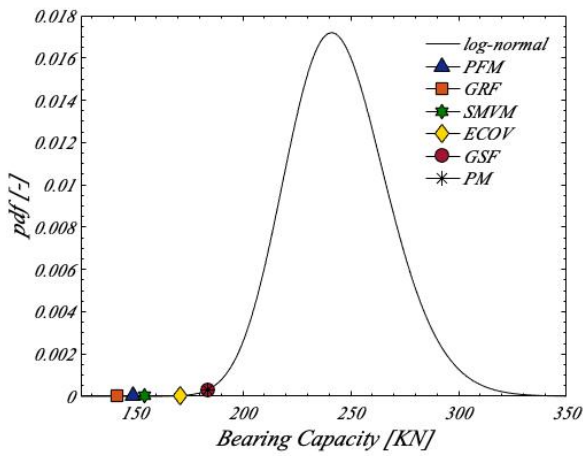
2

log-normal - $\mu_N = 759,2 \text{ KN}$ - $V_N = 0,1215$
 p-value=0,56



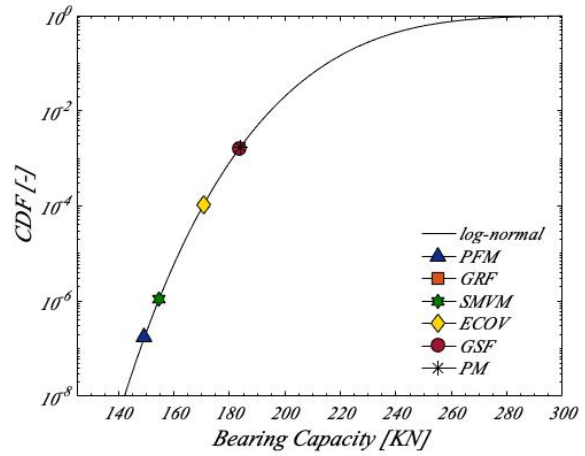
2

log-normal - $\mu_N = 759,2 \text{ KN}$ - $V_N = 0,1215$
 p-value=0,56



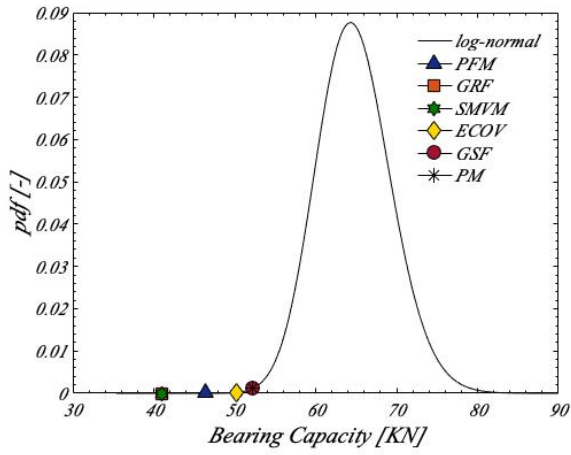
8

log-normal - $\mu_N = 244,5 \text{ KN}$ - $V_N = 0,1005$
 p-value=0,98

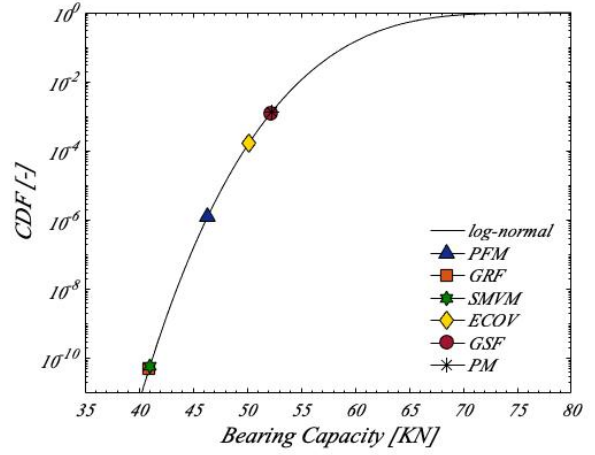


8

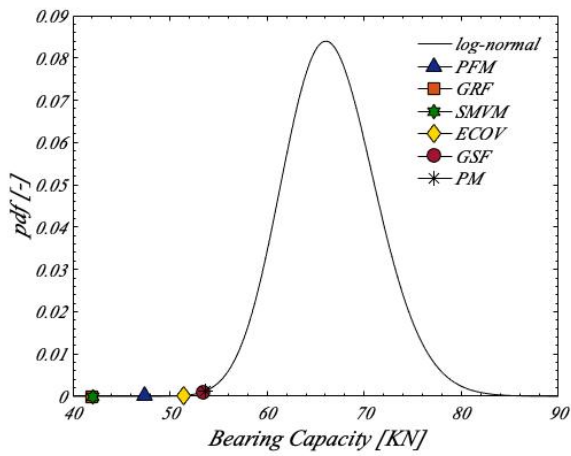
log-normal - $\mu_N = 244,5 \text{ KN}$ - $V_N = 0,1005$
 p-value=0,98



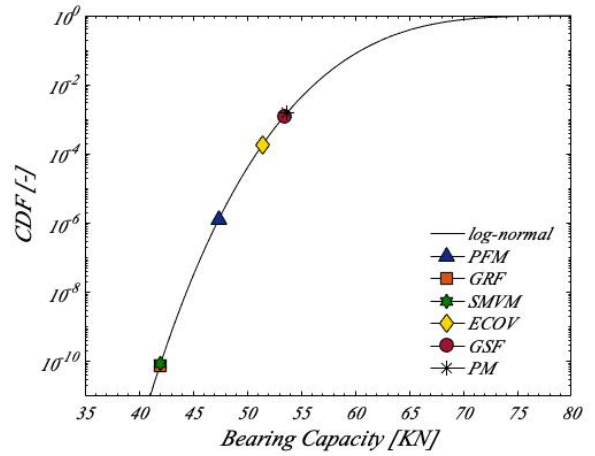
S28
 log-normal - $\mu_N = 64,8 \text{ KN}$ - $V_N = 0,0732$
 p-value=0,31



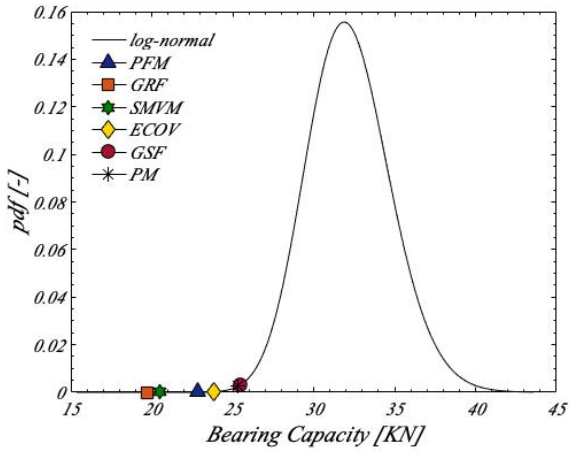
S28
 log-normal - $\mu_N = 64,8 \text{ KN}$ - $V_N = 0,0732$
 p-value=0,31



S30
 log-normal - $\mu_N = 66,6 \text{ KN}$ - $V_N = 0,0744$
 p-value=0,72

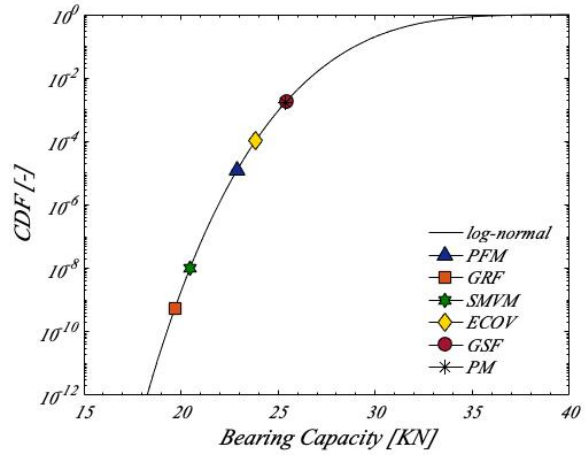


S30
 log-normal - $\mu_N = 66,6 \text{ KN}$ - $V_N = 0,0744$
 p-value=0,72



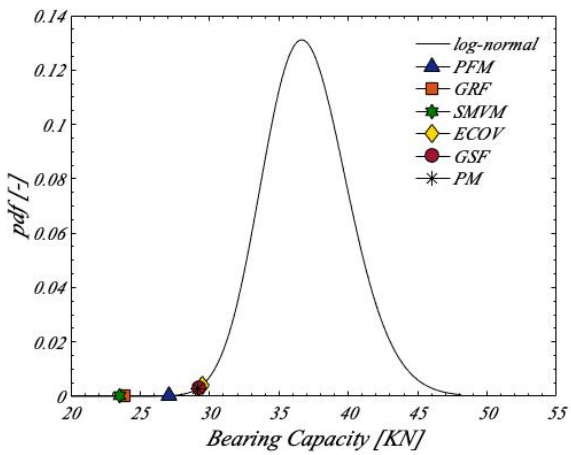
7

log-normal - $\mu_N = 32,2 \text{ KN}$ - $V_N = 0,0835$
p-value=0,85



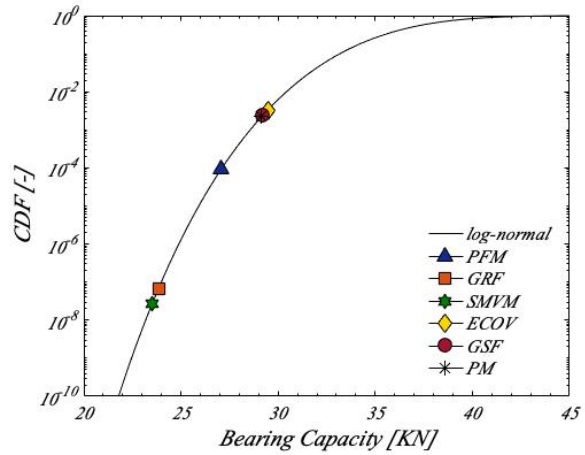
7

log-normal - $\mu_N = 32,2 \text{ KN}$ - $V_N = 0,0835$
p-value=0,85



17-A

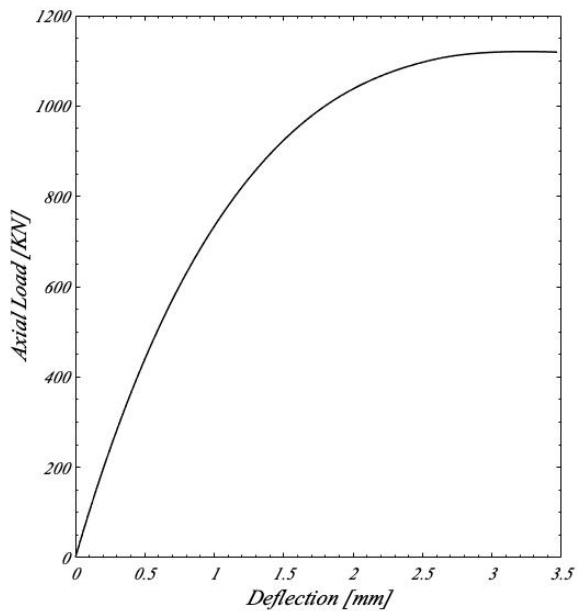
log-normal - $\mu_N = 37,0 \text{ KN}$ - $V_N = 0,0863$
p-value=0,80



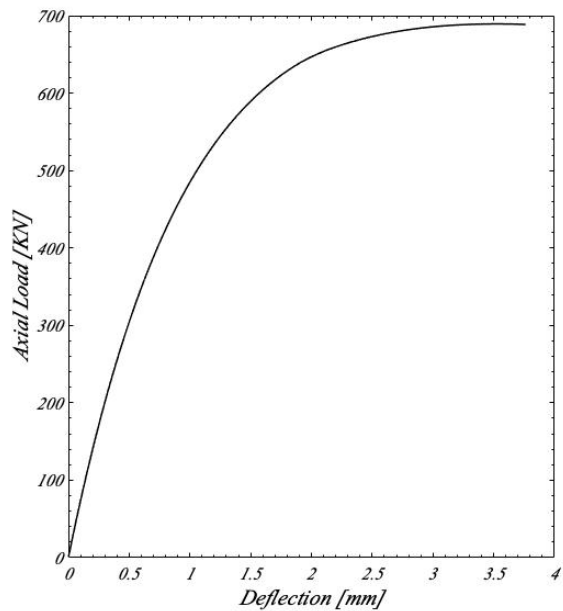
17-A

log-normal - $\mu_N = 37,0 \text{ KN}$ - $V_N = 0,0863$
p-value=0,80

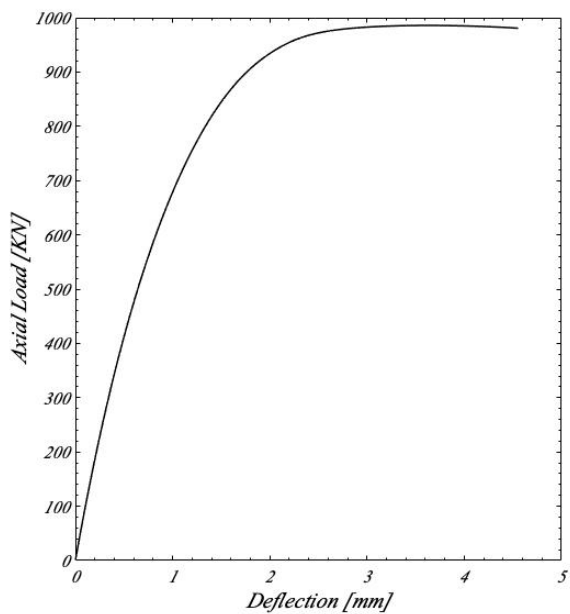
10 Appendix B – Graphics related to preliminary non-linear analyses (NLA1 and NLA2): Global axial load – deflection diagram and local fiber stress – strain diagram



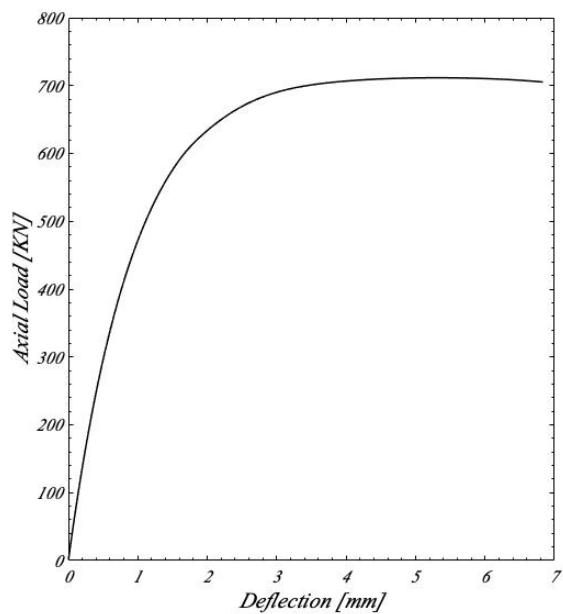
2L8-120R
NLA 1 - $l/h=9,7 - e_0/h=0,053$



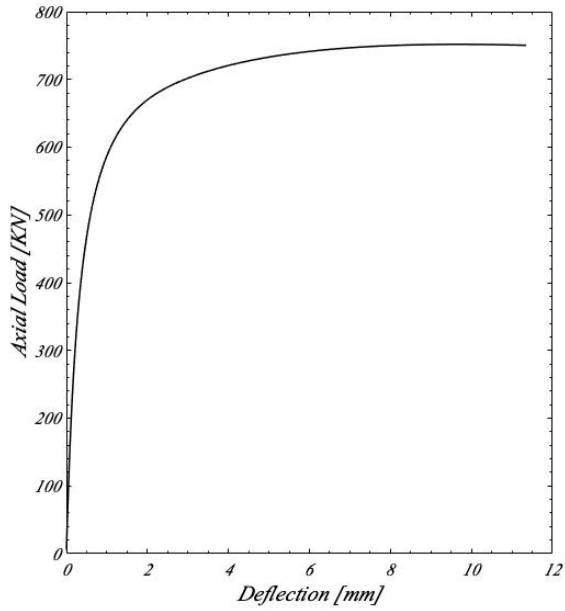
2L8-120R
NLA 2 - $l/h=9,7 - e_0/h=0,053$



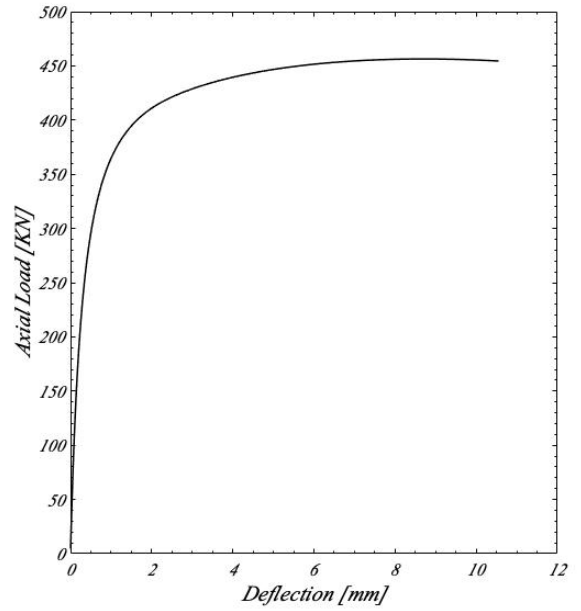
4L8-30
NLA 1 - $l/h=9,7 - e_0/h=0,053$



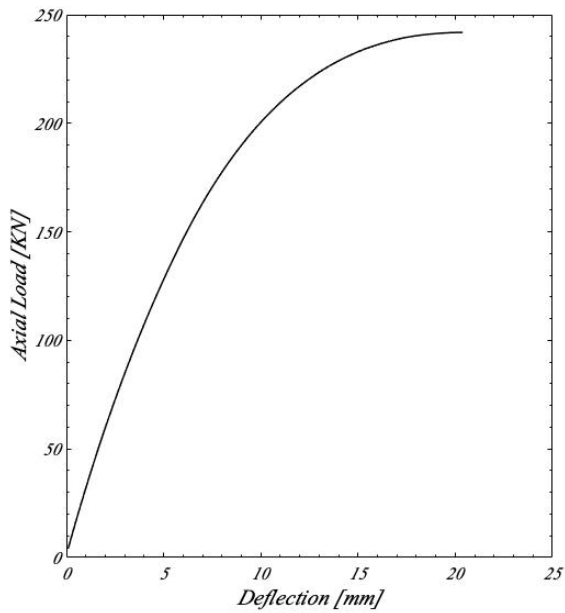
4L8-30
NLA 2 - $l/h=9,7 - e_0/h=0,053$



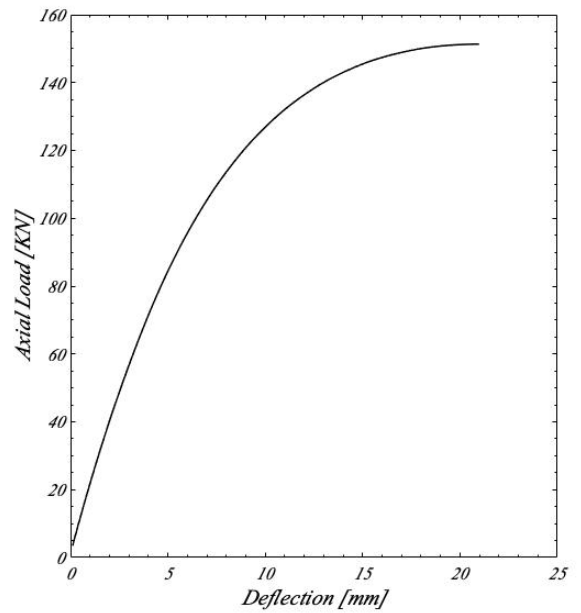
2
NLA 1 – $l/h=25,8 - e_0=0$



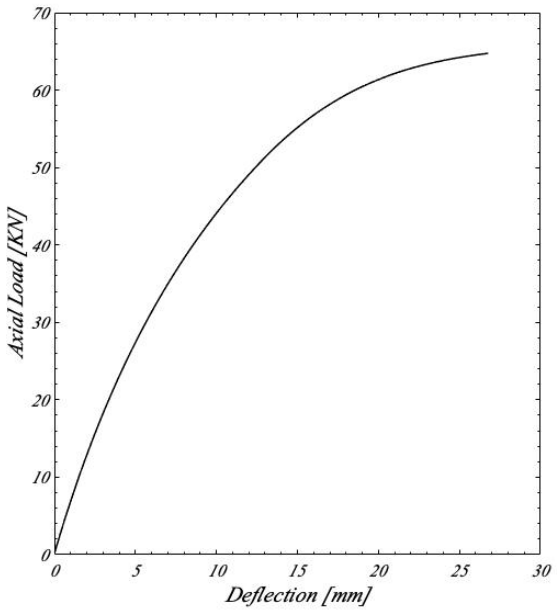
2
NLA 2 – $l/h=25,8 - e_0=0$



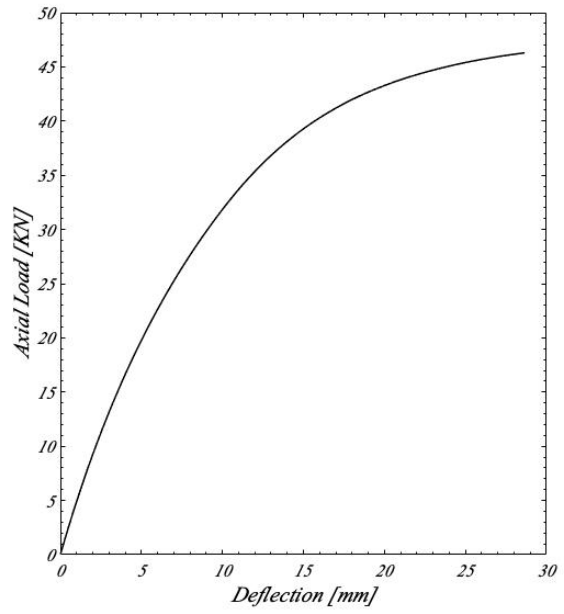
8
NLA 1 – $l/h=25,6 - e_0/h=0,200$



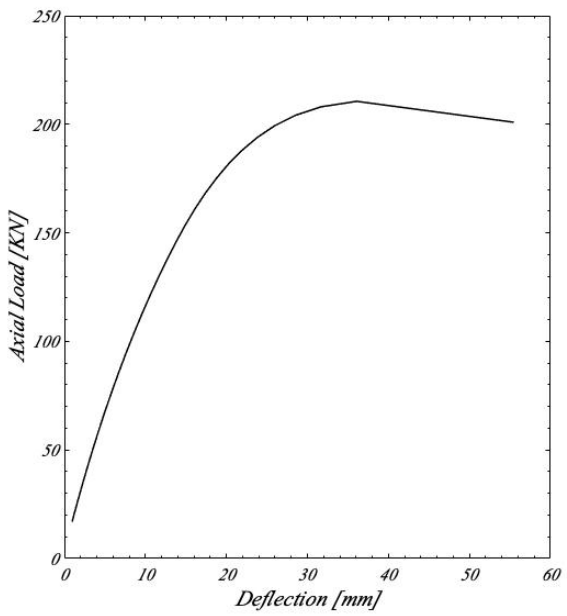
8
NLA 2 – $l/h=25,6 - e_0/h=0,200$



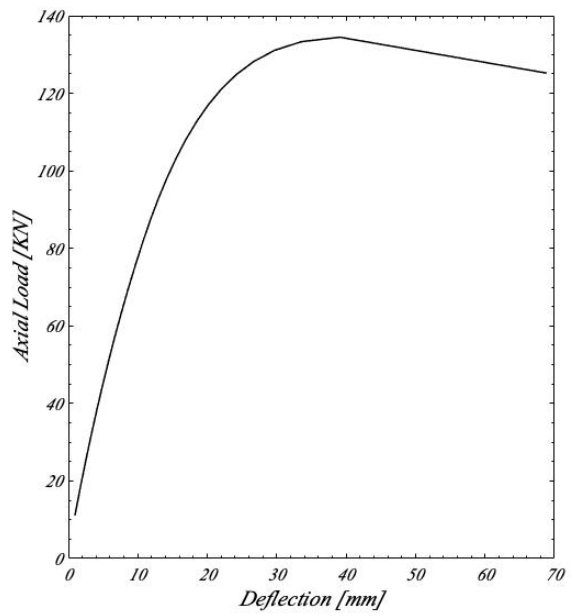
S28
NLA 1 – $l/h=48,1 - e_0/h=0,144$



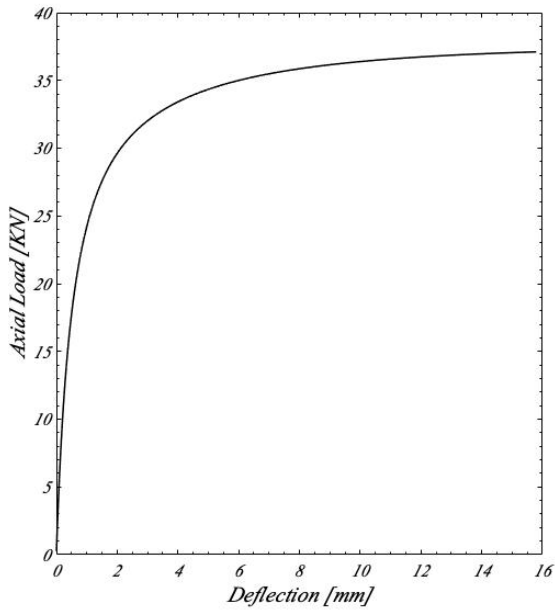
S28
NLA 2 – $l/h=48,1 - e_0/h=0,144$



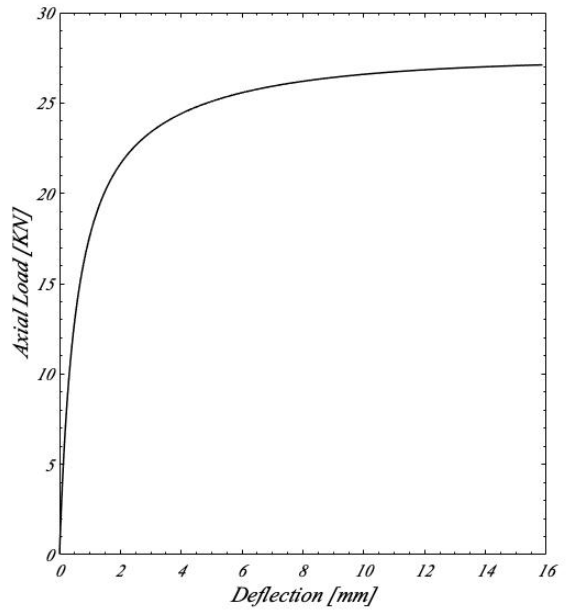
9
NLA 1 – $l/h=40,2 - e_0/h=0,200$



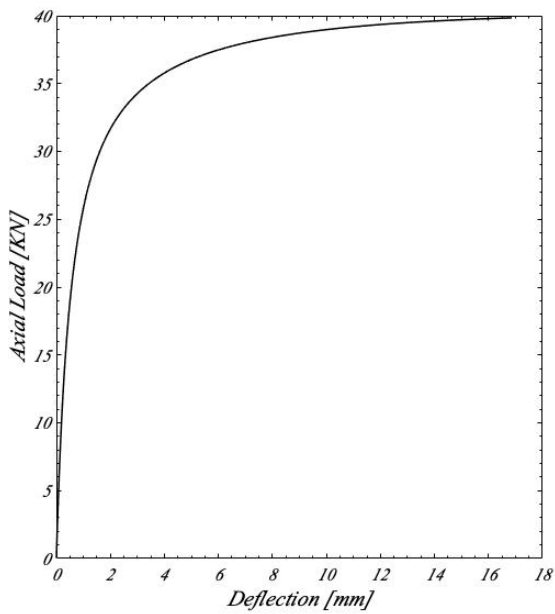
9
NLA 2 – $l/h=40,2 - e_0/h=0,200$



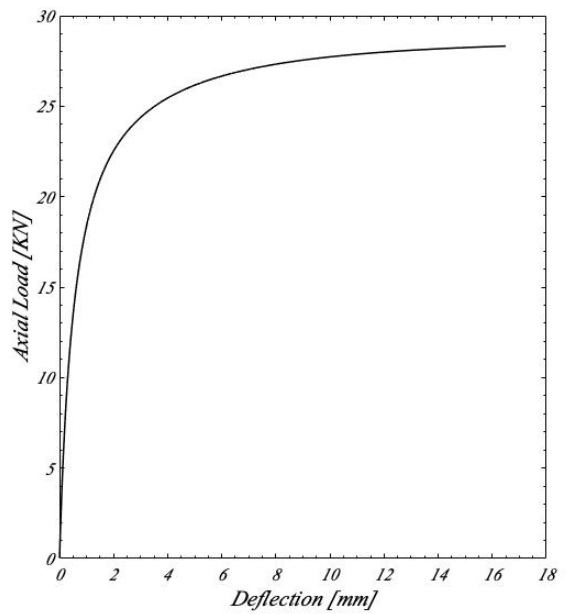
17-A
NLA 1 – $l/h=65 - e_0=0$



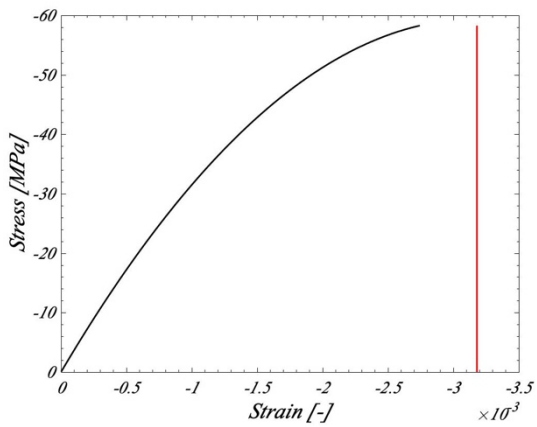
17-A
NLA 2 – $l/h=65 - e_0=0$



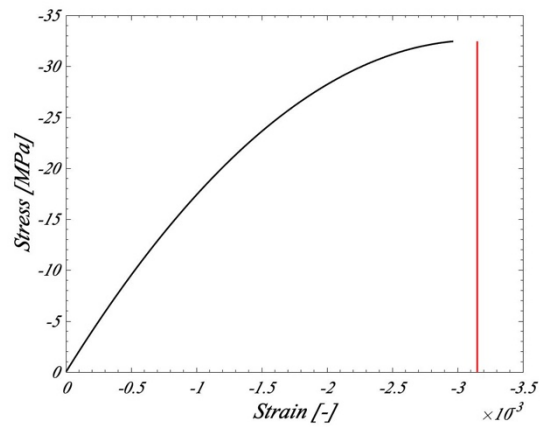
18
NLA 1 – $l/h=70,1 - e_0=0$



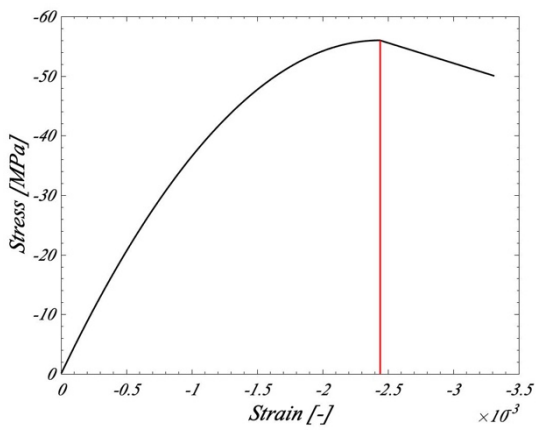
18
NLA 2 – $l/h=70,1 - e_0=0$



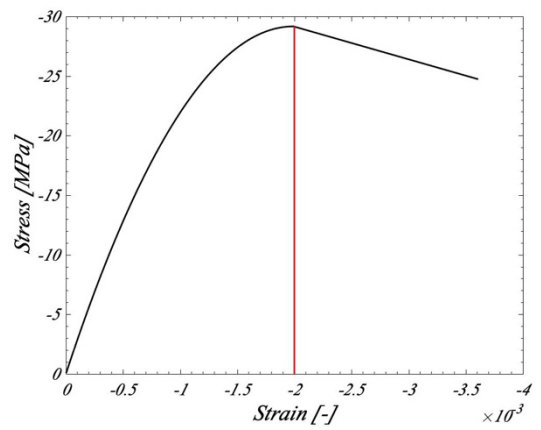
2L8-120R - NLA 1 - Confined concrete behavior



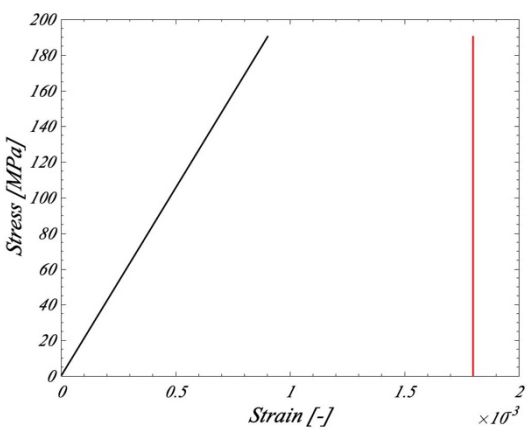
2L8-120R - NLA 2 - Confined concrete behavior



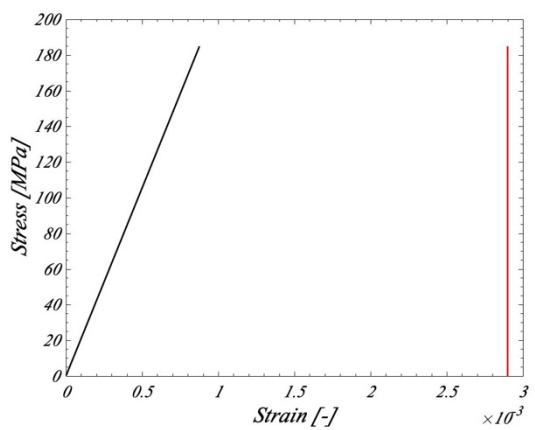
2L8-120R - NLA 1 - Unconfined concrete behavior



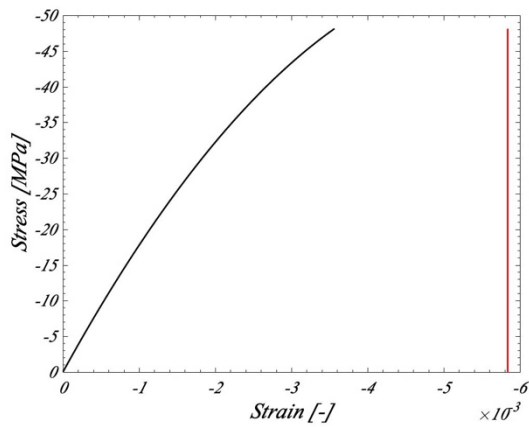
2L8-120R - NLA 2 - Unconfined concrete behavior



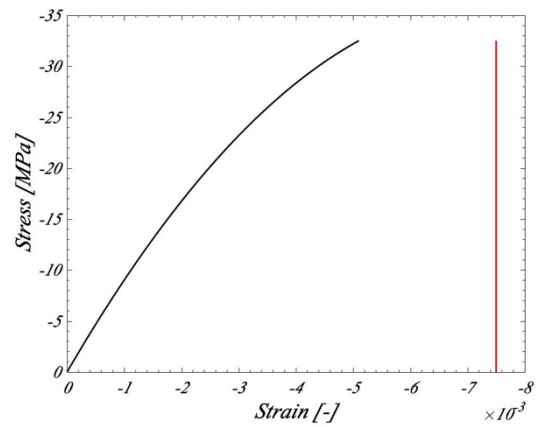
2L8-120R - NLA 1 - Steel behavior



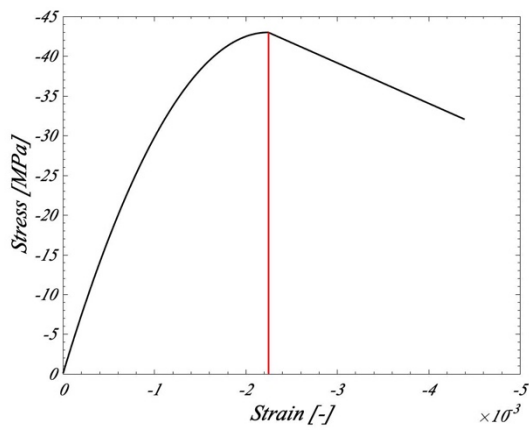
2L8-120R - NLA 2 - Steel behavior



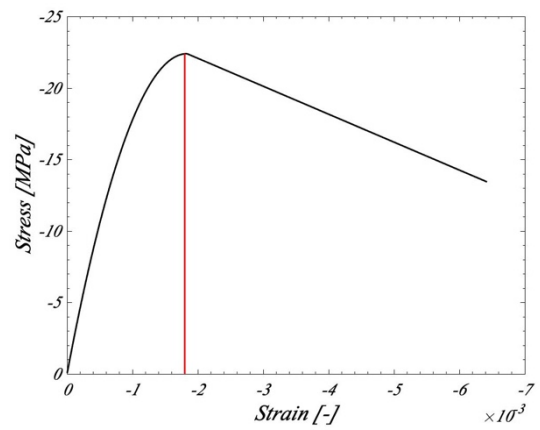
4L8-30 - NLA 1 - Confined concrete behavior



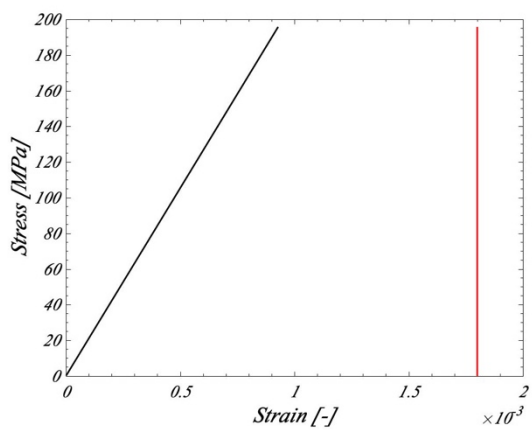
4L8-30 - NLA 2 - Confined concrete behavior



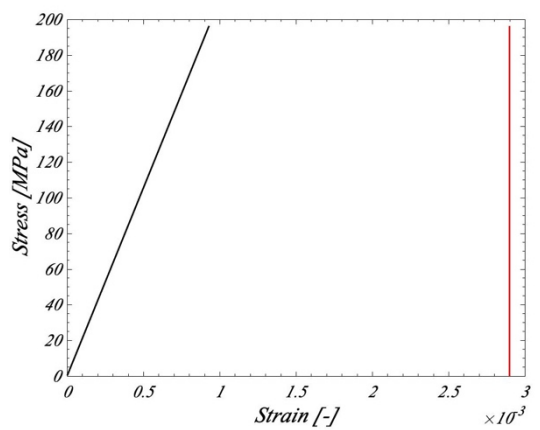
4L8-30 - NLA 1 - Unconfined concrete behavior



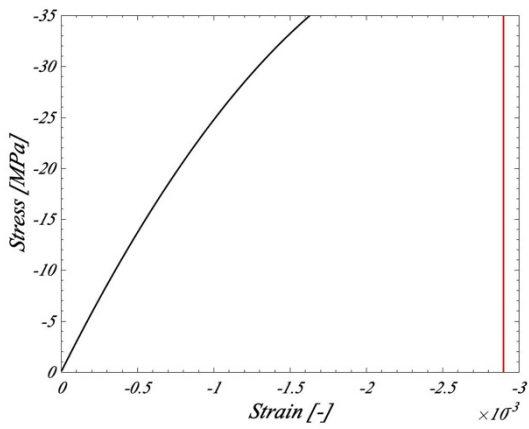
4L8-30 - NLA 2 - Unconfined concrete behavior



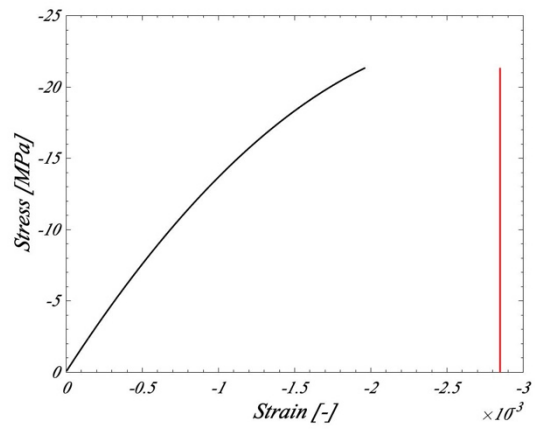
4L8-30 - NLA 1 - Steel behavior



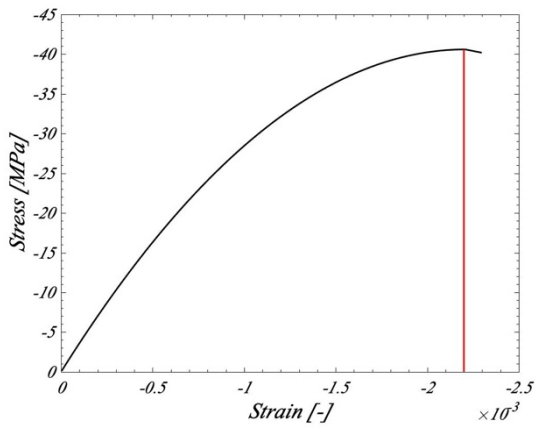
4L8-30 - NLA 2 - Steel behavior



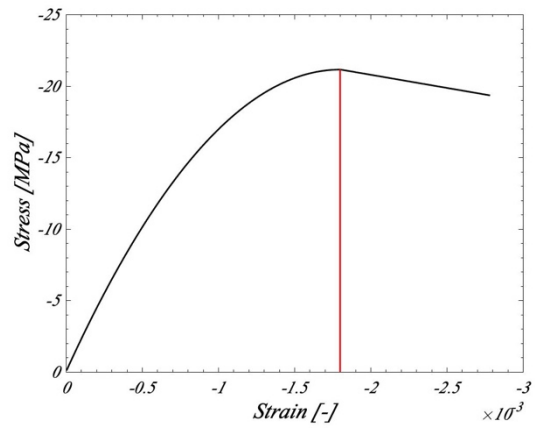
5.1 - NLA 1 - Confined concrete behavior



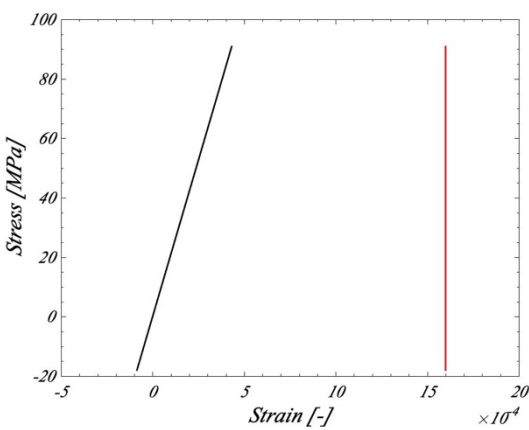
5.1 - NLA 2 - Confined concrete behavior



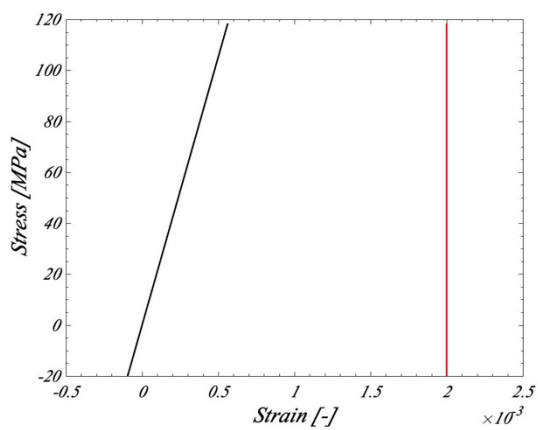
5.1 - NLA 1 - Unconfined concrete behavior



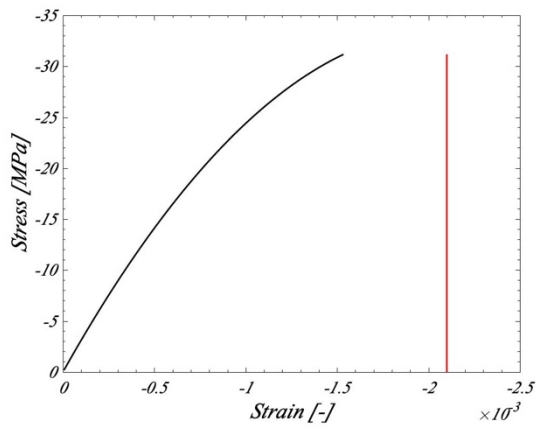
5.1 - NLA 2 - Unconfined concrete behavior



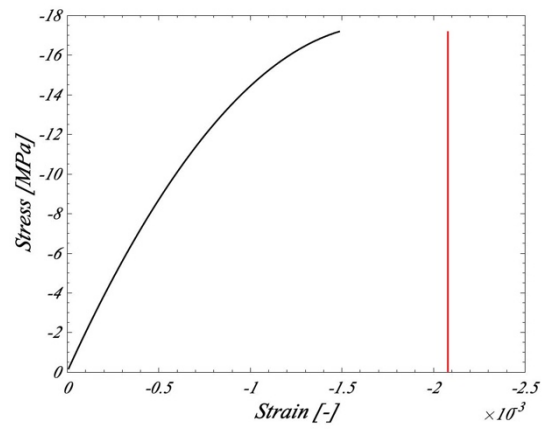
5.1 - NLA 1 - Steel behavior



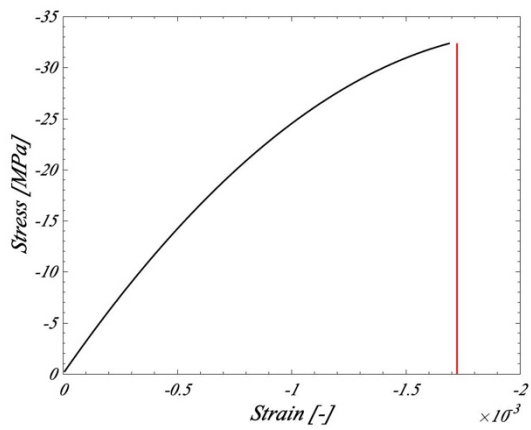
5.1 - NLA 2 - Steel behavior



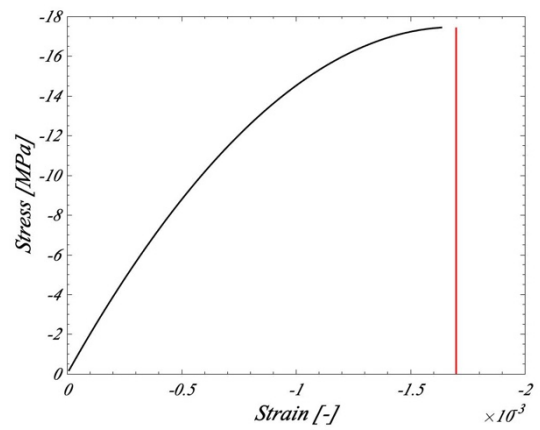
2 - NLA 1 - Confined concrete behavior



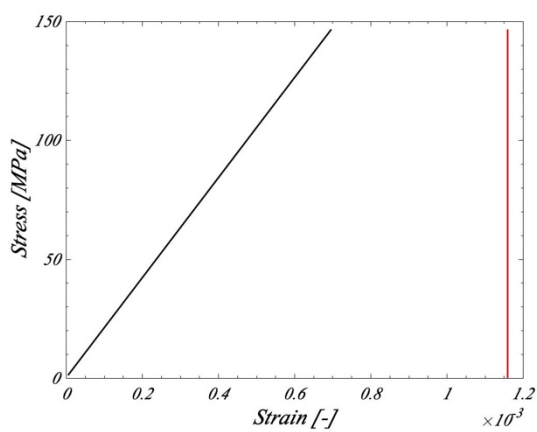
2 - NLA 2 - Confined concrete behavior



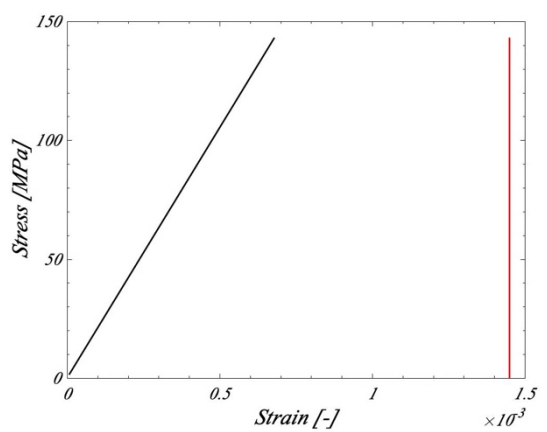
2 - NLA 1 - Unconfined concrete behavior



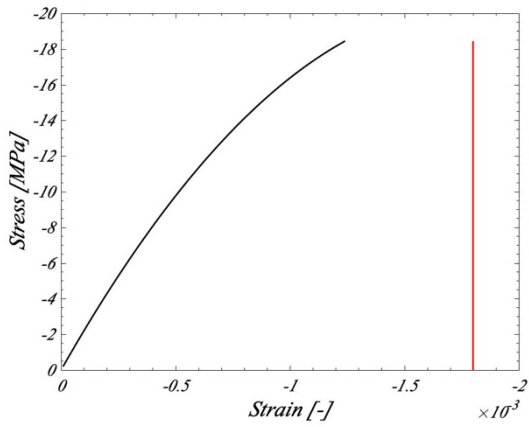
2 - NLA 2 - Unconfined concrete behavior



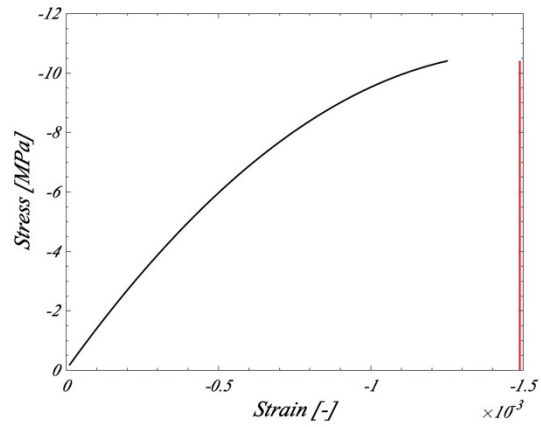
2 - NLA 1 - Steel behavior



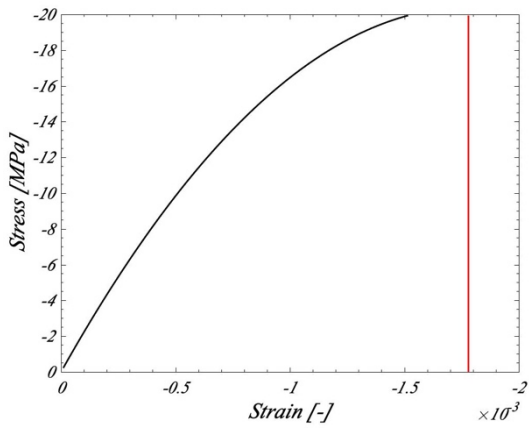
2 - NLA 2 - Steel behavior



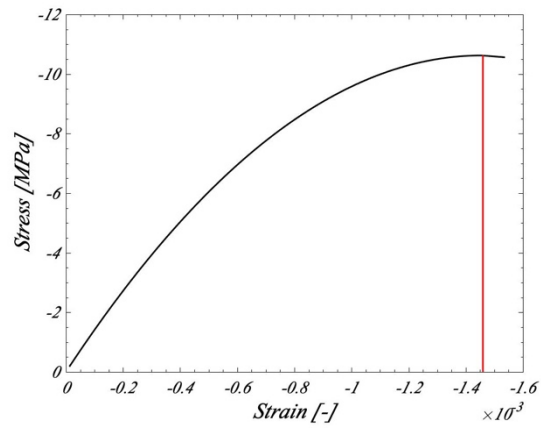
8 - NLA 1 - Confined concrete behavior



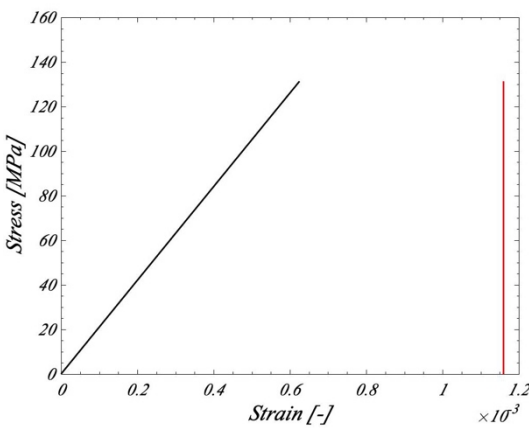
8 - NLA 2 - Confined concrete behavior



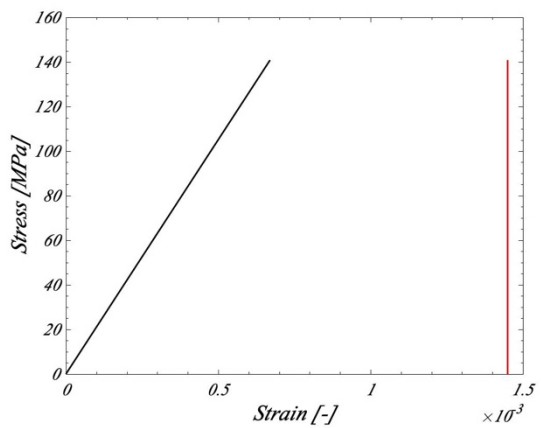
8 - NLA 1 - Unconfined concrete behavior



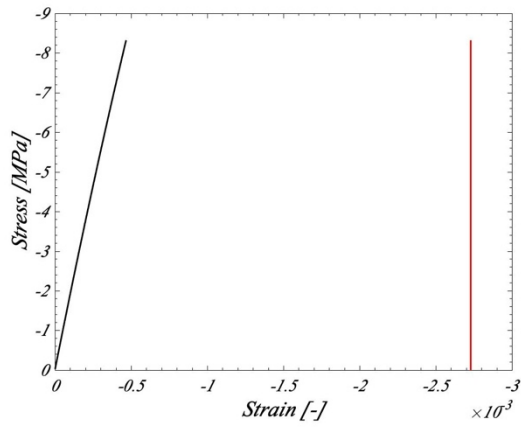
8 - NLA 2 - Unconfined concrete behavior



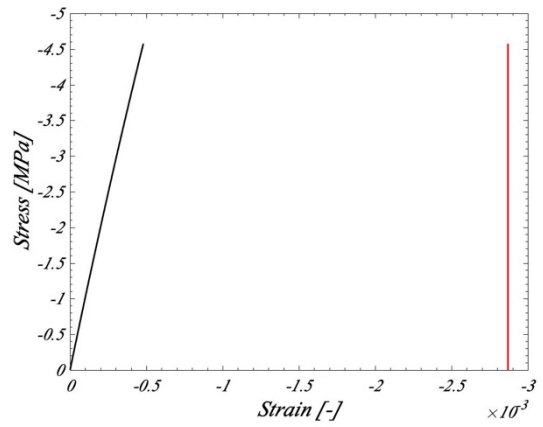
8 - NLA 1 - Steel behavior



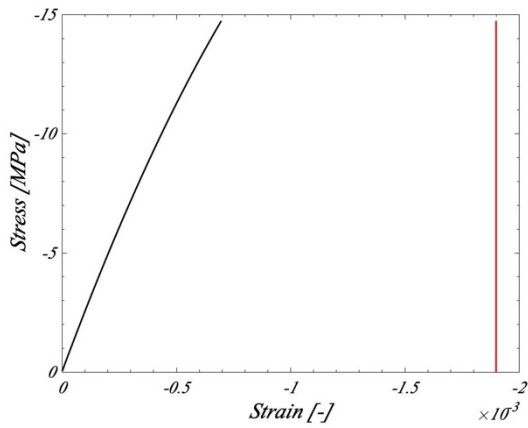
8 - NLA 2 - Steel behavior



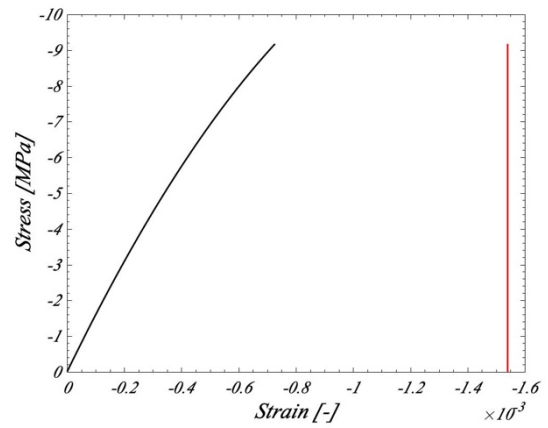
S28 - NLA 1 - Confined concrete behavior



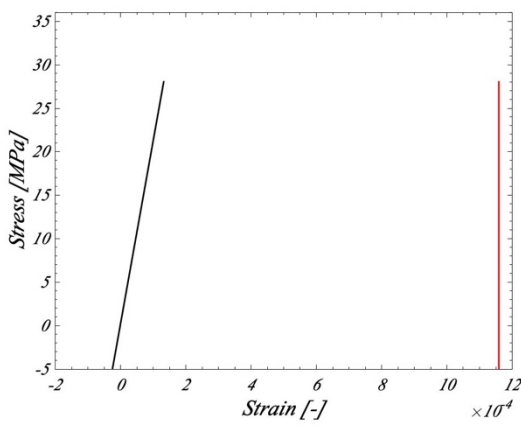
S28 - NLA 2 - Confined concrete behavior



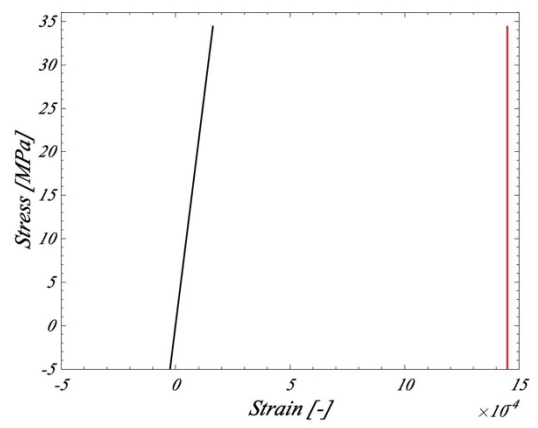
S28 - NLA 1 - Unconfined concrete behavior



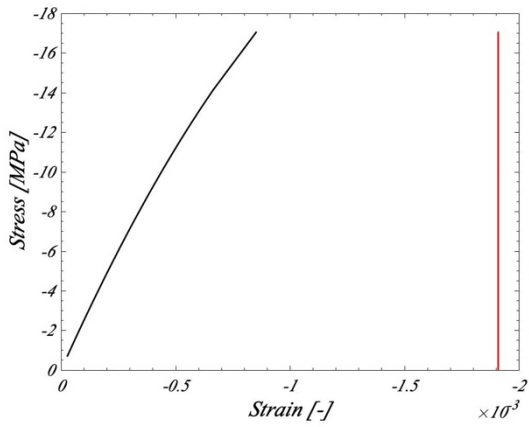
S28 - NLA 2 - Unconfined concrete behavior



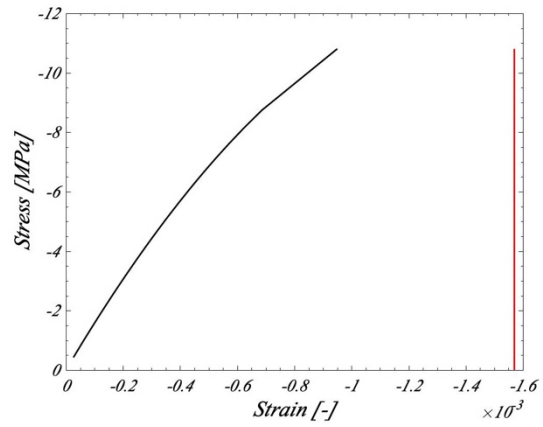
S28 - NLA 1 - Steel behavior



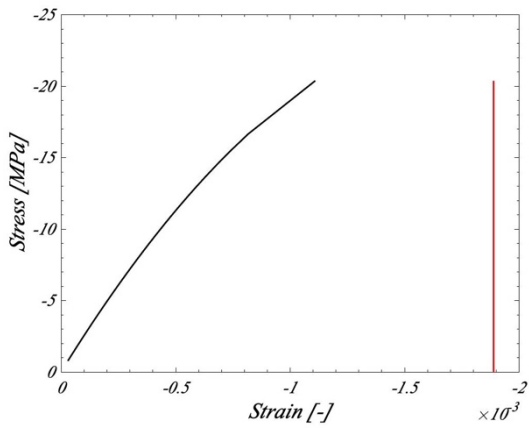
S28 - NLA 2 - Steel behavior



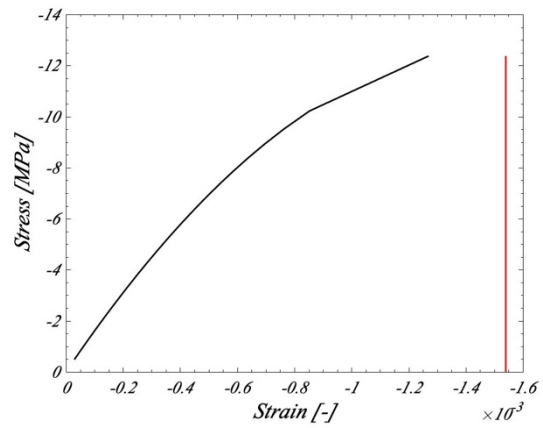
9 - NLA 1 - Confined concrete behavior



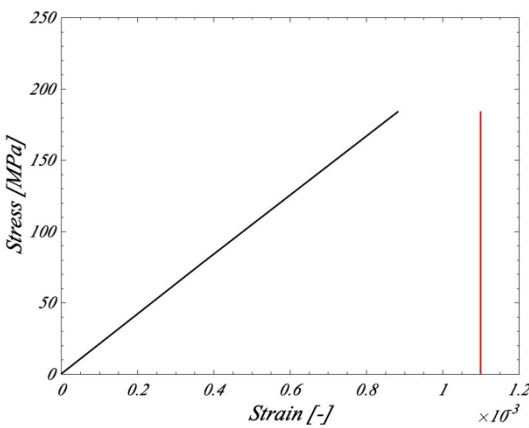
9 - NLA 2 - Confined concrete behavior



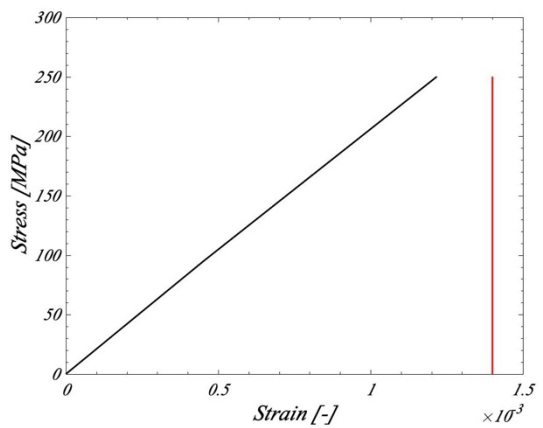
9 - NLA 1 - Unconfined concrete behavior



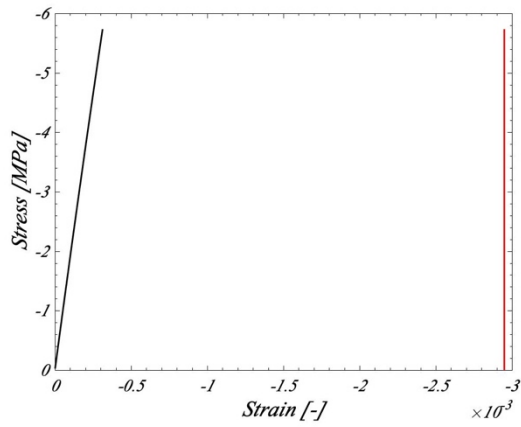
9 - NLA 2 - Unconfined concrete behavior



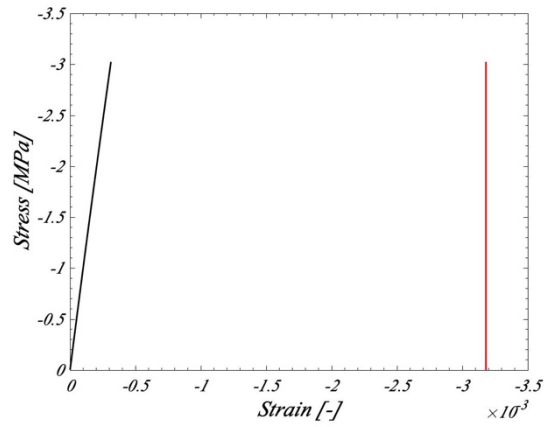
9 - NLA 1 - Steel behavior



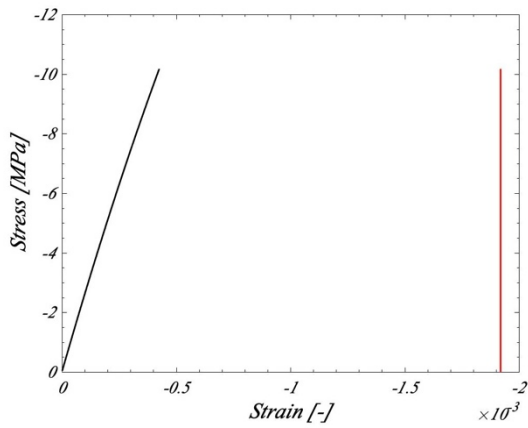
9 - NLA 2 - Steel behavior



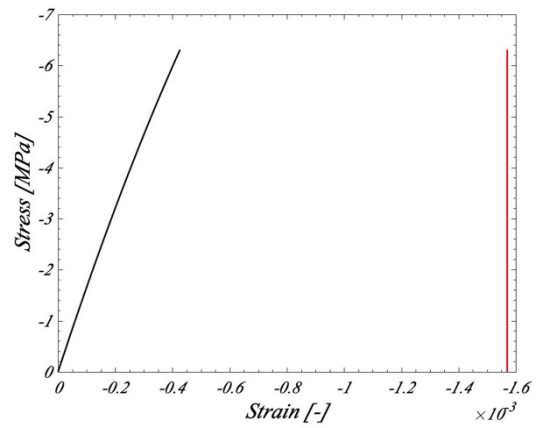
17-A - NLA 1 - Confined concrete behavior



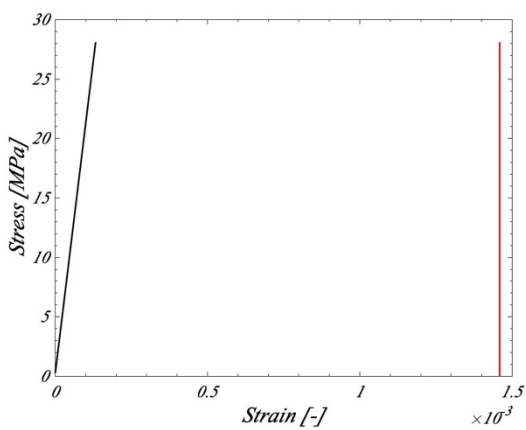
17-A - NLA 2 - Confined concrete behavior



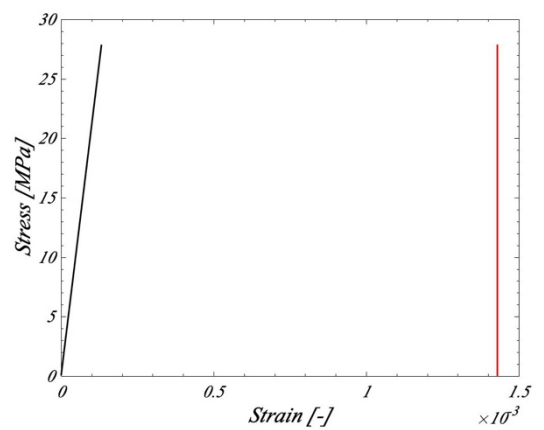
17-A - NLA 1 - Unconfined concrete behavior



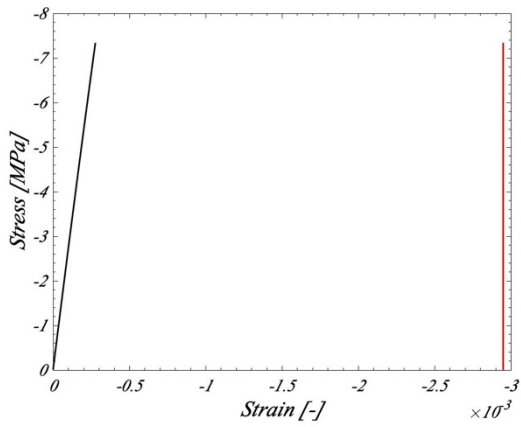
17-A - NLA 2 - Unconfined concrete behavior



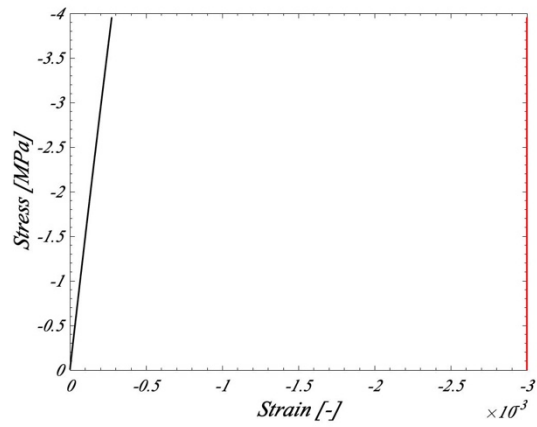
17-A - NLA 1 - Steel behavior



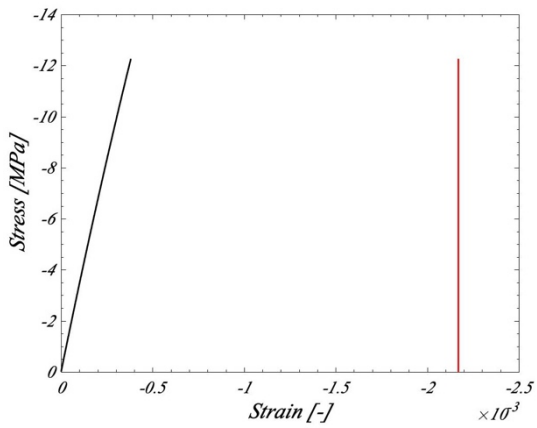
17-A - NLA 2 - Steel behavior



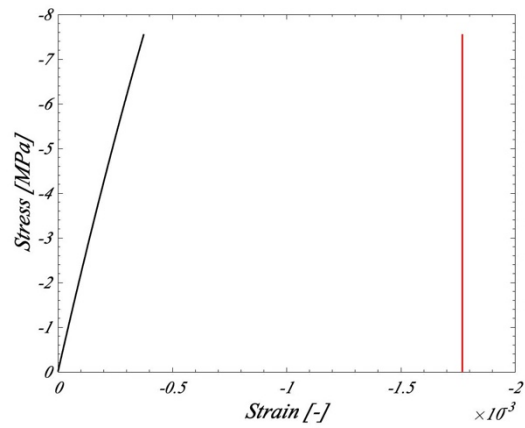
18 - NLA 1 - Confined concrete behavior



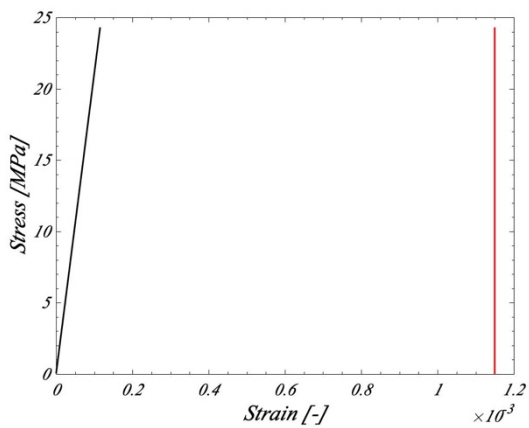
18 - NLA 2 - Confined concrete behavior



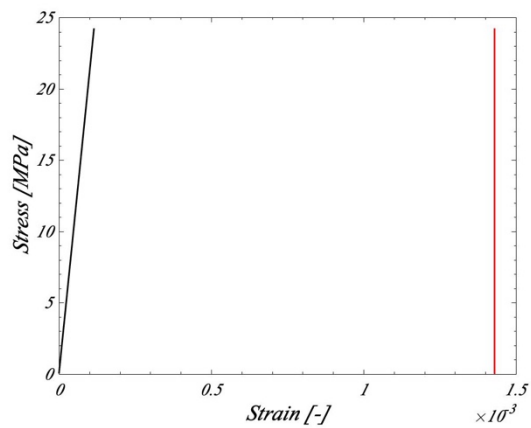
18 - NLA 1 - Unconfined concrete behavior



18 - NLA 2 - Unconfined concrete behavior



18 - NLA 1 - Steel behavior



18 - NLA 2 - Steel behavior

11 Appendix C – Example of OpenSees C++ code


```

#
set fccm 32.5694381629616;
set fccu 6.51388763259231;
set Eccm 31869.4974790669;
set epscc1 0.00315232672247369;
set epsccul 0.031;
set fcctm 2.29579699985319;
set Ect 708.316305291366;
#
# define UNCONFINED CONCRETE properties
#
set fcm 29.1698774497178;
set fcu 5.83397548994355;
set Ecm 30719.6781604866;
set epsc1 0.00199171762914162;
set epscul 0.0105;
set fctm 2.29579699985319;
set Et 708.316305291366;
#
# define STEEL properties
#
set fym 480;
set fsu 494.4;
set bs 0.03;
set Es 210000;
set epsy 0.00228571428571429;
set esh 0.045;
set epsu 0.07;
set Esh 576.000000000001;
set lsr 9.91735537190083;
#
#
# define ECCENTRICITY -----
#
set eh 8;
#
#
# define Column -----
#
set rin 400;
#
# ----- End -----
# -----

#
#
# ----- Define nodal coordinates -----
#
# In a 2D problem only the x and y coordinates need to be defined, using the node
command:
# node $nodeTag $X $Y
#
node 1 $eh -$rin;
node 2 0.0 -$rin;
node 3 0.0 0.0
node 4 0.0 [expr $Lcolonna/9];
node 5 0.0 [expr ($Lcolonna*2)/9];
node 6 0.0 [expr ($Lcolonna*3)/9];
node 7 0.0 [expr ($Lcolonna*4)/9];
node 8 0.0 [expr ($Lcolonna*5)/9];
node 9 0.0 [expr ($Lcolonna*6)/9];
node 10 0.0 [expr ($Lcolonna*7)/9];
node 11 0.0 [expr ($Lcolonna*8)/9];
node 12 0.0 $Lcolonna;
node 13 0.0 [expr $Lcolonna+$rin];
node 14 $eh [expr $Lcolonna+$rin];
#
#

```

```

# Boundary conditions are defined using fix command:
# fix $nodeTag DX DY RZ.
# where a fixed constraint is defined with a 1, a free constraint is define with 0
#
fix 1 1 0 0;
fix 14 1 1 0;
#
#
#
# ----- Define ELEMENTS & SECTIONS -----
-----
#
# Define materials for nonlinear columns
# -----
#
# CONCRETE
#
# This command is used to construct a UniaxialMaterial object which represents
uniaxial stress-strain relationships.
# uniaxialMaterial $matType $matTag $fck $epscl $fcu $epscl $lambda (ratio
betwn unloading slope at $epscl and initial slope) $ft $Et
#
# uniaxialMaterial Concrete02 [expr -$fck] [expr -$epscl] [expr -$fcu] [expr -
$epscl] 0.10 $fctm $Et
#
# Unconfined Concrete
uniaxialMaterial Concrete02 1 -$fcm -$epscl -$fcu -$epscl 0.10 $fctm $Et
#
# Confined Concrete
uniaxialMaterial Concrete02 2 -$fccm -$epscl -$fccu -$epscl 0.10 $fctm $Et
#
# STEEL
#
# uniaxialMaterial $matType $matTag $fy $Es $b (strain-hardening ratio) $R0 $CR1
$CR2 (parameters to control the transition from elastic to plastic branches)
#
#
#uniaxialMaterial Steel02 3 $fym $Es $bs 15 0.925 0.15
#
#
uniaxialMaterial ReinforcingSteel 3 $fym $fsu $Es $Esh $esh $epsu -DMBuck $lsr 0.8
#
#
uniaxialMaterial ReinforcingSteel 3 $fym $fsu $Es $Esh $esh $epsu -GABuck $lsr 2.0
0.0 0.5
#
#
# ----- Rigid link -----
-----
#
# rigidLink $type $masterNodeTag $slaveNodeTag
#
# type: beam (both the translation and rotation degrees of freedom are constrained)
#
#rigidLink beam 2 1
#rigidLink beam 4 5
#
#
# FIBER SECTION properties -----
-----
#
# ----- CROSS SECTION -----
-----
#
# La sezione è viene disposta con l'asse Z lungo la direzione 1
#
#
#

```



```

# element $eleType $eleTag $iNode $jNode$numIntgrPts $secTag (identifier for
previously-defined section object) $transfTag (identifier for previously-defined
coordinates-transformation object)
# COLUMN:

element nonlinearBeamColumn 1 3 4 5 1 3
element nonlinearBeamColumn 2 4 5 5 1 3
element nonlinearBeamColumn 3 5 6 5 1 3
element nonlinearBeamColumn 4 6 7 5 1 3
element nonlinearBeamColumn 5 7 8 5 1 3
element nonlinearBeamColumn 6 8 9 5 1 3
element nonlinearBeamColumn 7 9 10 5 1 3
element nonlinearBeamColumn 8 10 11 5 1 3
element nonlinearBeamColumn 9 11 12 5 1 3

#element elasticBeamColumn $eleTag $iNode $jNode $A $E $Iz $transfTag <-mass
$massDens> <-cMass>

element elasticBeamColumn 10 1 2 60000 30000 84375000 3
element elasticBeamColumn 11 2 3 60000 30000 84375000 3

element elasticBeamColumn 12 12 13 60000 30000 84375000 3
element elasticBeamColumn 13 13 14 60000 30000 84375000 3

set Vol [expr ($Lcolonna*$b*$h)]
set PCol [expr ($Vol*25/(1000000))]
# in N

# define GRAVITY -----
pattern Plain 1 Linear {
  load 2 0 $PCol 0
  # load 4 0 -$PCol 0
  # load 5 0 0 0
  # load 6 0 0 0
  # load 7 0 -$PCol 0
  # load 8 0 -$PCol 0
# DISTRUBUTED LOADS -----
-
# set Linfl 4000
# set G1 -0.0091
# set G2 -0.008
# set q1 [expr $G1*$Linfl]
# set q2 [expr $G2*$Linfl]
# eleLoad -ele 17 18 19 20 21 22 23 24 25 -type -beamUniform $q1
# eleLoad -ele 26 27 28 -type -beamUniform $q2
#}
# -----
# Start of analysis generation
# -----

# Create the system of equation, a sparse solver with partial pivoting
system BandGeneral

# Create the constraint handler, the transformation method
constraints Transformation

# Create the DOF numberer, the reverse Cuthill-McKee algorithm
numberer RCM

# Create the convergence test, the norm of the residual with a tolerance of 1e-12
and a max number of iterations of 10
test NormDispIncr 1.0e-13 1000 3

# Create the solution algorithm, a Newton-Raphson algorithm

```

```

algorithm Newton

# Create the integration scheme, the LoadControl scheme using steps of 0.05
integrator LoadControl 0.1

# Create the analysis object
analysis Static

# -----
# End of analysis generation
# -----

# -----
# Finally perform the analysis
# -----

# perform the gravity load analysis, requires 20 steps to reach the load level
analyze 10

# ----- maintain constant gravity loads
and reset time to zero
loadConst -time 0.0

puts "Model Built"

# Print out the state of elements
print ele 1

```

```

source Colonna.tcl

loadConst -time 0.0
puts "Gravity Analysis Completed"
puts "Cyclic Analysis Completed"
#display displacement shape of the column
recorder display "Displaced shape2" 20 20 500 500 -wipe

prp 300. 200. 1;
vup 0 1 0;
vpn 0 0 1;
display 1 5 40

# vup 0 0 1
# vpn 1 0 0 ----> vista Y-Z

# vup 0 1 0
# vpn 0 0 1 ----> vista X-Y

# vup 0 0 1
# vpn 0 1 0 ----> vista X-Z
# Set the gravity loads to be constant & reset the time in the domain
loadConst -time 0.0

# -----
# End of Model Generation & Initial Gravity Analysis
# -----

# -----
# Start of additional modelling for lateral loads
# -----

# Define lateral loads
# -----

# Set some parameters
set P 1.0;          # Reference lateral load

set dof 2
set nodo 1

# Set lateral load pattern with a Linear TimeSeries
pattern Plain 3 "Linear" {

    # Create nodal loads at nodes 3 & 4
    # nd    FX  FY  MZ

    load 1    0  $P    0.0
    # load 7    $H2 0.0  0.0

}

# -----
# End of additional modelling for lateral loads
# -----

# -----
# Start of modifications to analysis for push over
# -----

# Set some parameters
set dU 0.0010;     # Displacement increment
                  # Displacement increment
# Change the integration scheme to be displacement control

```

```

#                               node dof init Jd min max
integrator DisplacementControl $nodo $dof $dU 1 $dU $dU

# -----
# End of modifications to analysis for push over
# -----

# -----
# Start of recorder generation
# -----

#Fibra da analizzare su cc
set FibCCy [expr $H-$coverh]
set FibCCz [expr $B-$coverh]

set FibUCy [expr $H]
set FibUCz [expr $B]

# Stop the old recorders by destroying them
# remove recorders
nodeDisp 1 1
# Create a recorder to monitor nodal displacements
recorder Node -file DispV.out -node 1 -dof 2 disp
recorder Node -file DispO.out -node 8 -dof 1 disp
# Create a recorder to monitor base shear
recorder Node -file NForce.out -node 14 -dof 2 reaction
recorder Node -file VReaction.out -node 14 -dof 1 reaction
recorder Element -file CConcreteCompressed.out -ele 5 section 2 fiber -$FibCCy 0
2 stressStrain
recorder Element -file CConcreteTraction.out -ele 5 section 2 fiber $FibCCy 0 2
stressStrain
recorder Element -file UConcreteCompressed.out -ele 5 section 2 fiber -$FibUCy 0
1 stressStrain
recorder Element -file UConcreteTraction.out -ele 5 section 2 fiber $FibUCy 0 1
stressStrain
recorder Element -file Steel.out -ele 5 section 2 fiber $FibCCy $FibCCz 3
stressStrain
# recorder Element -file SScore.out -ele 1 section 3 fiber 0 50 1 stressStrain
# recorder Element -file SScover.out -ele 1 section 1 fiber 0 200 2 stressStrain
# recorder plot SScore.out "Stress-strain" 10 10 400 400 -columns 2 1
# recorder plot SScover.out "Stress-strain" 10 10 400 400 -columns 2 1
# recorder Element -file I29.out -ele 29 localForce
# recorder Element -file I35.out -ele 35 localForce
# recorder Element -file D29.out -ele section 1 deformation
# recorder Element -file D35.out -ele section 1 deformation

# End of recorder generation
# -----
# -----
# Finally perform the analysis
# -----

# Set some parameters
set maxU [expr 0.1*$Lcolonna]; # Max displacement
set currentDisp 0.0;
set ok 0

while {$ok == 0 && $currentDisp < $maxU} {

    set ok [analyze 1]

    # if the analysis fails try initial tangent iteration
    if {$ok != 0} {
        puts "regular newton failed .. lets try an initial stiffness for this step"
        test NormDispIncr 1.0e-4 2000
        algorithm ModifiedNewton
    }
}

```

```
        #-initial
        set ok [analyze 1]
        if {$ok == 0} {puts "that worked .. back to regular newton"}
        test NormDispIncr 1.0e-4 2000
        algorithm Newton
    }

    set currentDisp [nodeDisp $nodo $dof]
}

if {$ok == 0} {
    puts "Pushover analysis completed SUCCESSFULLY";
} else {
    puts "Pushover analysis FAILED";
}
```

*12 Appendix D – Different interpolations of Global Resistance
Factor γ_R related to several Safety Formats*

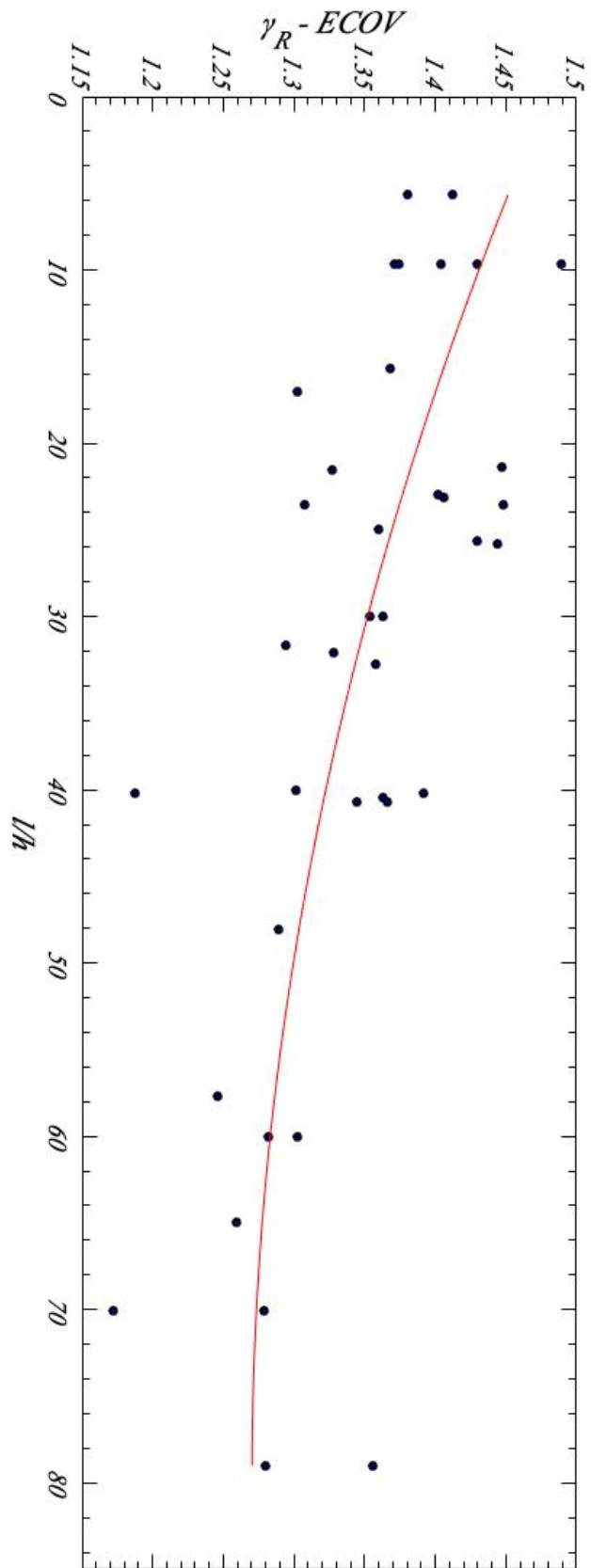


Figure 9.1 - Second order polynomial interpolation – ECOV

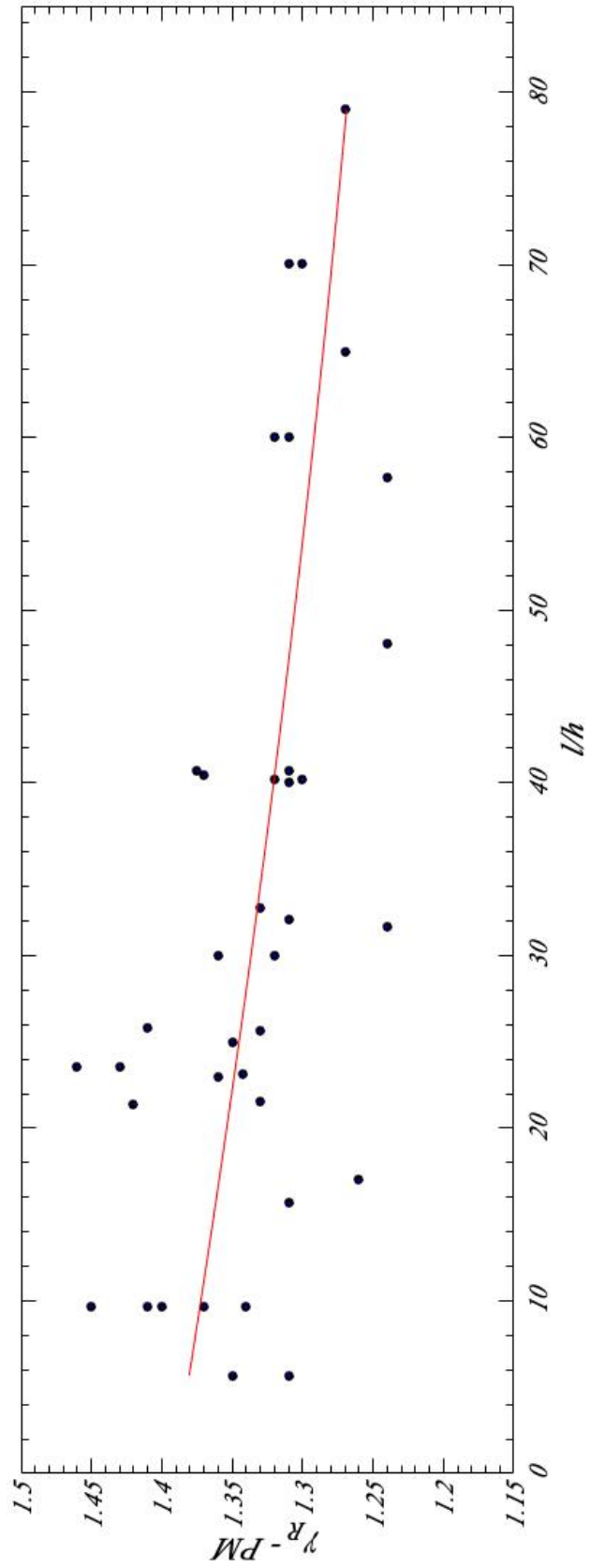


Figure 9.2 – First order polynomial interpolation – PM -GSF

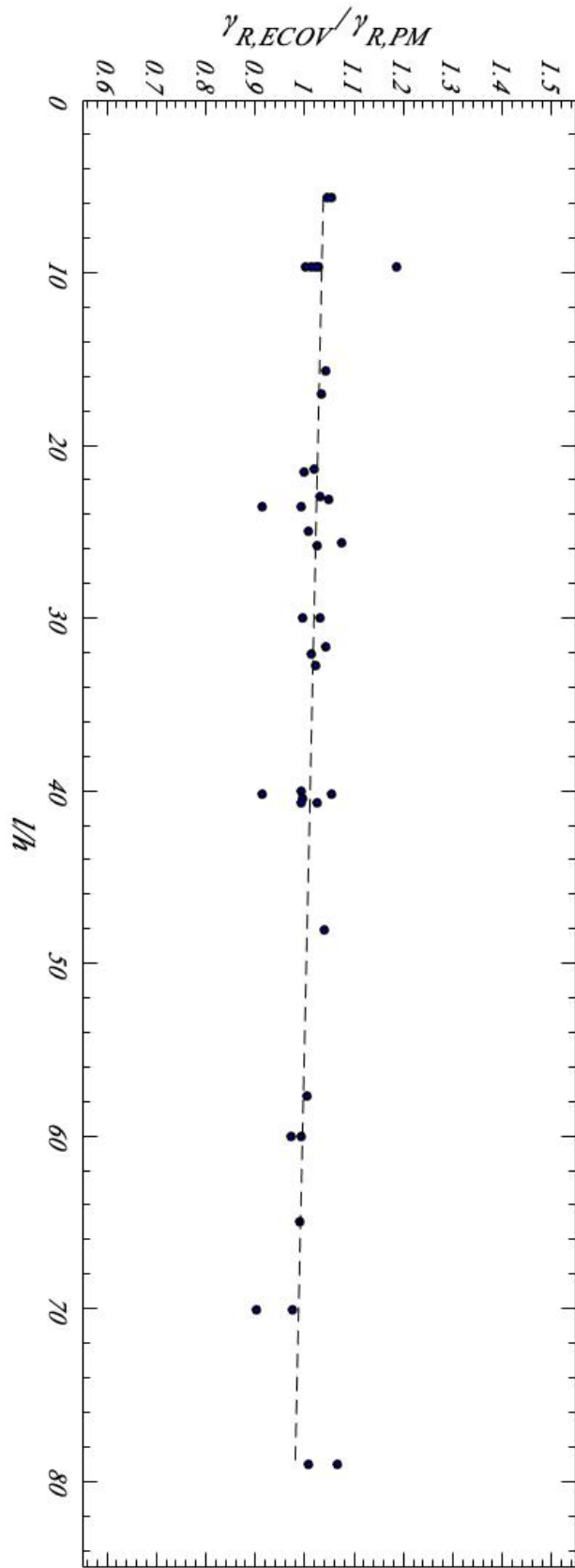


Figure 9.3 – Linear interpolation of ratio between $\gamma_{R,ECOV} / \gamma_{R,PM}$

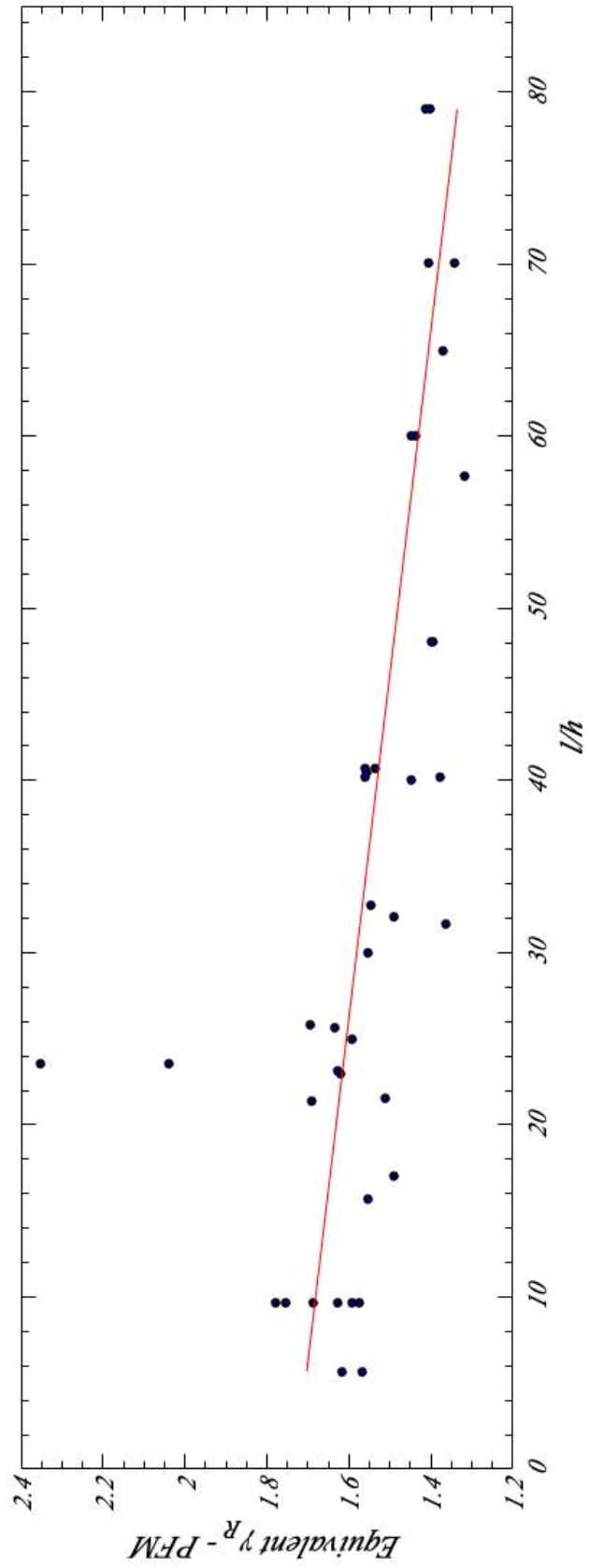


Figure 9.4 – First order polynomial interpolation – $\gamma_{R, \text{equivalent}}$ PFM

Bibliography

- [1] CEN. EN 1990: Eurocode – Basis of structural design, CEN, Brussels, 2013.
- [2] CEN. EN 1992-1-1: Eurocode 2 – Design of concrete structures. Part 1-1: general rules and rules for buildings, CEN, Brussels, 2014.
- [3] Robby Caspeele. *Introduction into structural reliability methods and structural system*. Ghent University, 2011.
- [4] CEB: *New developments in non-linear analysis methods. Bulletin information n°229*. CEB, Lousanne, 1995.
- [5] Hendrik Schlune, Mario Plos, and Kent Gylltoft. Safety formats for non-linear analysis of concrete structures. *Magazine of Concrete Research*, 64(7):563–574, 2012.
- [6] Armen Der Kiureghian and Ove Ditlevsen. *Aleatory or epistemic? does it matter? Structural Safety*, 31(2):105–112, 2009.
- [7] JCSS Probabilistic Model Code. Joint committee on structural safety. URL: www.jcss.ethz.ch, 2001.
- [8] G König, D Pommerening, and N TUE. Safety concept for the application of non-linear analysis in the design of concrete structures, general considerations. *CEB Bulletin No*, 229:13–31, 1995.
- [9] Milan Holický, Johan V Retief, and Miroslav Sykora. Assessment of model uncertainties for structural resistance. *Probabilistic Engineering Mechanics*, 45:188–197, 2016.
- [10] Milan Holický and Miroslav Sykora. Global resistance factors for reinforced concrete members. *Acta Polytechnica, CTU in Prague*, 2006.
- [11] Diego Lorenzo Allaix, Vincenzo Ilario Carbone, and Giuseppe Mancini. Global safety format for non-linear analysis of reinforced concrete structures. *Structural Concrete*, 14(1):29–42, 2013.
- [12] CEB FIB. Model code 2010. Technical report, 2010.
- [13] F. McKenna, G.L. Fenves, M.H. Scott, *Open system for earthquake engineering simulation*, University of California, Berkeley, CA, 2000.

- [14] Aykac B, Kalkan I, Aykac s, Egribiz EM. Flexural behavior of RC beams with regular square or circular web openings. *Engineering Structures*, 2013.
- [15] fib: fib Bulletin 56: Model Code 2010, first complete draft, vol.2, fib, Lousanne, 2010.
- [16] Jin-Keun Kim and Joo-Kyoung Yang. Buckling behaviour of slender high-strength concrete columns. *Engineering Structures*, 17(1):39–51, 1995.
- [17] A Mehmel, H Schwarz, KH Karperek, and J Makovi. Tragverhalten ausmit-tig beanspruchter stahlbetondruckglieder. institut für baustatik, eht, deutscher ausschuss für stahlbeton, heft 204, 1969.
- [18] Robert G Drysdale and Mark William Huggins. Sustained biaxial load on slender concrete columns. *Journal of the Structural Division*, 1971.
- [19] N Khalil, AR Cusens, and MD Parker. Tests on slender reinforced concrete columns. *Structural Engineer*, 79(18):21–3, 2001.
- [20] Luis P Saenz and Ignacio Martin. Test of reinforced concrete columns with high slenderness ratios. In *Journal Proceedings*, volume 60, pages 589–616, 1963.
- [21] Stephen J Foster and Mario M Attard. Experimental tests on eccentrically loaded high strength concrete columns. *Structural Journal*, 94(3):295–303, 1997.
- [22] VR Pancholi. *The Instability of Slender Reinforced Concrete Columns*. PhD thesis, University of Bradford, 1977.
- [23] Adriana Dracos. *Long slender reinforced concrete columns*. PhD thesis, Uni- versity of Bradford, 1982.
- [24] Satoshi IWAI, Koichi MINAMI, and Minoru WAKABAYASHI. Stability of slender reinforced concrete columns subjected to biaxially eccentric loads. 1986.
- [25] PH Chuang and FK Kong. Large-scale tests on slender, reinforced concrete columns. *Structural Engineer*, 75(23):410–16, 1997.
- [26] AC Barrera, JL Bonet, Manuel L Romero, and PF Miguel. Experimental tests of slender reinforced concrete columns under combined axial load and lateral force. *Engineering Structures*, 33(12):3676–3689, 2011.
- [27] Oskar Baumann. *Die Knickung der Eisenbeton-Säulen*. PhD thesis, ETH Zurich, 1935.

- [28] Bertagnoli G, VI Carbone. A finite element formulation for concrete structures in plane stress. *Structural Concrete*, 9(2):87–99, 2008.
- [29] Di Trapani F, VI Carbone. Analisi non lineare per l'ingegneria sismica, *Ph.D course, Turin*, 2017.
- [30] Cervenka V. Reliability-based non-linear analysis according to *fib Model Code 2010*, *Structures Concrete, Journal of the fib*, vol.14, March 2013.
- [31] Murat Saatcioglu and Salim R Razvi. Strength and ductility of confined concrete. *Journal of Structural engineering*, 118(6):1590–1607, 1992.
- [32] Murat Saatcioglu and Salim R Razvi. Confinement model for high-strength concrete. *Journal of Structural engineering*, 125(3):281–289, 1999.
- [33] Carpinteri A. *Scienza delle Costruzioni*, vol.2, *Pitagora, Bologna*, 1992.
- [34] Timoshenko, Gere. *Theory of elastic stability*, *McGraw-Hill*, 1963.
- [35] Viridis M. Assessment of aleatory and model uncertainties for non-linear analysis of reinforced concrete members, *Master's thesis, Turin*, 2018.
- [36] Sangiorgio, F: Safety Format for non-linear analysis of RC structures subjected to multiple failure modes, *Doctoral thesis, Stockholm, Sweden*, 2015.
- [37] Castaldo P, Gino D, Bertagnoli G, Mancini G. Partial safety factor for resistance model uncertainties in 2D non-linear finite elements analysis of reinforced concrete structures. *Engineering Structures*, 176(C), pp.746-762, September 2018.